JYU DISSERTATIONS 151

Jarno Kansanaho

Data-Driven Methods for Diagnostics of Rolling Element Bearings

UNIVERSITY OF JYVÄSKYLÄ
FACULTY OF INFORMATION TECHNOLOGY

JYU DISSERTATIONS 151

Jarno Kansanaho

Data-Driven Methods for Diagnostics of Rolling Element Bearings

Esitetään Jyväskylän yliopiston informaatioteknologian tiedekunnan suostumuksella
julkisesti tarkastettavaksi yliopiston Agora-rakennuksen auditoriossa 2
marraskuun 30. päivänä 2019 kello 12.

Academic dissertation to be publicly discussed, by permission of
the Faculty of Information Technology of the University of Jyväskylä,
in building Agora, auditorium 2, on November 30, 2019 at 12 o'clock noon.

JYVÄSKYLÄN YLIOPISTO
UNIVERSITY OF JYVÄSKYLÄ

JYVÄSKYLÄ 2019

Editors
Timo Männikkö
Faculty of Information Technology, University of Jyväskylä
Ville Korkiakangas
Open Science Centre, University of Jyväskylä

Permanent link to this publication: http://urn.fi/URN:ISBN:978-951-39-7936-2

ISBN 978-951-39-7936-2 (PDF)
URN:ISBN:978-951-39-7936-2
ISSN 2489-9003

ABSTRACT

Kansanaho, Jarno
Data-Driven Methods for Diagnostics of Rolling Element Bearings
Jyväskylä: University of Jyväskylä, 2019, 76 p. (+included articles)
(JYU Dissertations
ISSN 2489-9003; 151)
ISBN 978-951-39-7936-2 (PDF)

This thesis focuses on the research and development of the data-driven methods used to diagnose rolling element bearings (REBs) and evaluates the software architectural design of these data-driven methods. REBs are vulnerable components in machinery. Vibration-based condition monitoring is a very popular methodology for monitoring the health of REBs.

This research started with the development of methods to analyze and detect incipient local faults of REBs using vibration measurements. The main goal was to find weak vibration signatures generated by local faults in REBs. As a result, a flexible simulator was developed to analyze the vibrations of bearing faults and to evaluate vibration analysis methods, and a spline wavelet-based algorithm were introduced for fault detection.

An incipient bearing fault will become enlarged if a machine is run and the faulty bearing has not been replaced. The identification of different lifetime stages of wear evolution is part of the input data for bearing diagnostics and prognostics. A method to detect different lifetime stages of REBs according to their vibration signals was proposed based on an unsupervised learning method. The result of the unsupervised method was exploited in early fault detection utilizing supervised methods.

It is important to estimate the severity of a fault, and size is probably the best proxy for severity. Estimating the fault size of defective REBs is one of the top challenges in bearing diagnostics, especially when vibration measurements are used to determine the state of health. A novel method for feature ranking to estimate fault sizes for REBs was presented. Black-box classifiers were applied to detect non-linear relations between features, and it was concluded that the best metrics for basic diagnostics are not necessarily the best qualities for fault size estimation.

The final part of this research focuses on design at system-level. Software framework designs encapsulate fault detection and remaining useful life (RUL) estimation methods. As part of the tribotronic system, the object-oriented framework considers bearing applications and potentially extends them to other mechanical applications.

Keywords: Rolling element bearing, Bearing diagnostics, Vibration analysis, Feature extraction, Machine learning, Tribological system, Software framework

TIIVISTELMÄ (ABSTRACT IN FINNISH)

Kansanaho, Jarno
Tieto-ohjautuvia menetelmiä laakerien vikadiagnostiikkaan
Jyväskylä: University of Jyväskylä, 2019, 76 s. (+artikkelit)
(JYU Dissertations
ISSN 2489-9003; 151)
ISBN 978-951-39-7936-2 (PDF)

Väitöskirjatyöni käsittelee vierintälaakerien kunnonvalvonnassa käytettäviä vikadiagnostiikka-algoritmeja sekä ohjelmistoarkkitehtuurisuunnittelua kyseisten tieto-ohjautuvien menetelmien näkökulmasta.

Tutkimus aloitettiin kehittämällä menetelmiä, joilla analysoidaan ja voidaan havaita vierintälaakerien alkavat paikalliset viat värähtelymittauksia hyödyntämällä. Päätavoitteena oli löytää vierintälaakerien paikallisten vikojen aiheuttamat heikot värähtelyt. Konkreettisena tutkimustuloksena syntyi joustava simulaattori laakerivikojen värähtelyanalyysille ja värähtelyanalyysimenetelmien arviointiin sekä spline-väreitä hyödyntävä algoritmi vierintälaakerivian havaitsemiseen.

Vierintälaakerin vaurio suurenee, jos konetta käytetään edelleen, eikä laakeria ei vaihdeta. Vierintälaakerin vaurion etenemisen vaiheiden tunnistaminen on hyödyllistä vian vakavuuden arvioinnissa ja jäljellä olevan käyttöiän ennustamisessa. Tutkimuksessa sovellettiin valvomatonta oppimismenetelmää vierintälaakerin elinkaaren vaiheiden havaitsemiseksi värähtelysignaaleista. Valvomattoman menetelmän tulosta hyödynnettiin varhaisen laakerivian havainnoinnissa ohjattujen menetelmien avulla.

Viallisen vierintälaakerin vian vakavuuden arviointi voi olla hyvin haastavaa, erityisesti värähtelymittauksia käytettäessä. Tällöin piirreirrotus värähtelysignaaleista on välttämätöntä. Värähtelysignaalista laskettuja piirteitä on tutkittu ja niitä kehitetään laajasti. Piirteitä arvioidaan, kuinka hyvin niillä pystytään havainnoimaan laakerivika ja kuinka hyvin ne kuvaavat laakerivian vakavuuden tilaa tai sen elinkaaren vaiheita. Tässä tutkimuksessa sovellettiin koneoppimismenetelmiä vian koon arviointiin. Tuloksena syntyi uusi menetelmä värähtelysignaalien piirteiden arvioimiseen sovellettaessa vian koon arviointiin instanssipohjaisia luokittimia.

Tämän tutkimuksen viimeisessä osassa keskityttiin järjestelmätason suunnitteluun. Suunniteltu ohjelmistokehys kapseloi vikojen havaitsemisen ja jäljellä olevan käyttöiän arviointimenetelmät. Toteutettu ohjelmistokehys toimii osana tribotronista järjestelmää, jossa vierintälaakeri on tribologinen systeemi. Ohjelmistokehys tarjoaa mahdollisuuden laajentaa sen muihin tribologisiin systeemeihin.

Avainsanat: Vierintälaakeri, Laakerien diagnostiikka, Värähtelyanalyysi, Piirreirrotus, Koneoppiminen, Tribotroninen systeemi, Ohjelmistokehys

Author

Jarno Kansanaho
Faculty of Information Technology
University of Jyväskylä
Finland

Supervisor

Professor Tommi Kärkkäinen
Faculty of Information Technology
University of Jyväskylä
Finland

Reviewers

Professor (Emeritus) Kauko Leiviskä
Environmental and Chemical Engineering
University of Oulu
Finland

Assistant Professor Indrė Žliobaitė
Department of Computer Science
University of Helsinki
Finland

Opponent

D.Sc. (Tech.) Erkki Jantunen
Retired Chief Research Scientist, VTT
Finland

ACKNOWLEDGEMENTS

My PhD work began in a commissioned research project with ABB Marine and Ports. The project was initiated by Kari Saarinen from ABB Corporate Research. I am greatful for the co-operation with ABB Marine and Ports team. Thanks to Janne Peltola, Juha Pirkkalainen, Antti Laiho, Mika Kivistö and Jari Kivelä. I had an great opportunity to get hands on real-time systems development using the latest technologies, since the project was directed to product development. In addition to, some of the results were suitable for the scientific publications.

I made a research visit to University of South Wales (UNSW, Sydney, Australia) in summer 2018. The purpose of my visit was to start collaboration with the Tribology and Machine Condition Monitoring research group. Specialties of the research group are wear and fracture mechanisms, and machine condition monitoring using vibration, oil and wear debris analysis techniques. Outcome of my visit is a very big part of my PhD thesis. Thank you very much for your support, Zhongxiao Peng, Pietro Borghesani, Wade Smith and Bob Randall. I hope our co-operation will flourish in the upcoming future.

Many thanks to my supervisor Professor Tommi Kärkkäinen, who guided me through the process. We might have had some hard times during the work, but we kept the focus and finished the work. Awesome!

Heartfelt thanks and respect to my wife Päivi, who was able to listen to my stories about scientific publishing. Special thanks to my brother Karre, who always helps me.

This work is dedicated to my sons Johannes and Aatos.

LIST OF ACRONYMS

REB	Rolling Element Bearing
RUL	Remaining Useful Life
CBM	Condition Based Maintenance
CM	Condition Monitoring
P-F	Potential-to-Failure
ODM	Oil Debris Monitoring
DSP	Digital Signal Processing
LTI	Linear Time-Invariant
DTF	Discrete Fourier Transform
FFT	Fast Fourier Transform
STFT	Short-Time Fourier Transform
CWT	Continuous Wavelet Transform
DWT	Discrete Wavelet Transform
FIR	Finite Impulse Response
IIR	Infinite Impulse Response
BPFI	Ball Pass Frequency Inner
BPFO	Ball Pass Frequency Outer
BSF	Ball Spin Frequency
FTF	Fundamental Train Frequency
HFRT	High Frequency Resonance Technique
SNR	Signal-to-Noise Ratio

CPW	Cepstrum Pre-Whitening
SK	Spectral Kurtosis
TSA	Time Synchronous Averaging
ANC	Adaptive Noise Cancellation
SANC	Self Adaptive Noise Cancellation
EMD	Empirical Mode Decomposition
HHT	Hilbert-Huang Transform
IMF	Intrinsic Mode Function
k-NN	k-Nearest Neighbor
SVM	Support Vector Machine
NB	Naive Bayes

LIST OF FIGURES

LIST OF TABLES

CONTENTS

LIST OF INCLUDED ARTICLES

PI Jarno Kansanaho, Kari Saarinen and Tommi Kärkkäinen. Flexible Simulator for the Vibration Analysis of Rolling Element Bearings. *International journal of COMADEM*, 2017.

PII Jarno Kansanaho, Kari Saarinen and Tommi Kärkkäinen. Spline wavelet based filtering for denoising for vibration signals generated by rolling element bearings. *International journal of COMADEM*, 2018.

PIII Jarno Kansanaho and Tommi Kärkkäinen. Hybrid vibration signal monitoring approach for rolling element bearings. *In Proceedings of European Symposium on Artificial Neural Networks, Computational Intelligence and Machine Learning (ESANN 2019)*, 2019.

PIV Jarno Kansanaho, Tommi Kärkkäinen, Pietro Borghesani, Wade A. Smith, Robert B. Randall, Zhongxiao Peng. Feature ranking for fault size estimation of rolling element bearings. *Submitted to: Measurement*, 2019.

PV Jarno Kansanaho and Tommi Kärkkäinen. Software framework for Tribotronic system. *A preprint available at arXiv:1910.13764*, 2019.

1 INTRODUCTION

1.1 Background and motivation

Rolling bearing elements (REBs) are regularly used components in rotating machinery. The main function of REBs is to support shafts that rotate at different speeds and carry different loads. A bearing failure is the most common reason for machine breakdowns, which lead to significant economical, or even human, losses. Condition monitoring, a crucial part of condition-based maintenance, tries to prevent catastrophic failures from happening. Fault detection, fault diagnostics, and fault prognostics produce inputs for condition monitoring (Figure 1). Figure 1 presents the relationships between components related to condition monitoring.

Diagnostics covers the identification and quantification of a machine component fault, while prognostics covers the prediction of a component's future conditions, its remaining operational life, or the risk to complete operation (Heng et al., 2009; Sikorska et al., 2011). Detecting incipient faults enables better possibilities for planned maintenance actions. The fault severity assessment provides valuable information for RUL estimation that predicts the final operation time.

Vibration measurements are the most common condition monitoring method for bearing diagnostics. Compared to other online condition monitoring methods such as oil particle measurements, vibration measurement systems are affordable and scalable solutions. Moreover, vibration sensors are continually developed. Vibration measurements do not directly indicate a bearing's condition; thus, feature extraction is necessary. The sensitivity of vibration signals to disturbances makes the task more difficult.

Signal processing methods for vibration analysis are frequently developed for bearing diagnostics. Signal processing methods focus on the extraction of characteristic features from the vibration signals generated by REBs. The decision-making based on these extracted features can be considered the second step in signal processing approaches (Rai and Upadhyay, 2016). Features extracted from vibration signals include time domain, frequency domain, or time-frequency do-

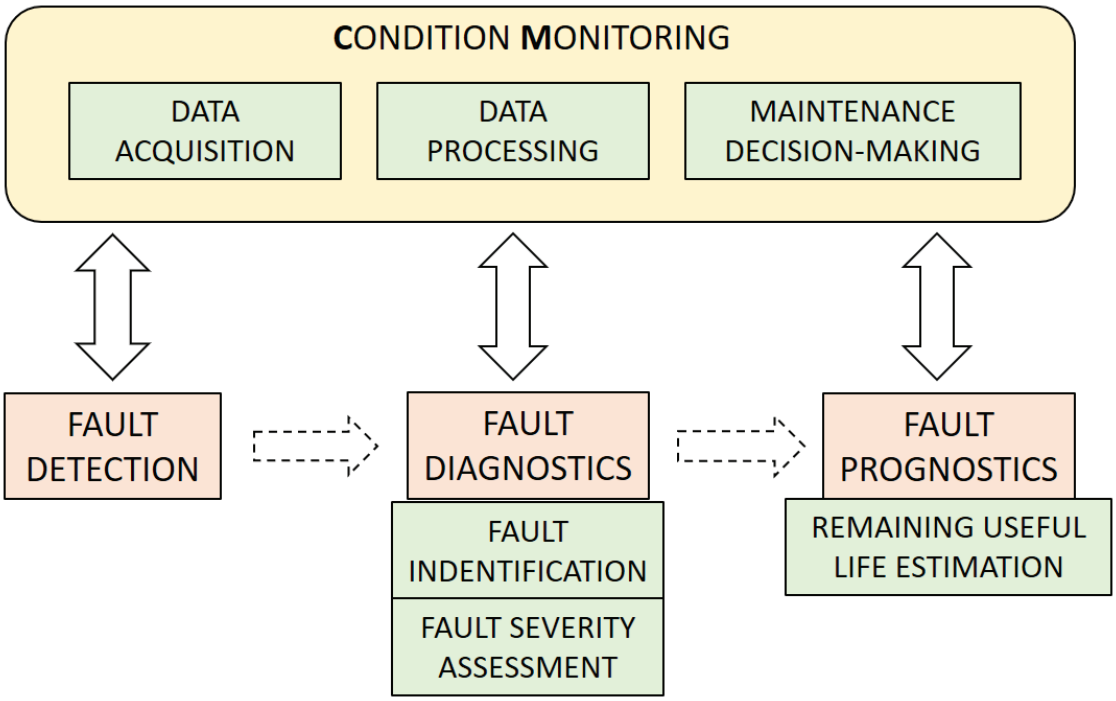

FIGURE 1 Key elements of condition monitoring.

main depending on the application. The most suitable features for diagnostics differ from features that are the most suitable for prognostics. Aside from data-driven methods, physical-based models have received attention in prognostics (Li et al., 1999, 2000; Luo et al., 2003b).

Detecting faults of incipient bearings can be as worthwhile as it is challenging. The operating conditions of bearings may consist of many other components that generate vibrations which overlap with the monitored bearing's vibrations. In such cases, extracting characteristic fault features requires sophisticated methods, such as the use of digital filters, transformations, and signal decomposition. Vibration signal features are usually high-dimensional and non-Gaussian, leading to problems when recognizing patterns (Zhao et al., 2014). This has led to the continual application of machine learning methods in bearing diagnostics and prognostics. However, such research should not rely on narrow datasets.

Fault severity assessment that provides valuable input for prognostics requires more background information regarding the health of a bearing other than fault detection. Direct information of the degradation of REBs should be acquired to map the actual degradation state using vibration signal features. In typical laboratory experiments, this requires the removal of a bearing. Finding a good degradation feature is essential for RUL estimation, which is a prognostic task.

Novel methods in the research of bearing diagnostics and prognostics are published in journals such as Mechanical Systems and Signal Processing, Measurement, Sound and Vibration, and Vibration and Control. Many of the published research studies are based on bearing vibration data collected from one bearing test rig. It is notable that one vibration dataset from Case Western University (CWRU, s. a.) has been studied in many research studies; see Table 3 in the

Appendix. Furthermore, bearing faults in this particular dataset were artificially produced; this leads to the conclusion that diagnostic and prognostic methods based on narrow datasets might not have good generalization capabilities.

Autonomous tribotronic systems control themselves based on measurements acquired from different sensors. In such a systems, REBs are components that are monitored, and their running parameters are adjusted based on the decisions made on outputs from diagnostic and prognostics algorithms. The requirements of real-time systems can significantly vary depending on the machinery. However, the key entities and functionalities in diagnostics and prognostics algorithms are generalizable. Software frameworks potentially allow software designs to be generalizable.

1.2 Research questions

RQ1: What methods can be applied for REB fault detection and how can the methods be analyzed?

RQ2: Can the different stages of wear evolution of REBs be determined?

RQ3: What are the most important vibration signal features, or indicators for fault diagnostics and severity estimation?

RQ4: How can bearing diagnostics and prognostic methods be encapsulated into an industrial software system?

2 ROLLING ELEMENTS BEARINGS

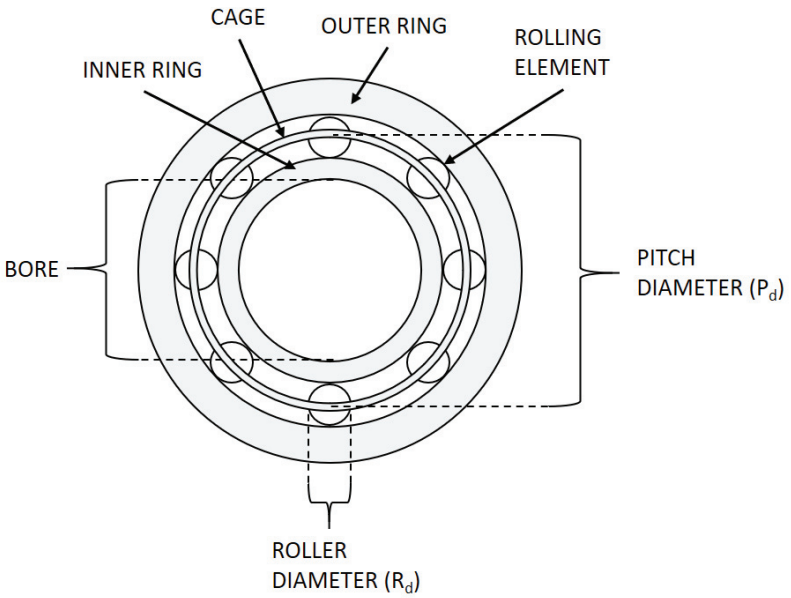

FIGURE 2 Main parts of a rolling element bearing.

Bearings are categorized as REBs or journal bearings based on their structures (Hamrock and Anderson, 1983). REBs contain rolling elements that have different shapes and can be spherical, cylindrical, tapered and needle-like (NTN, 2019). Journal bearings contain only sliding surfaces, no rolling elements. This research focuses on the study of REBs. The main parts of an REB are shown in Figure 2. A rotating shaft penetrates the bore of an REB. Rolling elements circulate the shaft between inner and outer rings touching the raceways. The function of the cage is to keep the rolling elements in the correct position and to prevent them from falling out (NTN, 2019). The inside of an REB is lubricated.

REBs are widely used in various machines, motors, wheels, cooling fans, etc., to support rotating shafts. Requirements for bearings vary depending on the machinery; for example, a large industrial motor has different requirements compared to a wheel on a car trailer. REBs are designed to carry axial and radial

loads, run at different speeds, operate in different conditions, etc. The magnitude and angle of the load are the most important bases for the selection of REBs (Ansaharju, 2009). Different types of REBs have been designed to meet various requirements. The most typical REBs are shown in Figure 3.

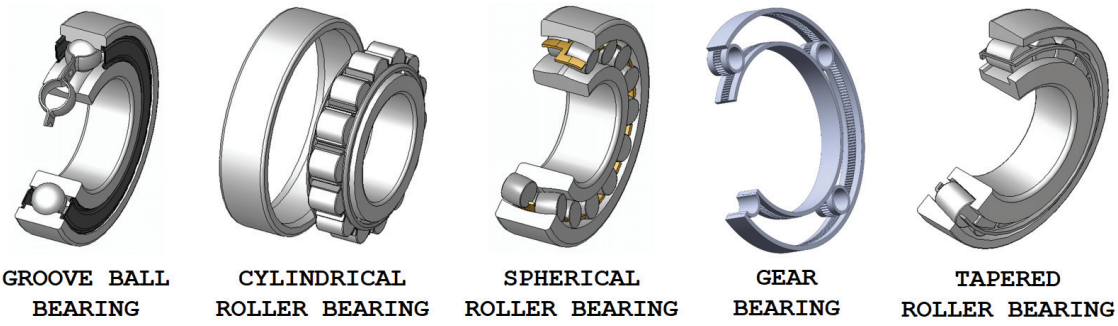

FIGURE 3 Different types of rolling element bearings (Silberwolf, 2006).

The most common type of REB is ball bearing, also called deep groove single row bearing, which carries axial and radial loads and can be used at high rotation speeds (Ansaharju, 2009). Typically, the inner ring is attached to the shaft in ball bearings. Cylindrical roller bearings can handle greater radial loads than ball bearings because cylindrical rolling elements have a larger area where the load can be distributed. Self-aligning, spherical roller bearings are designed to endure considerably heavy radial and axial loads at moderate speeds (Gonzales, 2015). The inner rings of these REBs include two raceways inclined at an angle to bearing axis. Spherical roller bearings are often used in wind turbines, pumps, and gear boxes. Roller elements of tapered roller bearings lean against the collar of the inner race that enables concurrent radial and axial loads (Ansaharju, 2009). Tapered roller bearings are used, for example, in the wheel shafts of cars.

Thrust bearings, also known as axial bearings, are designed to carry axial loads. Thrust ball bearings, high-speed duplex angular contact ball bearings and double direction angular contact thrust ball bearings are typical thrust bearings with ball-shaped rolling elements (NTN, 2019). In thrust bearings, the rolling elements are installed between plates that have rolling raceways. Thrust roller bearings can have cylindrical, needle, or tapered rolling elements.

2.1 Bearing failures

Bearing failure modes can be classified into six categories: fatigue, wear, corrosion, plastic deformation, fracture, and electric erosion Group (2012). The most common cause of bearing failure is fatigue (Sawalhi and Randall, 2011). Generally, REB defects are classified into distributed and localized defects. The distributed defects are surface roughness, waviness, misaligned races, and incorrectly sized rolling elements. Localized defects include cracks, pits, and spalls caused by fatigue on rolling surfaces (Tandon and Choudhury, 1999).

Wear, a measure of a bearing's condition, accumulates over time, and this cumulative wear is usually measured at selected times in machine condition monitoring systems (Christer and Wang, 1995). The presentation of wear evolution as a time series describes wear interaction and evolution at different lifetime stages. El-Thalji et al. introduced a five-stage descriptive model of wear evolution including: running-in, steady-state, defect initiation, defect propagation, and damage growth (El-Thalji and Jantunen, 2014). The five stage model is shown in Figure 4. Previously, two- and three-stage models of wear progress were presented (Jantunen, 2006; Schwach and Guo, 2006; Harvey et al., 2007; Yoshioka and Shimizu, 2009).

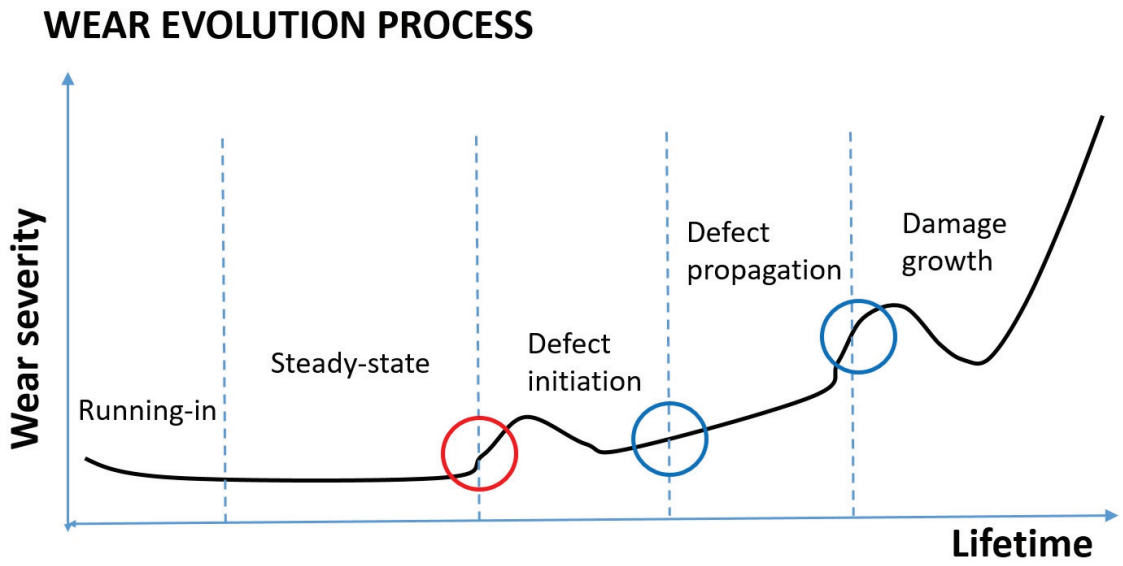

FIGURE 4 A five-stage descriptive model of wear evolution.

2.2 Condition Monitoring

When a measured variable directly determines a bearing failure, the condition monitoring method is direct. Respectively, when a measured variable provides associated information that is affected by the bearing condition, the condition monitoring method is indirect (Christer and Wang, 1995). Commonly used direct and indirect condition monitoring methods consist of the following (Jantunen, 2002; Dongre et al., 2013; Banjevic and Jardine, 2014; Wang et al., 2017): i) Indirect methods: vibration analysis, acoustic emission analysis, ultrasound and infrared analysis, physical basic quantities monitoring (heat, pressure), and electrical basic quantities monitoring (voltage, current, power, resistance); ii) Direct methods: oil debris analysis, corrosion monitoring, and visual inspection (boroscope, etc.).

Since a bearing failure is probable, condition monitoring is necessary to avoid catastrophic failures. The sensitivity of failure detection using different condition monitoring techniques is presented by a P-F curve (Moubray, 1999).

The P-F curve indicates time intervals between potential failure (P) and functional failure (F) using different types of condition monitoring techniques (Figure 5). Functional failure means the machine is inoperable.

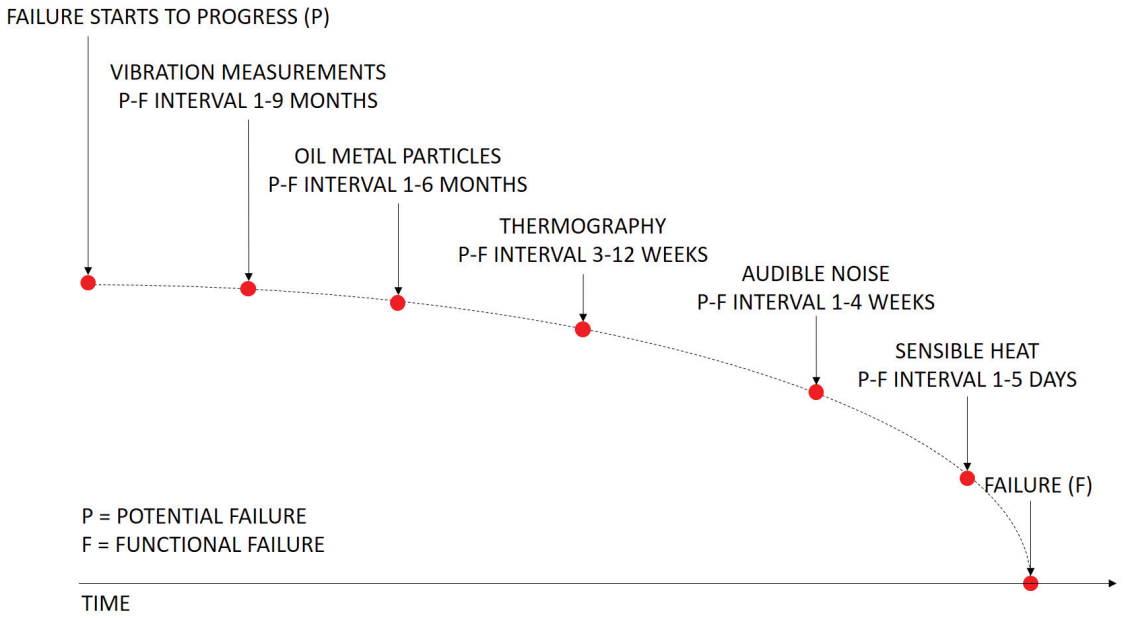

FIGURE 5 P-F curve.

It can be clearly seen from the P-F curve that vibration measurements and oil metal particle measurements provide the longest time interval between the potential failure detection and true functional failure. Hence, proper maintenance can be carefully and safely planned. However, the installation of sensors plays a crucial role with respect to reliable fault detection.

Vibration sensors interpret vibration values indirectly from mechanical and optical quantities. Vibration sensors are categorized into contacting and a non-contacting sensors according to their measurement principles. Moreover, contacting and non-contacting sensors are divided into path, speed, and acceleration measurement (Ruhm, 2010): i) Path measurement: potentiometric transmitter, linear variable differential transformer; ii) Speed measurement: principle of electrodynamics, seismometer (principle of inertia); iii) Acceleration measurement: piezoelectric, piezo-resistive, resistive, and inductive sensors. Path measurement sensors convert linear displacement into an electrical signal. Commonly used accelerometers exploit the piezoelectricity of certain materials. Due to the variety of applications, first, a suitable vibration sensor needs to be chosen based on measurement requirements. Vibration sensor installation is crucial for reliable measurements and so forth for successful condition monitoring. The length of a signal path should be as short as possible (Siemens, 2016). However, environmental conditions also affect the sensors' final positions. Figure 6 shows a simplified example of vibration sensor installation.

Unlike vibration analysis, analysis of lubrication oil of a mechanical system provides direct and reliable information of wear (Bozchalooi and Liang, 2009).

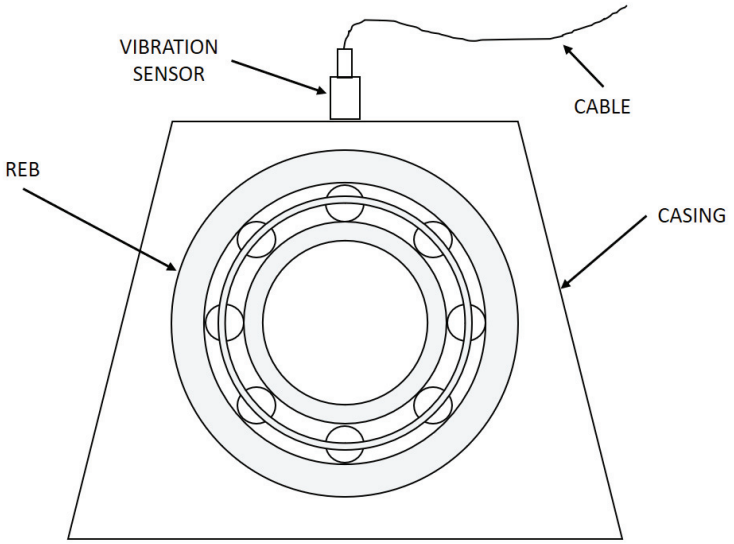

FIGURE 6 Simplified example of installation of a vibration sensor.

Metallic debris indicating a faulty bearing can be detected at the early failure state using an oil debris monitoring system. In practice, oil debris monitoring (ODM) is based either on regularly taken oil samples analyzed in the laboratory (off-line analysis) or on ODM sensors, which are able to detect metal particles on-line (Dupuis, 2010; Dempsey et al., 2011). The actual oil debris data is a time-series, indexed in a chronological order, that represents the amount of metal particles. It is possible to use oil debris data itself as a degradation parameter. However, installation of oil debris sensors is more cumbersome than vibration sensors.

2.3 Tribotronic system

A tribotronic system unites tribological system, sensors, real-time control system, and actuators (Glavatskih and Hoglund, 2008). The tribotronic system is autonomous; measured data from sensors is processed through a real-time control unit and, based on the unit's response, the tribological system is controlled. Such tribological systems include REBs, gears, and seals. Figure 7 presents the components of a tribotronic system and their interactions.

Due to a variety of assets properties, high resolution data, and rather complex algorithms, it is necessary to both plan and document software design. Without any software architectural design in large and complex systems, it is very likely that a software will become difficult to maintain and error-prone. One of the main goals in software engineering is to reuse existing code (Bosch et al., 2000). Since the emergence of object-oriented design, design patterns, software platforms, and software frameworks, software implementations have become more maintainable and reusable. Software frameworks are a key technique in the implementation of software platforms. An important property of a software

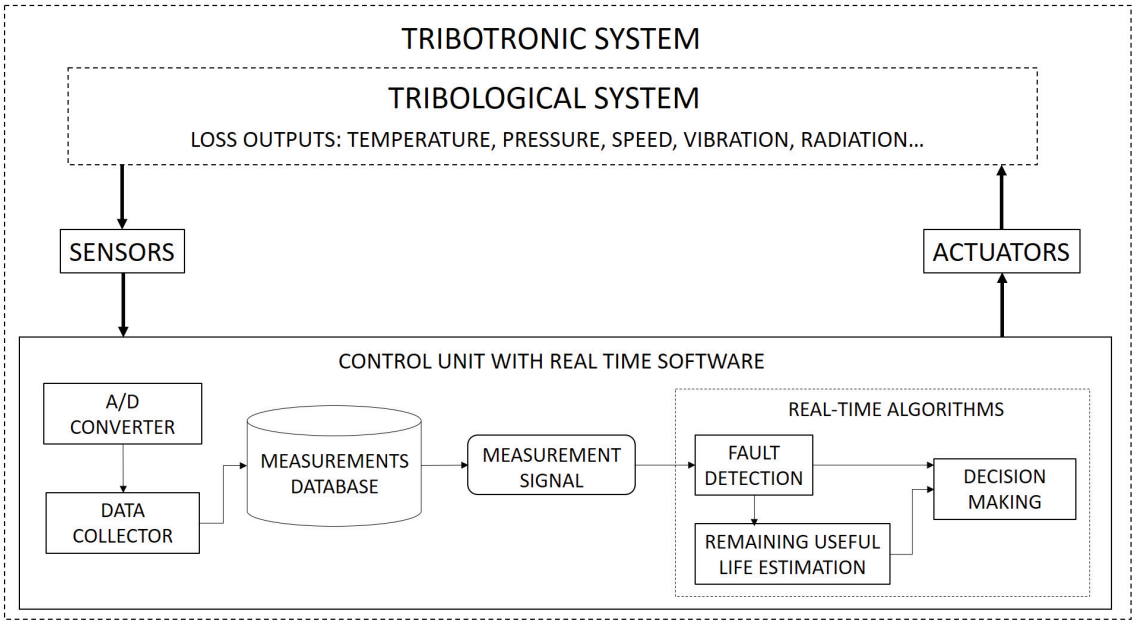

FIGURE 7 Data process flow in tribotronic system.

framework is inversion control, which enables the framework itself to call a user's implemented methods (Johnson and Foote, 1988). Without using frameworks in the software development, a lot of code would be written repeatedly. There exists several types of software frameworks, such as abstract, white-box, black-box, plug-in, layered, and hierarchical frameworks (Koskimies and Mikkonen, 2005).

A control unit in a tribotronic system may incorporate complex algorithms that require the exploitation of several entities, since the software's architectural design is essential. More importantly, a tribological system should be interchangeable from the architectural design perspective; e.g. the tribological system could be REB which would be replaced with gear. Real-time algorithms for fault detection and RUL estimation should be compatible for other tribological systems. Progressive data flow in the control unit could be represented as a pipes-and-filters architectural design (Philipps and Rumped, 1999). From the framework perspective, the tribological system could be considered a plug-in and the inheritance could be the specialization mechanism.

3 DIGITAL SIGNAL PROCESSING

The basics and some common techniques in digital signal processing will be briefly introduced in this chapter, and Chapter 4^{th} references these techniques again.

3.1 Discrete digital signals

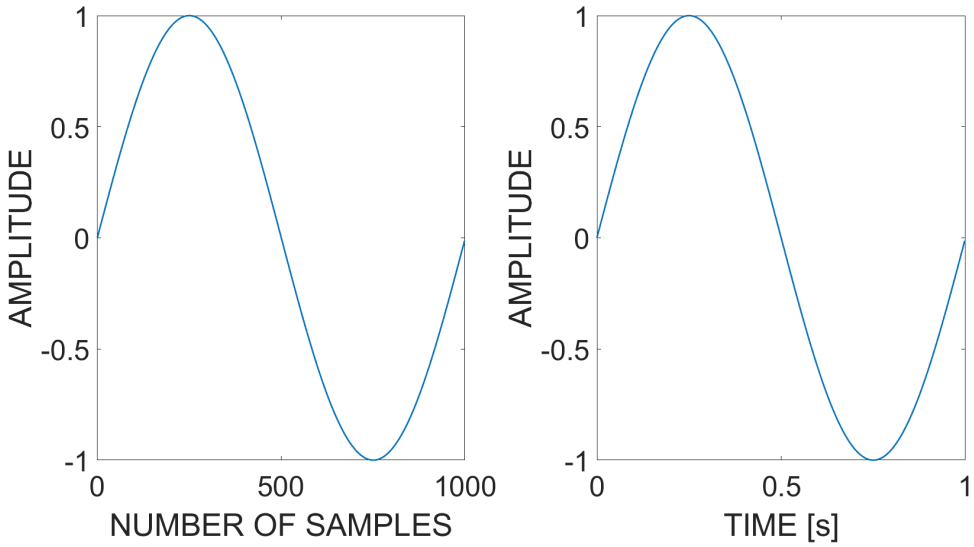

FIGURE 8 Sinusoidal pulse with sampling frequency of 1000 Hz.

Analog-to-Digital (A/D) converters change analog signals [V] to discrete digital signals [0 1]. After conversion, digital filtering removes possible noise or disturbances caused by non-relevant sources. Sampling frequency F_s defines the resolution of a signal. Sampling frequency demonstrates how many samples are recorded per second:

$$F_s = 1/T, \tag{1}$$

where T is the time interval between recorded measurements. Figure 8 shows a discrete signal with a sampling frequency of 1000 Hz. The signal describes one sinusoidal pulse ($2\Pi t$). The number of samples in the signal is 1000 (left side of Figure 8) and its duration is one second (right side of Figure 8).

To completely reconstruct a continuous signal, the sampling frequency of a signal must be at least two times the highest frequency component in the signal (Nyquist, 1928). If the sampling frequency of the signal is less than prerequisite set by Nyquist, aliasing will occur, which is a process that causes high frequency components of a signal to be indistinguishable (Gonzalez and Woods, 2008).

The unit impulse (on the left in Figure 9) is the response of the unit sample function in the discrete systems. The unit sample function is:

$$\delta(n) = \begin{cases} 1, & \text{when n = 0,} \\ 0, & \text{when n} \neq 0. \end{cases}$$

Any discrete sequence can represent translated and weighted series of unit samples:

$$x(n) = \sum_{n=-\infty}^{\infty} x(k)\delta(n-k), \tag{2}$$

where $k \in \mathbb{Z}$ and $x(k)$ is the k^{th} sample of the input sequence.

The input of the linear (discrete) time invariant system (LTI) is the unit impulse $\delta(n)$ and the output is the impulse response $h(n)$ (on the right in Figure 9). If the impulse response of the LTI-system is known then all the other responses can be calculated (Mitra, 2005).

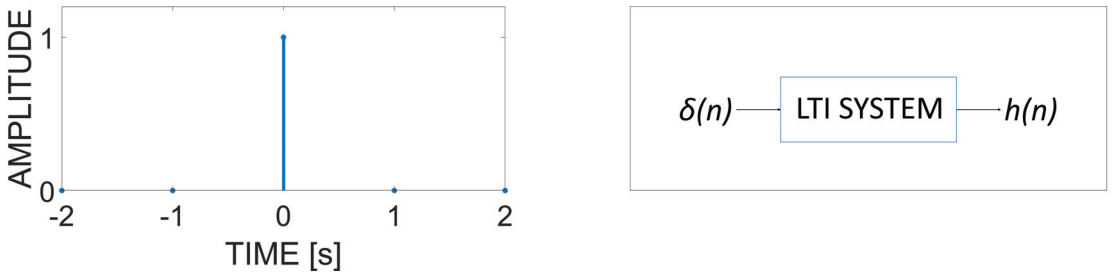

FIGURE 9 Unit impulse $\delta(n)$ (left). LTI system output, impulse response $h(n)$ (right).

The impulse response of a system is utilized by convolution. The impulse response of the discrete system can be determined from its impulses. The response to the input signal is the sum of all impulse responses:

$$x(n) = \sum_{n=-\infty}^{\infty} x(k)h(n-k) : x(n) * h(n) \rightarrow convolution \tag{3}$$

Convolution requires that the system is additive, homogeneous, and time invariant.

3.2 Discrete Fourier Transform

The discrete-time Fourier transform (DTFT) converts the time domain signal samples to the frequency domain components. When an input signal is a non-periodic discrete signal and the result is periodic discrete signal, the transform is referred as the DTFT. In case, an input signal is a periodic discrete signal and the result is periodic discrete signal, the transform is referred as the discrete Fourier transform (DFT). The result of the DFT, $X(\omega)$, is a complex-valued function of frequency. The DFT is the set of samples N of taken at frequencies spaced by ω_{fs}/N in the Nyquist band (Tretter, 2008). The DFT of signal $x(n)$ is (Mitra, 2005):

The discrete-time Fourier transform (DTFT) converts the time domain signal samples into the frequency domain components. When an input signal is a non-periodic discrete signal and the result is a periodic discrete signal, the transform is referred to as the DTFT. In cases where an input signal is a periodic discrete signal and the result is periodic discrete signal, the transform is referred to as a discrete Fourier transform (DFT). The result of the DFT, $X(\omega)$, is a complex-valued function of frequency. The DFT is the set of samples N of taken at frequencies spaced by ω_{fs}/N in the Nyquist band (Tretter, 2008). The DFT of signal $x(n)$ is (Mitra, 2005):

$$X(k) = \frac{1}{N}\sum_{n=0}^{N-1} x(n) W_N^{-kn}, \tag{4}$$

where $k = (0, 1, .., N-1)$, N is the length of the fundamental period, W_N is the n'th root of unity, i is the imaginary unit and n is the sample index of the signal. Using the Euler formula, W_N can be presented:

$$W_N = e^{\left(\frac{2\Pi i}{N}\right)} = cos\Big(\frac{2\Pi kn}{N}\Big) - i \cdot sin\Big(\frac{2\Pi kn}{N}\Big), \tag{5}$$

where *sin* and *cos* functions are referred to as the basis functions. Replacing W_n with Euler's representation, the DFT becomes:

$$X(k) = \frac{1}{N}\sum_{n=0}^{N-1} x(n)\Big[cos\Big(\frac{2\Pi kn}{N}\Big) - i \cdot sin\Big(\frac{2\Pi kn}{N}\Big)\Big]. \tag{6}$$

The inverse discrete Fourier transform (IDFT) is given by (Mitra, 2005):

$$X(k) = \frac{1}{N}\sum_{n=0}^{N-1} x(n) W_N^{kn}. \tag{7}$$

Both the DFT and the IDFT can be represented in the matrix form. The DFT operation for the sequence becomes a multiplication operation between a matrix and a vector. The transformation matrix is called the DFT matrix, W:

$$\begin{bmatrix} 1 & 1 & 1 & \dots & 1 \\ 1 & \omega & \omega^2 & \dots & \omega^{(N-1)} \\ \vdots & \vdots & \vdots & \ddots & \vdots \\ 1 & \omega^{N-1} & \omega^{2(N-1)} & \dots & \omega^{(N-1)(N-1)} \end{bmatrix},$$

where $\omega = \frac{2\Pi i}{N}$.

3.2.1 Fast Fourier Transform

The Fast Fourier transform (FFT) is an efficient algorithm to calculate the DFT. The FFT factorizes the DFT matrix into a product of sparce factors. Algorithm complexity of the FFT is $Nlog_2N$ and N^2 for the DTFT. N depends on the number of points that is $N = 2^p$; e.g. if p = 10 then $N^2 = 1048576$ and $Nlog_2N = 10240$.

FFT algorithms apply two main strategies for factorization; decimation in time (DIT) and decimation in frequency (DIF). The DIT strategy divides the summation operation of the DFT into sums over the odd and even indexes of a signal.

$$X(k) = \sum_{m=0}^{\frac{N}{2}-1} x_{2m} e^{-\frac{2\Pi i}{N}(2m)k} + \sum_{m=0}^{\frac{N}{2}-1} x_{2m+1} e^{-\frac{2\Pi i}{N}(2m+1)k}, \tag{8}$$

where $2m$ refers to sums of the even-numbered indexes and $2m + 1$ to sums of the odd-numbered indexes.

A pair-wise computation of these operations is called a FFT butterly (Figure 10). The Cooley-Tukey algorithm is a popular FFT algorithm that uses the DIT strategy (Cooley and Tukey, 1965). There are several Cooley-Tukey algorithm derivatives such as radix-2, radix-4, radix-8 and split-radix (Ghissoni et al., 2010).

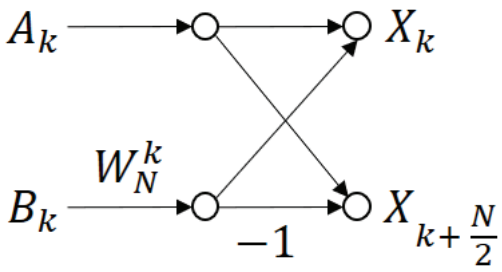

FIGURE 10 FFT butterfly describes a pair-wise computation of the FFT algorithm.

3.2.2 Amplitude and power spectrum

The DFT results a complex number representation of an input in frequency domain. Amplitude and power spectra are a convenient ways to plot spectral intensities versus frequencies. The definitions for the amplitude spectrum A_k and the power spectrum P_k (Tan, 2008):

$$A_k = \frac{1}{N}|X(k)| = \frac{1}{N}\sqrt{X(k)^2_{REAL} + X(k)^2_{IMAG}}, \tag{9}$$

$$P_k = \frac{1}{N^2}|X(k)|^2 = \frac{1}{N^2}X(k)^2_{REAL} + X(k)^2_{IMAG}, \tag{10}$$

where $X(k)_{REAL}$ is the real part of the DFT and $X(k)_{IMAG}$ is the imaginary part of the DFT. The frequency resolution for the spectra is $f_{res} = \frac{f_s}{N}$.

Spectral leakage is an unwanted phenomenon that occurs because of the convolution operation that creates new frequency components on spectrum calculations (Tan, 2008). The windowing is used to reduce the spectral leakage in the DFT. However, the windowing might increase the spectral leakage on some sections of the spectral and decrease it on other sections (Harris, 1978).

3.2.3 Short-time Fourier transform

The short-time Fourier transform (STFT) is a piece-wise transform that calculates the sinusoidal frequency and phase content of the local sections of a signal. The discrete time STFT is defined (Gröchenig, 2001):

$$STFT(k,\omega) = \sum_{n \in Z} w[n-k]x[n]e^{-jnT\omega}, \tag{11}$$

where w is the window function, $k = mN/2$ for even N and $k = m(N-1)/2$ for odd N, with N as the length of a signal and $m \in Z$. An example of the window function is the Hanning window $w[n] = sin^2(\Pi(n-1)/N)$, where $n = 1, .., N$.

3.3 Modulation and demodulation

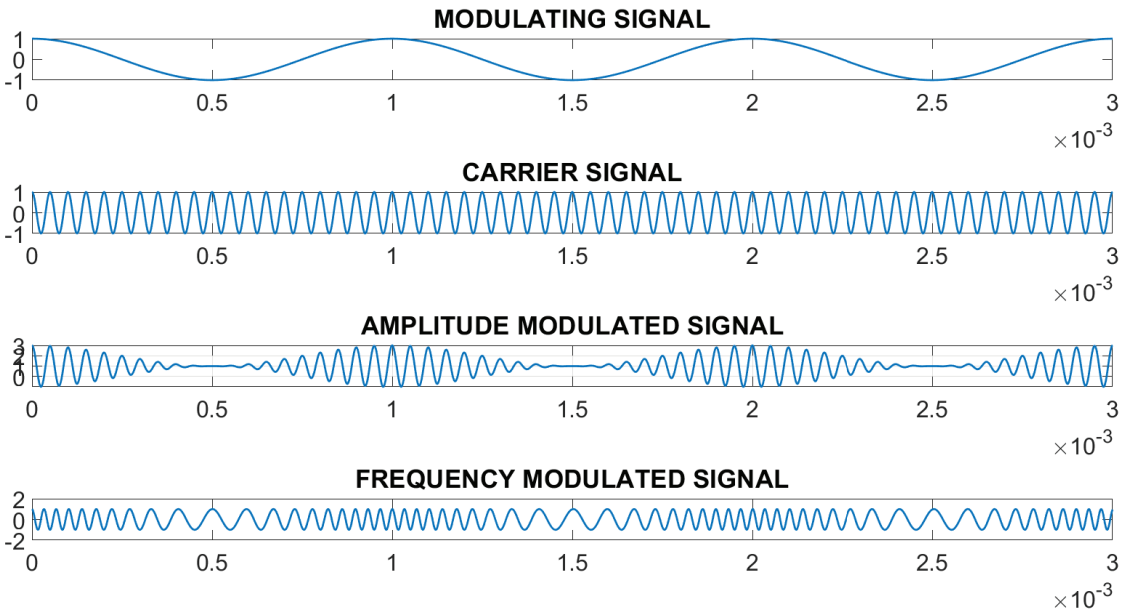

FIGURE 11 Examples of amplitude and frequency modulation.

Modulation is a notable process in telecommunications and digital signal processing. Modulation is a process which combines a waveform signal, called a modulating signal, into another waveform signal, called a carrier wave. The transmission properties of the carrier wave are significantly better than the modulating signal. Signal waveforms can be modulated by either amplitude or frequency. Amplitude modulation linearly transforms the amplitude of the carrier

wave. In the frequency modulation, the frequency or phase angle of the carrier wave is modulated. Figure 11 shows examples of amplitude- and frequency-modulated signals. The modulating signal is combination of two sinusoidal pulses (at the top of Figure 11). The frequency of the carrier signal is 20 Hz in the frequency modulation.

Demodulation is the opposite operation of modulation. Several techniques can be used for amplitude demodulation, including square-law demodulation (Tretter, 2008), envelope demodulation with Hilbert transform (Tretter, 2008; Feldman, 2011), and coherent demodulation (Grami, 2019). Frequency demodulation techniques include zero-crossing demodulation (Carlson, 1975) and quadrature demodulation (Gallager, 2008).

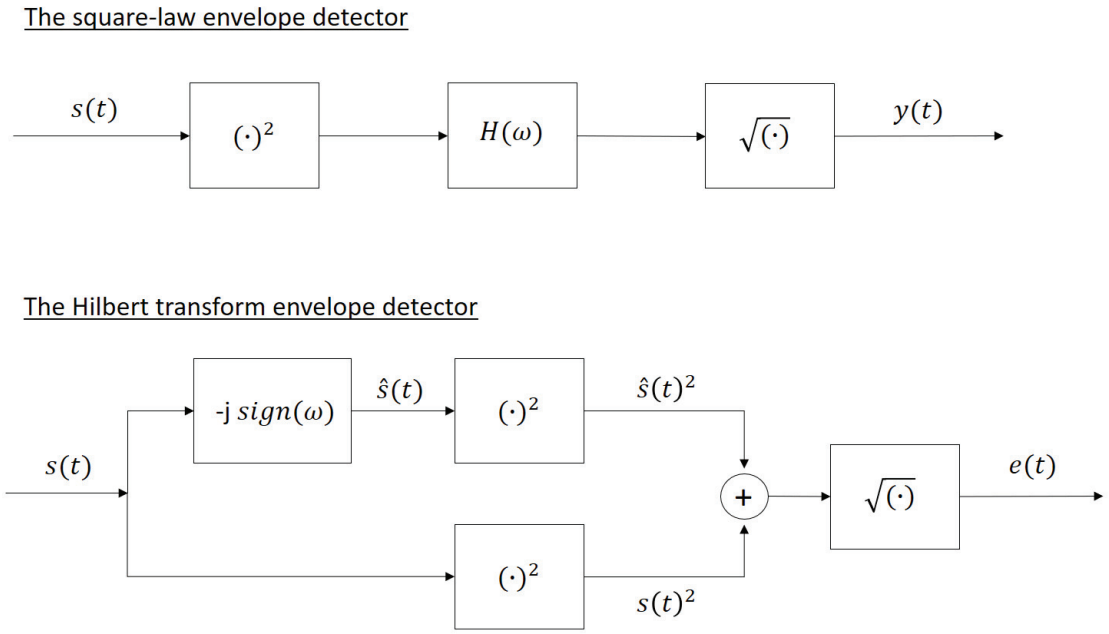

FIGURE 12 The square law and the Hilbert transform envelope detectors.

The square-law demodulation includes successive operations: the squaring operation, lowpass filtering and square-root operation (upper portion of Figure 12). The definition for the input (transmitted) signal $s(t)$:

$$s(t) = A_c[1 + k_a m(t)]cos(\omega_c t), \tag{12}$$

where $m(t)$ is the modulation signal (lowpass baseband), A_c is the amplitude, and ω_c is the angular frequency of the carrier wave. The sampling rate of the input signal $s(t)$ must be at least $4(\omega + W)$ to prevent aliasing and the lowpass filter $H(\omega)$ must operate on samples of $s^2(t)$ taken at rate $4(\omega + W)$ (Tretter, 2008). W is the cut-off frequency of the modulation signal.

The Hilbert transform has been used in vibration analysis more than 30 years (Feldman, 2011). What follows is the definition for the Hilbert transform in time domain:

$$\hat{x}(t) = x(t) * \frac{1}{\pi t} = \frac{1}{\pi}\int_{-\infty}^{\infty} \frac{x(\tau)}{t-\tau} d\tau, \tag{13}$$

where * is the convolution operator. In other words, when a signal is passed through a filter with impulse response $\frac{1}{\pi t}$, the Hilbert transform has been applied on the signal. The Hilbert transform is a linear operation that shifts the phase angle by 90° in the frequency domain. The operations of the Hilbert transform envelope detector are shown in Figure 12. The definition of the input signal was defined in the equation 12.

3.4 Wavelet Transforms

The wavelet transform enables multi-resolution analysis with dilated windows. The wavelet transform is a constant relative bandwidth analysis (Kovacevic and Vetterli, 1995). Using dilation and translation, the wavelet transform can efficiently extract the time-frequency features of a signal (Kumar et al., 2013). It is an excellent tool for the analysis of non-stationary signals. The frequency resolution increases and the time resolution decreases when the wavelet transform is done at sequentially wide scales. Like Fourier transforms, the wavelet-transform concludes the basis-function called mother wavelet.

3.4.1 Continuous wavelet transform

The continuous wavelet transform (CWT) transforms signal to a two-dimensional time-scale joint representation. The idea of the CWT is to continuously calculate scalable function by moving this function continuously over a signal. As result, the wavelet coefficients are acquired. However, the bases of the scalable functions become non-orthogonal, which makes wavelet coefficients redundant (Sheng, 2000). The definition of the CWT as the function of time is:

$$T(a,b) = \int_{-\infty}^{\infty} f(t)\psi^{*}_{(a,b)}(t)dt, \tag{14}$$

where ψ is the mother wavelet and * refers to complex conjugation. The mother wavelet is:

$$\psi_{(a,b)}(t) = \frac{1}{\sqrt{a}}\Big(\frac{t-b}{a}\Big), \tag{15}$$

where a is the scaling (dilation) parameter, and b if the translation parameter. The parameter a controls the window length and affects the frequency resolution; large a for better frequency resolution.

3.4.2 Discrete wavelet transform

The time-scale joint representation of a discrete wavelet transform (DWT) is a grid along the scale and time axes. The discrete wavelet is a piecewise continuous function. The discretisation of the wavelet is done by sampling the time-scale axis at discrete intervals. Usually, dyadic sampling is used with a geometric sequence

of ratio two. The DWT as a function of time is:

$$\psi_{(i,j)}(t) = \frac{1}{\sqrt{2^i}}\left(\frac{t - 2^i j}{2^i}\right), \tag{16}$$

where the dilation term is 2^i and the translation term is $2^i j$.

The DWT can be represented in sequences of high- and low-pass filters, as shown in Figure 13 (Vetterli and Herley, 1992), where g[n] is the low-pass filter and h[n] is the high-pass filter.

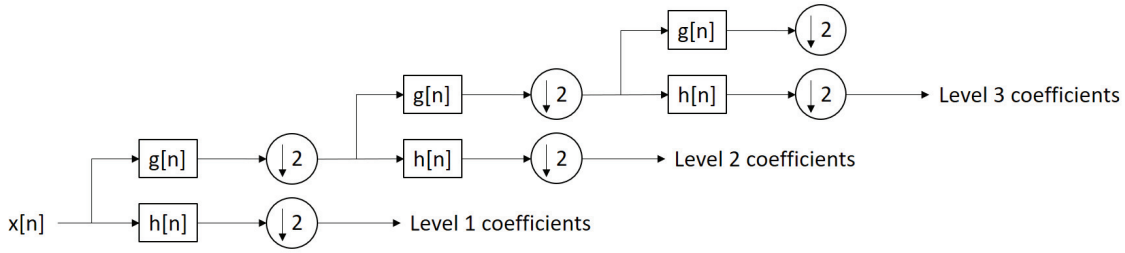

FIGURE 13 The DWT as sequences.

3.5 Digital Filters

3.5.1 Finite impulse response filters

The impulse response of the finite impulse response (FIR) filter has finite length. Convolution with impulse response of the FIR filter removes desired frequencies from the signal: The impulse response of the finite impulse response (FIR) filter has finite length. Convolution with the impulse response of the FIR filter removes desired frequencies from the signal, as:

$$y(n) = \sum_{k=0}^{N} h[k]x[n-k], \tag{17}$$

where h is the impulse response of the FIR filter, x is the original signal, and y is the filtered signal (Mitra, 2005).

An FIR filter is defined based on requirements of a filter's phase and amplitude responses. Phase responses are usually linear and amplitude responses are specified for pass-, transition- and stop bands. The basic idea of a FIR filter design is to find appropriate coefficients and determine an accurate filter order. A common technique is the FIR convolution that is a cross-correlation between the original signal and the impulse response of the pulse shape that is to be filtered (Oppenheim et al., 1983). A moving average filter is a simple FIR filter.

3.5.2 Infinite impulse response filters

The impulse response of the infinite impulse response (IIR) filter has an infinite length. The general form of the IIR filter is:

$$Y(e^i\omega) = H(e^i\omega)X(e^i\omega), \tag{18}$$

where $H(e^i\omega)$ is the frequency response of the filter. In practice, the IIR filter is implemented in terms of the difference equation:

$$y(n) = \sum_{k=0}^{K} a_k x(n-k) + \sum_{m=0}^{M} b_m y(n-m), \tag{19}$$

where m, a_k and b_m are the IIR coefficients (Mitra, 2005).

Butterworth, Chebyshev, Bessel, and elliptic filters are different types of IIR filters. Compared to FIR filters, IIR filters require fewer calculations and memory and they perform better from narrow transition bands (Mitra, 2005). However, FIR filters are easier to implement to linear phases and to match the desired frequency response (Mitra, 2005).

3.5.3 Wavelet filter banks

The construction of wavelet filter banks concludes the analysis and synthesis functions that perform the composition of the original spectrum using sub-spectral components. The wavelet transform is orthogonal when the analysis and synthesis function sets are the same. For the biorthogonal transform, these function sets are different. A common technique for computing wavelet transforms is to use two-channel perfect reconstruction (PR) filter banks: a low-pass filter $g(z)$ and high-pass filter $h(z)$ form an analysis filter bank and a low-pass filter $H0(z)$ and high-pass filter $H1(z)$ form a synthesis filter bank (Figure 14).

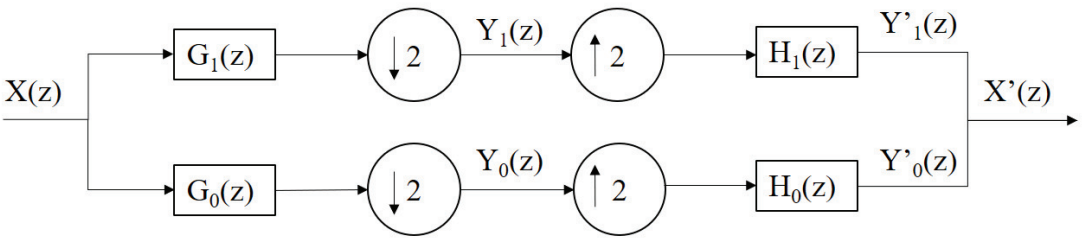

FIGURE 14 Two-channel wavelet filter bank.

4 VIBRATION ANALYSIS OF ROLLING ELEMENT BEARINGS

Vibration analysis is a key technique in the condition monitoring of REBs. Vibration analysis of REBs exploits different (digital) signal processing methods. Vibration measurements do not provide direct information regarding the health of REB, and, therefore, feature extraction is necessary. This implies different applications of signal processing methods. The sensitivity of vibration signals to disturbances makes the task more difficult. Features of vibration signals can be separated into six categories: i) time-domain features; ii) frequency-domain features; iii) time-frequency-domain features; iv) phase-space dissimilarity measurements; v) complexity measurements; vi) other features (Caesarendra and Tjahjowidodo, 2017).

Recently, Rai et al. (Rai and Upadhyay, 2016) reviewed signal processing methods utilized in the fault diagnosis of REBs and the methods were ordered in the chronological stages:

I Time domain methods (statistical moments, autoregressive model, etc.), time-frequency domain methods (DWTs), bispectral and power density methods, adaptive noise canceling, envelope analysis.

II Autoregressive model (improvements), bispectral analysis, wavelet transform, matching pursuit, cyclostationary methods, spectral kurtosis and kurtogram, entropy, morphological feature extration methods, empirical mode decomposition.

III Spectral kurtosis and kurtogram (improvements), cyclostationary methods, wavelet based approaches, empirical mode decomposition (improvements), morphological signal processing, matching pursuit order tracking, data reduction tools, cepstral analysis.

A variety of signal processing methods have been developed for the vibration analysis of REBs. The selection of a suitable technique depends on the bearing application in question. In some cases, the required techniques may be rather simple. However, the detection of incipient bearing faults requires more advanced

techniques, especially in environments where other sources create disturbing vibrations. The vibration analysis methods used in this research are presented in this chapter.

4.1 Vibrations generated by rolling element bearings

Randall (2008) defined a taxonomy for different signal types:

- stationary and non-stationary
- stationary → random and deterministic
- deterministic → periodic and quasi-periodic
- non-stationary → continuous and transient
- continuous → continuously varying and cyclostationary

Cyclostationary processes are non-stationary processes whose statistics are periodically varying (Antoni, 2006). Vibration signals generated by REBs can be modelled as pseudo-cyclostationary (Randall and Antoni, 2011). The term "pseudo" refers to the randomness by caused by jitter. The terms "quasi-cyclostationary" and "pseudo-quasi-cyclostationary" have also been used in research publications (Antoni et al., 2004; Estupiñan et al., 2007).

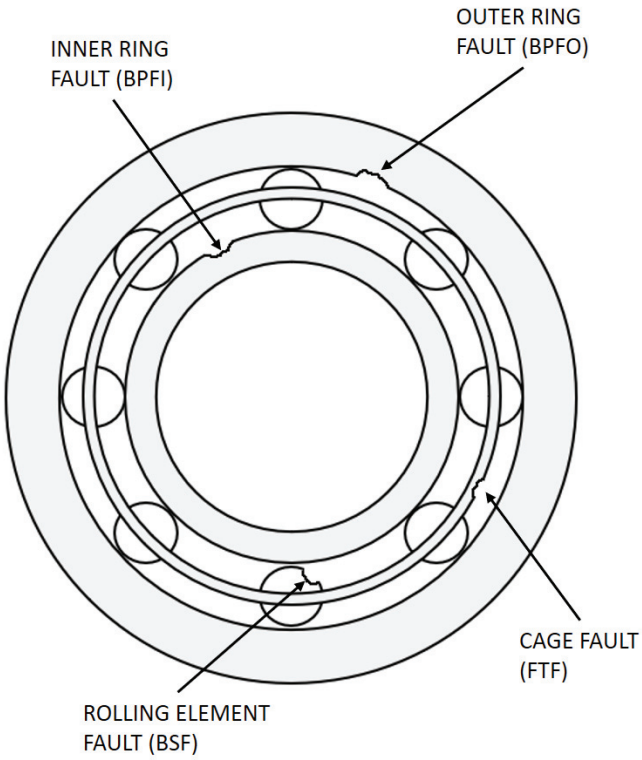

FIGURE 15 Local faults of REB.

The vibrations generated by REBs include the vibrations of the raceway rings, the vibrations of the cages, rolling element passage vibrations, vibrations

due to the surface waviness on the inner and outer raceways, vibrations generated by flaws, vibrations due to contamination, and seal vibrations (Momono and Noda, 1999). Other than flaw vibrations, the presented vibrations of the REBs can be considered normal. Bearing fault signals, which include flaw vibrations, have a deterministic part and a stochastic part. The stochastic part is pseudo-cyclostationary and is very often small because of the low-pass filtering effect of random jitter, combined with the band-pass filtering effect of resonances that are excited (Randall et al., 2001). The spacing between these impulses usually varies between 1-2% due to slippage resulting from the variation of the load angle of the rolling element (Barszcz and Sawalhi, 2012).

4.2 Local faults in REBs

Local faults occur in the different parts of REBs: the inner race, outer race, rolling elements and cage. Figure 15 shows common local faults. The resonances of the bearing parts and housing structure emerge when a rolling element strikes a localized defect, and an exponentially decaying ringing is generated (Tandon and Choudhury, 1999; Kiral and Karagülle, 2003). Vibrations in the 2–20 kHz range, are commonly measured by acceleration sensors. Ultrasound and acoustic emission measurements cover considerably higher frequencies.

When a defective part of a bearing hits other elements of the bearing, a series of impacts will occur at a rate dependent on the bearing's geometry. The impacts appear periodically in time, if the shaft is rotating at a constant speed. Each part of an REB has its own frequency of occurrence based on the geometric dimension of the REB. These frequencies are called the characteristics fault (defect) frequencies of the REB and include the outer race (the ball pass frequency of the outer race [BPFO]), the inner race (the ball pass frequency of the inner race [BPFI]), the ball or roller (the ball spin frequency [BSF]), and the gage (the fundamental train frequency [FTF]) (Randall and Antoni, 2011). Table 1 lists the characteristic fault frequencies and the corresponding equations, where N_b is the number of rolling elements, B_d is the diameter of the rolling element, P_d is the pitch diameter, and $RotSpeed$ refers to the shaft rotation speed.

Many research studies exploit simulation models of bearing faults. McFadden and Smith (1984) introduced an impulse model of a single fault that considers the load distribution and moving location of impacts:

$$f(t) = \int_{i=-\infty}^{\infty} \delta(t - iT)P(\theta), \tag{20}$$

where δ is the impulse function, T is the time between consecutive impacts, θ is the angle of rotation, and P is the load distribution function.

Since then, new impulse models for faulty bearing have been proposed. The results of these studies have added multiple faults, random fluctuations, the effect of surface roughness, and the effect of multiple interferences (McFadden and Smith, 1985; Ho and Randall, 2000; Rohani and Mba, 2011; Liang and Faghidi,

TABLE 1 Characteristic fault frequencies of REBs.

Fault type	Equation
BPFI	$\frac{N_b}{2}\left(1+\frac{B_d}{P_d}cos\theta\right)*RotSpeed$
BPFO	$\frac{N_b}{2}\left(1-\frac{B_d}{P_d}cos\theta\right)*RotSpeed$
BSF	$\frac{P_d}{2B_d}\left(1-\left(\frac{B_d}{P_d}cos\theta\right)^2\right)*RotSpeed$
CAGE	$\frac{1}{2}\left(1-\frac{B_d}{P_d}\right)*RotSpeed$

2014). The bearing impulse model used in this research was presented by Liang and Faghidi (2014) with modulation terms for shaft rotation and random jitter added as follows:

$$r(t) = Asin(\omega_{rot}t)e^{-\beta\tau}cos(\omega_{res}t+\varphi)+\sum_{k=1}^{K}L_k cos(\omega t), \tag{21}$$

where A is the amplitude of the vibration signal, ω_{rot} is the rotation frequency, β is the structural damping characteristic, ω_{res} is the frequency of the exited resonance, φ is the phase angle, and L_k is the frequency of the k^{th} interference component.

The spectrum of a modulated signal contains sidebands spaced at the modulation frequency (Randall, 2010). The passage of the local fault through the load zone or a varying transmission path between the impact point and the vibration measurement point can result amplitude modulation of impulses responses (Ho and Randall, 2000). The spectrum of such a signal would consist of a harmonic series of frequency components spaced at the bearing defect frequency with the highest amplitude around the resonant frequency (Figure 16).

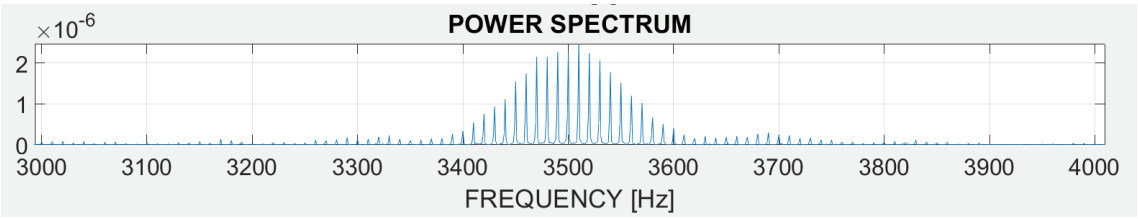

FIGURE 16 Modulation sidebands (10 Hz) at the resonant frequency (3500 Hz).

4.3 Envelope analysis

Envelope analysis, also known "high frequency" resonance technique, is used to resolve the amplitude modulation of vibration signals. The impulses generated by bearing faults excite "high frequency resonances" and the resulting signal appears as a sequence of transient and impulsive vibrations (Gao et al., 1998). The characteristic frequencies of these impulses can be detected from the envelope spectrum of a vibration signal. The resonances excited by an incipient bearing fault exists in higher frequencies than the resonances excited by a grown bearing fault. Figure 17 presents the simulated vibration signal of a faulty bearing and the power spectrum and envelope spectrum of the signal. The repetition rate of the fault pulse is 10 Hz, and the resonant frequency of the pulse is 3500 Hz. White noise was added to the signal (SNR = 1.5) and no random fluctuations were present. Resonant frequency is seen in the power spectrum. The fundamental frequency of the fault pulse and its harmonics are present in the envelope spectrum. The harmonics are integer multiples of the fundamental frequency.

The vibration signals of REBs acquired from real machinery are most likely affected by other machine components that interfere with vibration analyses. Deterministic vibrations generated by gears, shafts, and motors affect the measured signal (Borghesani et al., 2013). It is common that "low frequency" components are filtered out using a high-pass filter or a band-pass filter if resonances are expected to appear in certain frequency area. However, these filtering techniques are quite simple, and more sophisticated methods are needed for vibration signals that contain multiple interferences.

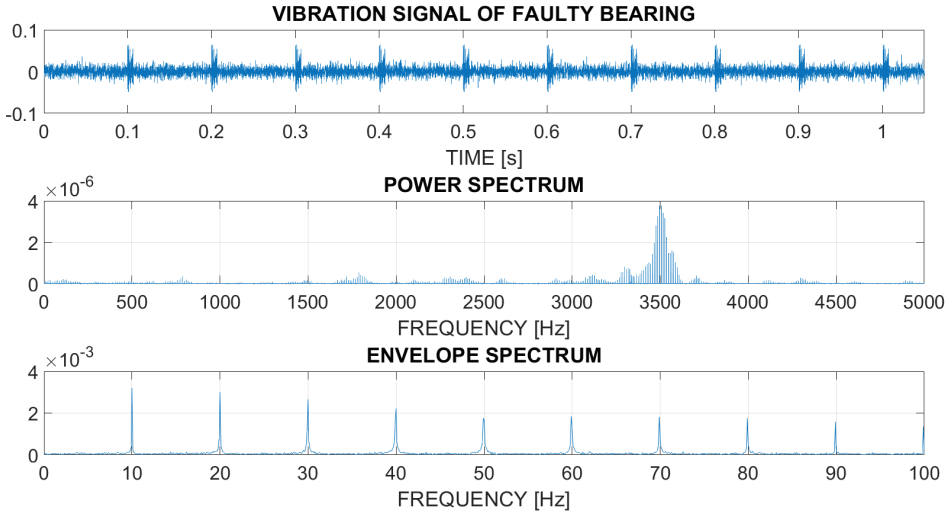

FIGURE 17 Envelope analysis of faulty bearing signals.

4.4 Cepstrum pre-whitening

Cepstrum analysis is a non-linear signal processing technique. The real cepstrum is defined as the IDFT (Eq.7) of the logarithm of the DFT (Eq.4) of a signal (Bogert et al., 1963):

$$CEPSTRUM_{REAL} = \left| IDFT\big(\log(|DFT(X)|)\big) \right|. \tag{22}$$

The shaft harmonics of a vibration signal are the periodical and deterministic excitations that produce a spectrum with multiple harmonics of the first excitation frequency (Borghesani et al., 2013). The peak amplitudes of the real cepstrum correspond to the multiple harmonics of the vibration signal. The definition for the cepstrum pre-whitening is as follows:

$$X_{CPW} = IDFT \frac{DFT(X)}{|IDFT(X)|}. \tag{23}$$

The cepstrum pre-whitening performs the following steps: 1) the real cepstrum is set to zero, 2) transformation to the frequency domain, 3) recombination with the original phase, 4) inverse transformation to the time domain. Pre-whitening removes the deterministic excitations and resonance effects from the signal (Borghesani et al., 2013).

4.5 Spectral kurtogram

The spectral kurtosis (SK), the frequency domain kurtosis, is a powerful tool to reveal the non-Gaussian components of a signal in the frequency domain (Dwyer, 1983). The SK represents a kurtosis at each frequency line in order to discover the presence of hidden non-stationarity properties and to indicate in which frequency bands these occur (Antoni, 2007). The SK is calculated by using the STFT (Eq.11) (Antoni, 2006):

$$SK = \frac{\langle |STFT(k,\omega)|^4 \rangle}{\langle |STFT(k,\omega)|^2 \rangle} - 2, \tag{24}$$

where $\langle . \rangle$ is the time-average operator.

Antoni and Randall (2006) presented the concept of the kurtogram. The kurtogram displays the SK as a function of frequency and of spectral resolution. The kurtogram can reveal, for example, the resonant frequencies of a REB fault. Hence, the kurtogram can be used as a basis for a band-pass filter design. Further, Antoni (2007) developed an algorithm to reduce the computational complexity of the kurtogram calculation. Figure 18 shows a kurtogram of the simulated vibration signal presented in Figure 17. Enhancements of the kurtogram have been proposed, including an adaptive SK and the protrugram (Wang et al., 2016).

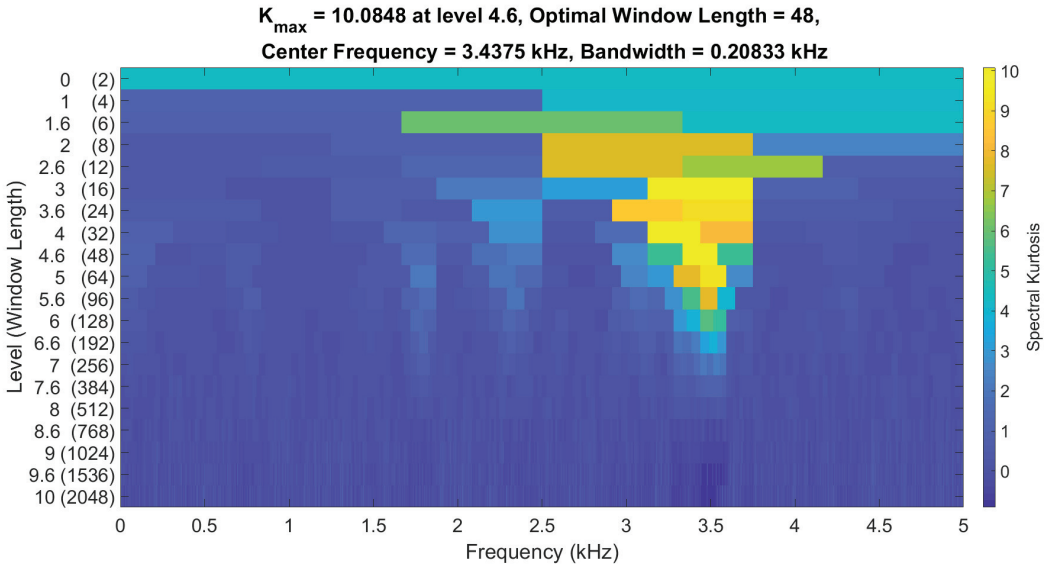

FIGURE 18 The fast kurtogram of a vibration signal of a faulty bearing.

4.6 Wavelet analysis

The wavelet transform has been used for signal demodulation and optimal bandpass filter design (Qiu et al., 2006). The wavelet transform has also been successfully applied for bearing fault detection (Prabhakar et al., 2002; Seker and Ayaz, 2003; Luo et al., 2003a; Lou and Loparo, 2004). Fault features extracted by wavelet transform can be based on wavelet coefficients, wavelet energy, singularity based, and wavelet function (Peng and Chu, 2004). However, there is no standard method to select the wavelet function for a specific purpose; as such, the wavelets do not have a standard status in fault diagnostics (Peng and Chu, 2004). Breakdown points, trends, and discontinuities in higher derivatives are detectable by using wavelet analysis (Kumar et al., 2013).

Tse and Wang (2011) introduced the sparsogram, which uses the binary wavelet packet transform for signal decomposition and the sparsity measure of the decomposition levels for bearing fault detection. Later, the sparsogram was expanded for the optimization of the Morlet wavelet filter Tse and Wang (2013). Complex frequency B-spline wavelets (CFBSW) have been used for bearing fault detection by adjusting the wavelet to correspond to the fault pulse (Paliwal et al., 2014).

The newest enhancements to the wavelet transform is empirical wavelet transform (EWT) which decomposes a signal based on the segmentation of the Fourier spectrum (Kedadouche et al., 2016). The EWT extracts different modes of a signal, and the resulting modes are applied to construct a wavelet filter bank (Gilles, 2013).

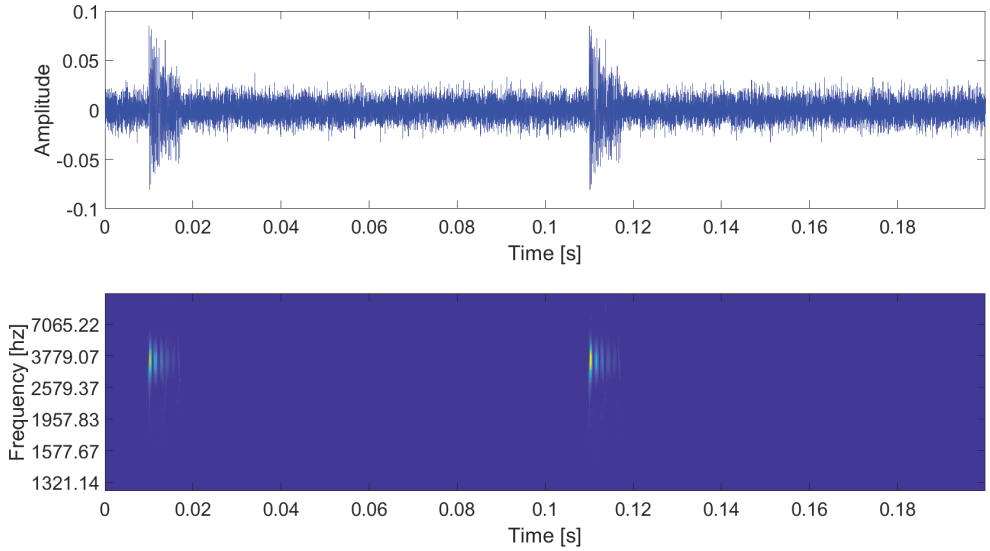

FIGURE 19 CWT analysis of a vibration signal of a faulty bearing.

4.7 Other popular techniques for vibration analysis

Time synchronous averaging (TSA) can be used to remove discrete frequency components with the minimal disruption of the residual signal (Randall and Antoni, 2011). The removal of harmonics requires resampling, which is achieved with the synchorization of a signal using order tracking (Randall and Antoni, 2011). Order tracking involves sampling a signal at constant increments of the shaft angle (Fyfe and Munck, 1997). Usually, the phase information of the shaft is acquired using a tachometer. Later, a tachometer-less TSA approach was proposed (Siegel et al., 2012).

Adaptive noise cancellation (ANC) can be used to separate two uncorrelated components from a signal. The idea is to find a linear transfer function that can be applied to a chosen reference part of the original signal (Randall, 2010). When the result is subtracted from the original signal, the uncorrelated components are separated. Self-adaptive noise cancellation (SANC), an extension of the ANC, exploits the delayed version of the original signal as another signal in the process (Randall, 2010). The SANC expects that another component is deterministic and that yet another is random.

Empirical mode decomposition (EMD) enables analysis nonlinear and nonstationary properties of a signal. Empirical mode decomposition (EMD) splits a signal into intrinsic mode functions (IMF) (Huang et al., 1998). Compared to wavelet decomposition, EMD does not require a predefined basis for the signal, which makes it adaptive-like (Peng et al., 2005). The Hilbert-Huang transform (HHT) combines of the EMD and the Hilbert spectral analysis. The Hilbert spectrum reveals instantaneous frequencies of IMFs. The HHT is popular in bearing diagnostics (Yu et al., 2005; Yang et al., 2007; Zhao et al., 2013).

Bispectrum analysis involves higher order spectra (Nikias and Mendel, 1993).

It analysis has been shown to detect the modulation phenomena and the type of the defects better than Fourier analysis in bearing diagnostics (Yiakopoulos and Antoniadis, 2005; Alwodai et al., 2013; Rehab et al., 2014).

5 MACHINE LEARNING

Machine and deep learning methods have increasing been applied in bearing fault diagnosis (Zhang et al., 2019; Hoang and Kang, 2019). However, the generalization of these methods has been cumbersome. The biggest weakness of deep learning methods is the selection of hyper-parameters, which is done with time-consuming "trial and error" principle (Hoang and Kang, 2019). Many research studies on the fault diagnostics of REBs, use traditional black-box classifiers such as the k-nearest-neighbor (k-NN) and the support vector machines (SVM) (Wang et al., 2014a; Baraldi et al., 2016a; Tian et al., 2016; Gryllias and Antoniadis, 2012; Zhang et al., 2013; Du et al., 2014; Wen et al., 2015a; Saidi et al., 2015; Li et al., 2016a,b; Saari et al., 2019). The basic idea is to train classifiers with features of vibration signals whose health state is known. Further, classifiers are used to classify features of new vibration signals to diagnose the health state of REBs.

Usually, a number of fault samples in condition monitoring domain is limited. Instance-based classifiers do not require a large number of training samples to be accurate (Yang et al., 2005; Gryllias and Antoniadis, 2012), unlike deep learning methods. The machine learning methods used in this research are introduced in the following sections of this chapter.

5.1 On feature engineering

Features are inputs in a model in data-driven approaches. Feature extraction refers to cases where a new, smaller-dimensional set of features is created from an original set (e.g. by transform). The process of selecting a subset of relevant features is called feature selection or variable selection. The removal of redundant or irrelevant features should not cause a loss of information. The objectives of feature selection can be three-fold (Guyon and Elisseeff, 2003; Moradi and Rostami, 2015): to improve the performance of the model (classifiers), to provide faster and more cost-effective models than using all the available features, and to improve understanding of the data generation process.

John et al. (1994); Kohavi and John (1997) proposed the division of a set of features into irrelevant, weakly relevant, and strongly relevant. In (Zare and Niazi, 2016), the category of weakly relevant features was further divided into redundant and non-redundant features. The identification of such a division is a search problem, and many techniques and approaches exist for this purpose, for example, exhaustive searching, branch-and-bound-algorithms, evolutionary approaches etc. (see, e.g., (Miller, 1990; Liu and Motoda, 1998; Huang et al., 2008; Liang et al., 2017)). A forward search involves adding new features one-by-one or group-by-group to the model, whereas backward elimination refers to the removal of individual or sets of features during the search process.

The intrinsic assumption behind feature selection is that there is some redundancy among the features. Liu et al. (Liu and Motoda, 1998) divided feature selection criteria measuring the redundancy into five groups: information measures, distance measures, dependency measures, consistency measures, and accuracy measures. Depending on the constituents present when constructing a criterion, two basic approaches for feature selection can be used: the filter approach and the wrapper approach (John et al., 1994).

The benefits of feature selection are as follows: i) it reduces effect of the curse of dimensionality ii) it reduces overfitting, and iii) it speeds-up training (Guyon and Elisseeff, 2003). The curse of dimensionality arises when the ratio between features and observations is high; in the k-NN classification it, results in the phenomenon that observations might have no nearby neighbors (James et al., 2013). A model with too many adjustable parameters usually leads to overfitting, which means that noise of the data is fitted (Sovilj, 2014). By selecting optimal features, the misclassification and the training time of classifiers are reduced (Hu et al., 2007). The features calculated from the vibration signals generated by REBs are usually high-dimensional and non-Gaussian, leading to a pattern recognition problems (Zhao et al., 2014). It is typical that dimensionality reduction methods, such as Principal Component Analysis, Kernel Principal Component Analysis, and Linear Discriminant Analysis are applied to vibration signal features (Zhang et al., 2013; Zhao et al., 2014; Dong and Luo, 2013).

5.2 Unsupervised learning

In the unsupervised learning, one attempts to model the structure or distribution of unlabeled input data. Clustering, the most common technique for this purpose, involves the unsupervised classification of patterns into groups (clusters) by joining together similar points (Jain et al., 1999). Over the years, many clustering approaches and algorithms have been developed, for instance, density-based, probabilistic, grid-based, and spectral clustering (Aggarwal and Reddy, 2013). However, the two most common and mostly used groups of clustering algorithms are partitional and hierarchical clustering algorithms (Jain, 2010; Zaki et al., 2014).

5.2.1 Fuzzy c-means clustering

K-means clustering is the most popular partitional type of algorithm that attempts to partition a set of data points into k number of distinct, crisp clusters. K-means clustering positions k number of centroids (prototypes), one for each cluster, and then recursively searches the best centroids based on the nearest mean. Fuzzy clustering algorithms, especially fuzzy c-means (FCM) clustering, which was originally developed by Ruspini (Ruspini, 1969), generalize the k-means by allowing data points to belong to multiple clusters. This relation is represented with a membership function.

The FCM algorithm was further developed by Dunn (1973) and Bezdek (1973). The algorithm minimizes the objective function (Bezdek, 1981):

$$J_m = \sum_{i=1}^{D} \sum_{j=1}^{N} u_{ij}^m \left\| x_i - c_j \right\|^2, \tag{25}$$

where D is the number of data points, N is the number of clusters, m is a fuzzy partition matrix exponent to control the overlap of the clusters, u_{ij} is the degree of membership of x_i in the cluster j, x_i is the i^{th} observation in the d-dimensional measurement data, c_j is the d-dimensional center of the cluster, and $\left\|*\right\|$ is the Euclidean norm measuring the similarity between the measured data and its center.

5.3 Supervised learning

Supervised learning refers to training a predictive model, or its parameters, by using a labelled data. A predictor is then used to evaluate labels for new, unseen data. Supervised learning algorithms try to approximate the mapping function between input variables and output variables. Classification and regression problems are typical supervised learning problems. Classification algorithms attempt to assign new data points to pre-defined categories. Regression algorithms attempt to predict numeric values for new data points.

5.3.1 k nearest neighbor algorithm

The k-NN classification rule was originally introduced by Cover and Hart (Cover and Hart, 1967). The k-NN rule is a sub-optimal non-parametric procedure for the assignment of a class label to an input pattern based on the class labels represented by the k closest neighbors (Keller et al., 1985). The k-NN rule is applicable on data that is in the metric space, and it does not make assumptions regarding the distribution of data. k is the number of nearest data points used in the classification.

An example of the principle of the k-NN classifier is shown on the left side of Figure 20. A triangle is classified into a group of rectangles when k is three. When k is five, the triangle is classified into a group of stars. Euclidean distance,

used as a dissimilarity measure, satisfies the three following properties: positivity, symmetry, and triangle inequality.

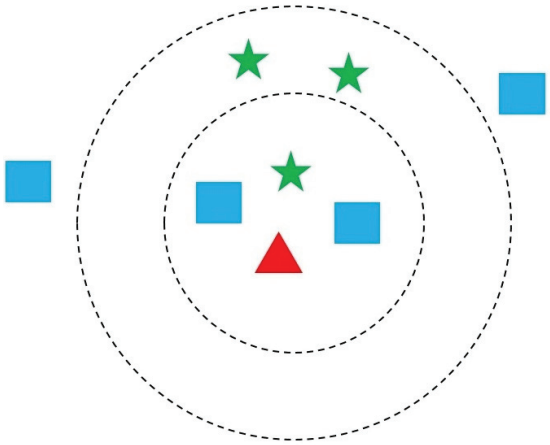

FIGURE 20 k-nearest-neighbor classification example.

The k-NN is an "instance based" learning method. Unlike inductive learning methods, instance-based learning methods do not include an explicit description of the target function (Mitchell, 1997). Instance-based learning approximates real-valued or discrete-valued target functions (Mitchell, 1997). The k-NN trains the examples and finds the k-NN of the new instance (test sample) (Wagh et al., 2012). The k-NN classifier algorithm for each test example $y \in Y$:

1. Compute the distance $r(y, x)$ between y and each training example $(x, c) \in X$,

2. Select $X(k, y) \in X$, the set of the "k nearest" training examples to y,

3. $$Class(y) = \underset{v \in [1..C]}{\operatorname{argmax}} \sum_{(y,c) \in (k,y)} \delta_{(v,c)}, \tag{26}$$

where x is the input data, $Y = y_i, i = 1, .., N$ is the training data, and $c_j, j = 1, .., C$ is the set of predefined classes.

5.3.2 Support Vector Machine

An SVM is a supervised machine learning algorithm that can be used for both classification and regression problems. An SVM is a binary classifier that searches an optimal separating hyperplane to separate classes from each other (Vapnik, 2000). The simplest SVM classifier is the so-called hard-margin classifier, that is applicable when training data is linearly separable, meaning which the two hyperplanes clearly separate the data (Figure 17).

The definition of the separating hyperplane is $w^T + b = 0$, where w is the normal vector of the hyperplane and b is a scalar constant. The marginal hyperplanes are $w^T + b = 1$ and $w^T + b = -1$. The sample vectors on the marginal hyperplanes are called support vectors. The SVM algorithm tries to solve parameter

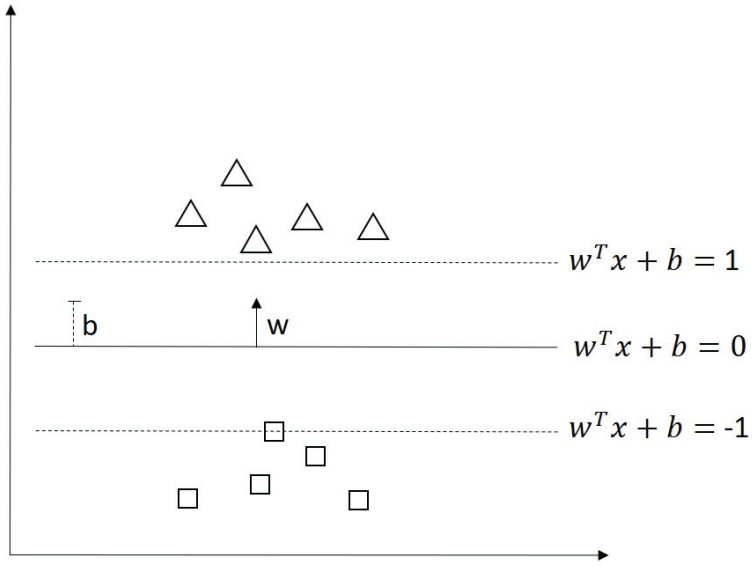

FIGURE 21 Support vector machine (principle).

w and b so that the distance between the hyperplanes is maximal. Otherwise, it minimizes the length of w so that it is orthogonal to the two hyperplanes: when $y_i = w^T x_i + b >= 1, y_i \in [-1, 1]$. Using Lagrange's method for the minimization results in the following equation: $L(w, b) = \frac{1}{2}|w| - \sum_{i=1}^{N} \alpha_i [y_i(w^T x_i + b) - 1]$, when $\alpha \geq 1$.

The classification function for unclassified feature vector x:

$$f(x) = sign\Big(\sum_{i:x_i \in SV} (y_i \alpha_i K(x_i, x) + b\Big), \tag{27}$$

where $K(x_i, x)$ refers to the "linear like" kernel. The sign of the function defines the resulting class $[-1, 1]$.

In practice, a non-linear kernel transformation is performed because the patterns are not linearly separable (Saidi et al., 2015). The nonlinearity of the SVM and the corresponding class boundaries can be obtained from the famous kernel-trick using nonlinear transformation through a high-dimensional feature space (Zaki et al., 2014). The feature vectors are transformed to Hilbert space using a non-linear transform: $x_i^T x_j \rightarrow \theta(x_i)^T \theta(x_j)$. The dot product of the transform is called a kernel. Commonly used kernels are the polynomial kernel ($K(x_i, x_j) = e^{-}|x_i - x_j|/2\sigma^2$) and the radial basis kernel ($K(x_i, x_j) = (x_i^T x_j + 1)^p$).

As such, multiclass problems can be reduced to multiple binary classification problems that can be solved separately. SVMs use error-correcting output codes (ECOC) framework to combine binary problems to address the multiclass problems (Dietterich and Bakiri, 1995). The ECOC framework uses different decoding strategies, which are implemented by the coding design (Escalera et al., 2010). The most commonly used coding designs are one-versus-all and one-versus-one. The one-versus-one coding design considers all possible pairs of classes while the one-versus-all discriminates a given class from all other classes.

Disadvantages of the one-versus-all coding design is that the binary classifiers might have different scales and the training sets are not balanced (Bishop, 2006).

5.3.3 Naive Bayes

The naive Bayes (NB) classifier is a probabilistic classifier that is based on Bayes' theorem. Bayes' theorem is a formula that describes the probability of an event, based on prior knowledge of conditions that might have an effect on the event (Ziegel, 1989):

$$P(y|x) = \frac{P(x|y)P(y)}{P(x)}, \tag{28}$$

where x and y are events, and $P(x) \neq 0$. $P(y|x)$ (resp. $P(x|y)$) is the likelihood of event y (resp. x) occurring given that x (resp. y) is true. $P(x)$ and $P(y)$ are the marginal probabilities of observing x and y independently of each other.

The NB classifier considers the prior probability of the predicted class when the likelihood of that class is calculated (Zaki et al., 2014). The naiveness of NB means that the input features are assumed to be statistically independent of each other; thus, the predicted class is the one that maximizes the posterior probability (Domingos and Pazzani, 1997). The NB classifier is configured based on the distribution of the teaching data. A Bayesian posterior is calculated from the distribution of the training data. Gaussian (normal) distribution is commonly used.

6 SUMMARY OF INCLUDED ARTICLES AND RESEARCH CONTRIBUTIONS

6.1 Flexible Simulator for the Vibration Analysis of Rolling Element Bearings

6.1.1 Publication details

The first version of the article (PI) was published in the proceedings of the 29th International Congress on Condition Monitoring and Diagnostic Engineering Management (COMADEM 2016). The main author had an oral presentation at the COMADEM 2016 conference that was held at Xi'an Jiaotong University, Shaanxi, P.R. China in August of 2016. The main editor suggested that the article be extended (+50%) so that it could be published in the International Journal of COMADEM. The manuscript was extended and then it was submitted to the International Journal of COMADEM. The manuscript was accepted and it published in the journal (2/2017).

The paper presents a flexible computer simulator that is used for the simulation and visualization of vibration signals generated by REBs and for testing of vibration analysis methods. This approach tries to overcome challenges in bearing fault detection in real-world environments, where the weak bearing fault signatures experience interference from noise from different external sources and internal mechanical components. The parametric models of the impulse responses for different vibration components are adjustable, and the simulation models can be verified by loading a real-world vibration signals samples into the simulator.

6.1.2 Scientific and personal contributions

A novel property of the flexible simulator is the feedback mechanism, that uses information obtained from vibration analysis to adjust a parametric impulse response models. The disturbance modeling by using wavelets offers a new way to test digital filters on problematic vibration analysis scenarios. The flexible simu-

lator is the main author's invention.

The main author implemented the simulator with LabVIEW. The conference paper was written with the help of the co-author's docent Kari Saarinen and professor Tommi Kärkkäinen. The simulator was presented for the first time at the COMADEM 2016 conference. The extended version of the article was reviewed by both of the co-authors. The vibration data acquisition and data pre-processing were done by the main author.

6.2 Spline wavelet based filtering for denoising vibration signals generated by rolling element bearings

6.2.1 Publication details

The first version of the article (PII) was published in the proceedings of the 30th International Congress on COMADEM 2017. The main author had an oral presentation at the COMADEM 2017 conference that was held in University of Central Lancashire, Preston, United Kingdom in July of 2017. The main editor suggested that the article be extended (+50%) so that it could be published in the International Journal of COMADEM. The manuscript was extended and then it was submitted to the International Journal of COMADEM. The manuscript was accepted and it was published in the journal (4/2018).

Spline wavelets have received little attention in bearing fault detection. The article presents the fundamentals of spline wavelets and a denoising algorithm for the vibration signals generated by REBs. The algorithm can be applied for bearing fault detection. The motivation for this research was initialized during the development of the flexible simulator that was presented in the previous paper, where biorthogonal spline wavelets where used to model disturbances.

6.2.2 Scientific and personal contributions

Such a brute force algorithm that covers a large number of biorthogonal spline wavelets has not been seen in the research field of bearing fault detection. Spline wavelet decomposition reveals bearing fault pulses clearly, which enables the possibility to study the entry and exit events related to bearing fault size.

The conference paper was written entirely by the main author. It was reviewed by the co-author's docent Kari Saarinen and Professor Tommi Kärkkäinen. The extended journal paper was reviewed by Professor Tommi Kärkkäinen. The spline wavelet denoising algorithm was implemented by the main author. The vibration data acquisition and data pre-processing were done by the main author.

6.3 Hybrid vibration signal monitoring approach for rolling element bearings

6.3.1 Publication details

The identification of different lifetime stages of REBs has been studied, as presented in Chapter 2. This paper studies unsupervised clustering approaches to detect the different lifetime stages of REBs using vibration measurements. Since, vibration measurements are an indirect condition monitoring approach, feature extraction is necessary to establish of appropriate degradation features. A method to detect different lifetime stages of REBs according to their vibration signals was proposed based on an unsupervised learning method. The paper also presents a bearing fault detection approach using unsupervised clustering results as bases for supervised methods.

6.3.2 Scientific and personal contributions

The paper presented a novel hybrid vibration "signal based" condition monitoring method. The method enables the identification of different life-time stages of REBs and early bearing fault detection. A comparison of supervised methods was performed. However, the data set was small. To generalize the methodology, further testing using bearing vibration data from other sources is required. Hence, the degradation feature selection can be improved.

The main author applied a fuzzy clustering approach to detect of different life-time stages of REBs. Professor Tommi Kärkkäinen implemented of the cross validation technique to evaluate of feature saliency. The paper was written by the main author and it was reviewed by Professor Tommi Kärkkäinen. The vibration data acquisition and data pre-processing were done by the main author.

6.4 Feature ranking for the fault size estimation of rolling element bearings

Research related to fault severity estimation of REBs, started during my research visit University New South Wales (Australia, Sydney) from 25 June to 20 July 2018. Since then, the research reported in this paper was conducted in collaboration with the Tribology and Machine Condition Monitoring (TMCM) research group. Key persons of the TMCM group include: Associate Professor Zhongxiao Peng, Dr. Pietro Borghesani, Dr. Wade Smith, and Emeritus Professor R.B. Randall.

6.4.1 Publication details

The research tried to solve challenges resulting from the fault severity of REBs using vibration measurements. Incipient bearing fault detection and fault severity estimation where, the size is probably the best proxy, are challenging. A novel method for feature ranking to achieve the fault size estimation of REBs was presented. "Instance based" classifiers (k-NN, SVM) were applied to detect the nonlinear relations between vibration signal features. It was concluded that the best metrics for basic diagnostics are not necessarily the best for the fault size estimation. Even if, the fault size estimation results are convincing, further research using REBs with different properties is needed.

6.4.2 Scientific and personal contributions

The research used bearing vibration data from three different bearings and three different test rigs. The vibration signal feature subset is unique. The classifiers were taught based on features calculated from one test bearing. The fault size estimation was done for all three bearings; meaning that two of the bearings were completely unknown. An analysis of the features reveal the most relevant features to estimate the fault size of REBs when the chosen classifiers were used. The feature ranking process of features of vibration signals was completely novel and it is reproducible.

The TMCM research group advised the researchers on the feature selection process. They provided the bearing vibration data gathered from their bearing test rig and other sources. The feature extraction algorithms for the new statistical features were provided by Dr. Pietro Porghesani. The main author developed the feature extraction and feature ranking processes with the help of other team members. The evaluation of the classifiers was done by the author. The article was written in co-operation with Professor Tommi Kärkkäinen and the TMCM research group.

6.5 Software framework for Tribotronic Systems

6.5.1 Publication details

The increasing capabilities of sensors and computer algorithms require a structural support to solve recurring problems. Autonomous tribotronic systems are self-regulating based on feedback acquired from interacting surfaces in relative motion. This paper introduced a description of a software framework for a tribotronic system. An example application is an REB installation with a vibration sensor. The presented plug-in framework offers functionalities for vibration data management, feature extraction, fault detection, and remaining useful life estimation. The framework was demonstrated with bearing vibration data acquired

from NASA's prognostics data repository. The plug-in implementations are easy to update, and new implementations are easily deployable even in run-time. The proposed software framework improves the performance, efficiency and reliability of a tribotronic system. In addition, the framework facilitates evaluation of the configuration complexity of the plug-in implementation.

6.5.2 Scientific and personal contributions

As the final part of this thesis, an "object oriented" software framework was designed and developed for tribotronic systems. This publication (manuscript) summarizes the main concepts of this Ph.D. work. It assembles and validates the individual parts of this thesis work, namely, feature extraction from vibration signals, fault detection, and RUL estimation. It highlights the central algorithms and shows reliable results through demonstration. The framework generalizes the main elements that were discovered in the research work done in bearing diagnostics and prognostics.

The main author came up with the idea of a software framework after reading a publication in which of the concept of the tribotronic system was introduced (Glavatskih and Hoglund, 2008). The main contribution is a novel plug-in framework that evolved during the work. Such a software framework and it's evaluation has not been previously established. The main author designed the framework and implemented the tribotronic plug-in for REBs. The publication was written by the main author. It was reviewed by Professor Tommi Kärkkäinen.

7 CONCLUSIONS

The main topics of this research are bearing diagnostics, vibration analysis, early fault detection, fault severity estimation, RUL estimation, and system design. As mentioned in earlier, fault severity is a diagnostics task. Table 2 summarizes involvement of the topics in different publications.

TABLE 2 Summary of research topics in articles.

RESEARCH TOPICS	PI	PII	PIII	PIV	PV
Bearing diagnostics	X	X	X	X	X
Vibration analysis	X	X	X	X	X
Early fault detection	X	X	X		X
Fault severity estimation			X	X	X
RUL estimation					X
System design	X				X

With the exception of system design, all the topics focus on the actions that provide feedback to condition monitoring. However, a system is a realization of condition monitoring. The last publication brings together all the research topics, combines diagnostics and prognostics algorithms, and demonstrates them in a carefully established software framework.

7.1 Answers to research questions

RQ1 (What methods can be applied for REB fault detection and how can the methods be analyzed?)

Fault detection indicates when the state of an REB changes from normal condition to defective. Fault detection based on vibration measurements is dependable on the requirements set for its sensitivity and how the environmental conditions. Traditional statistical indicators are very sensitive to disturbances,

which makes fault detection unreliable. An envelope analysis can provide accurate results, but vibrations generated by other sources might disturb the analysis. A variety of methods have been developed to make fault signatures more easily detectable including filtering, decompositions and transformations. Typically, research based on certain fault detection cases shows the good or remarkable capabilities of the fault detection algorithm introduced. However, it is not evident that one algorithm works across scenarios. Simulation is a powerful tool to investigate capabilities of different fault detection algorithms.

RQ2 (Can the different stages of wear evolution of REBs be determined?)

Wear, one of the failure modes in REBs, accumulates over time. Since, wear is monitored cumulatively, representational quantity should be at least monotonic. The metal particles count in oil, which is monitored by direct condition monitoring, gives a good indication of wear and transitions between the life-stages of wear evolution. It is more challenging to find an effective vibration signal feature to describe the wear-state of REBs. Some methods exist to evaluate the effectiveness of degradation features and to recognize transitions states from feature data. However, the SNR of features might need smoothing in order to fill degradation parameter requirements. Unsupervised methods can be used blindly to classify features of vibration signals into different groups. As a result, a combination of features provide a model, that can be used for the identification of different life-time stages.

RQ3 (What are the most important vibration signal features, or indicators for fault diagnostics and severity estimation?)

Finding a better status indicator is a continuous challenge. Fault detection should be done early to be reliable and for RUL estimation to certain. Diagnostics indicators have been developed and justified to describe the different properties of vibration signals. Further, finding out the physical meaning of the indicators is very valuable. It is clear that envelope analysis is effective for fault detection if fault signatures dominate a measured vibration signal. However, a statistical time-domain features might show good correlation to fault size on some circumtances. As research shows, in different cases using different bearings in different conditions, generalization is very challenging. Machine and deep learning methods offer new models based on selected features to be indicators for bearing diagnostics and prognostics. However, the generalization of these models requires that the underlying data is some how normalized. Further, different combinations of features might produce equally effective models.

RQ4 (How can bearing diagnostics and prognostic methods be encapsulated into an industrial software system?)

As a part of the tribotronic system, the designed object-oriented software framework implements bearing applications and provides the possibility to extend it to other mechanical applications. The framework supports condition monitoring data management, feature extraction, fault detection, and RUL estimation, all of which are central tasks in bearing diagnostics and prognostics. The unique tribotronic framework was demonstrated using bearing vibration data acquired from NASA's data repository. The framework improves the performance, efficiency, and reliability of a tribotronic system. The configuration complexity of the plug-in implementation is low, and it can be introduced to users of an industrial software system.

7.1.1 Generalization of diagnostics methods for REBs

Generalization of bearing diagnostics methods is very important aspect. Like point out in this thesis, published research papers related to bearing diagnostics rely on narrow data sets. Very often presented diagnostics methods and algorithms are often shown to be generalizable only in the presented bearing application. Availability of high quality data seems to be a problem. Getting the vibration data from companies or other research institutions is hard. It is almost indispensable to own hardware that bearings can be tested and appropriate data acquired for the analysis. The fourth (PIV) paper presented a unique feature ranking process for vibration signals acquired from three different bearings and three different test rigs in which different running parameters were used. The feature ranking process includes a specific feature normalization to avoid problems cause by the fact, that the feature data acquired from different environments have different distributions. Since, the results are very promising, it is very important to acquire more vibration data from different bearings, which are operated in different environments and conditions. Further, the presented tribotronic plug-in framework offers flexible and robust platform to bring new condition monitoring data and methods for bearing diagnostics.

7.2 Future work

One of the focal points of the future work will be the exploitation of the tribotronic plug-in framework. The performance of the framework will be tested on embedded systems. A new plug-in implementation will be developed to be deployed in another tribotronic system, that is, gears. Also other implementations of feature extraction, fault detection and RUL estimation will be tested. Computationally expensive operations can be evaluated on GPUs in order to reduce running times. Configuration complexity of the framework requires more advanced metrics than just the number meta parameters because some of the parameters require pre-calculations.

Further focal points of the future work will be the research and develop-

ment of fault severity estimation methods using vibration measurements. More data is needed to better test the features under different operating environments and for larger bearings. In addition, all types of bearing faults have to be taken into account. Different noise filtering methods will be applied depending on the measurement conditions. Further, the physical link between fault severity and found features is not yet clear. Focus will be on developing features that are able to describe the time span between events linked to the spall size. Finally, the generalization of the developed methods must be proven over a large data set.

YHTEENVETO (SUMMARY IN FINNISH)

Väitöskirjatyössäni käsitellään vierintälaakerien kunnonvalvonnassa käytettäviä vikadiagnostiikka-algoritmeja sekä ohjelmistoarkkitehtuurisuunnittelua kyseisten tieto-ohjautuvien menetelmien näkökulmasta.

Laakerit ovat yleisin koneissa käytettävä komponentti. Laakereita käytetään mm. moottoreissa, pyörissä ja puhaltimissa. Vioittunut laakeri on yleisin syy koneiden rikkoutumiseen. Laakereiden kuntoa valvotaan eri menetelmillä esimerkiksi värähtely-, lämpötila- ja öljypartikkelimittauksilla. Ideaalisen laakerien kunnonvalvontamenetelmän tulisi pystyä havainnoimaan laakerivika mahdollisimman aikaisessa vaiheessa, jotta vältytään ei-toivotuilta äkkinäisiltä konerikoilta, jotka voivat aiheuttaa merkittäviä taloudellisia tappioita ja pahimmissa tapauksissa ihmishenkien menetyksiä. Kehitetyt menetelmät hyödyntävät vierintälaakerien kunnonvalvonnassa käytettävien värähtelymittalaitteiden mittausdataa. Värähtelymittaus on yleisin vierintälaakerien kunnonvalvonnassa käytettävä menetelmä. Kehitetyillä vikadiagnostiikka-algoritmeilla pyritään havaitsemaan alkava laakerivika, tunnistamaan laakerivian etenemisen eri vaiheet ja arvioimaan vian vakavuutta. Algoritmeissa käytetään kehittyneitä signaalinkäsittely- ja koneoppimisalgoritmeja. Tutkimuksessani on käytetty teollisista koneista ja laboratorioista saatua värähtelydataa.

Vianhavainnointimenetelmä ilmaisee, kun laakerin kunnontila muuttuu normaalista vialliseksi. Värähtelysignaaleihin perustuva viantunnistus riippuu sille asetetuista vaatimuksista herkkyyden ja sen toimintaympäristön suhteen. Suuri määrä menetelmiä on kehitetty helpottamaan laakerivian aiheuttamien piirteiden löytämistä värähtelysignaalista; digitaaliset suodattimet, transformaatiot ja hajotelmat. Usein tutkimuksissa esitetään uuden vianhavainnointimenetelmän tuloksia yhdessä ympäristössä, mikä ei takaa menetelmän yleistystä kaikkiin ympäristöihin. Tietokoneavusteinen simulaatio on tehokas keino eri vianhavainnointimenetelmien toimivuuden testaamiseen.

Laakereista mitattujen värähtelysignaalien piirteistä vikaantumisentilaa luotettavasti kuvaavan piirteen löytäminen on huomattavasti vaikeampaa kuin esimerkiksi käytettäessä voiteluöljyn metallipartikkelien määrää. Valvomattomien oppimismenetelmien käyttäminen värähtelysignaalien piirteiden luokitteluun on hyödyllistä laakerin kulumisen eri vaiheiden tunnistamisessa, koska tuloksena saatu malli perustuu usean piirteeseen. Valvottujen oppimismenetelmien käyttö vian vakavuuden arvioimisessa vaatii monipuolisen värähtelysignaalien piirrejoukon ja piirteiden huolellisen normalisoinnin, jotta menetelmien yleistys olisi parempi.

Väitöskirjatyössäni kehitetty oliopohjainen ohjelmistokehys soveltuu autonomisten tribotronisten systeemien reaaliaikaisesti toimiviin ohjausyksiköihin. Ohjelmistokehys kapseloi kunnonvalvontamittausten datan hallinnan, piirreirrotuksen, vianhavainnoinnin ja jäljellä olevan eliniän ennustamisen.

REFERENCES

Aggarwal, C. C. & Reddy, C. K. 2013. Data clustering: algorithms and applications. CRC press.

Alwodai, A., Wang, T., Chen, Z., Gu, F., Cattley, R. & Ball, A. 2013. A study of motor bearing fault diagnosis using modulation signal bispectrum analysis of motor current signals. Journal of Signal and Information Processing 04, 72-79. doi:10.4236/jsip.2013.43B013.

Ansaharju, T. 2009. Koneenasennus ja kunnossapito. WSOY.

Antoni, J., Bonnardot, F., Raad, A. & Badaoui, M. E. 2004. Cyclostationary modelling of rotating machine vibration signals. Mechanical Systems and Signal Processing 18 (6), 1285 - 1314. doi:10.1016/S0888-3270(03)00088-8.

Antoni, J. & Randall, R. 2006. The spectral kurtosis: application to the vibratory surveillance and diagnostics of rotating machines. Mechanical Systems and Signal Processing 20 (2), 308 - 331. doi:10.1016/j.ymssp.2004.09.002.

Antoni, J. 2006. The spectral kurtosis: a useful tool for characterising non-stationary signals. Mechanical Systems and Signal Processing 20 (2), 282 - 307. doi:10.1016/j.ymssp.2004.09.001.

Antoni, J. 2007. Fast computation of the kurtogram for the detection of transient faults. Mechanical Systems and Signal Processing 21 (1), 108 - 124. doi:10.1016/j.ymssp.2005.12.002.

Antoni, J. & Borghesani, P. 2019. A statistical methodology for the design of condition indicators. Mechanical Systems and Signal Processing 114, 290 - 327. doi:10.1016/j.ymssp.2018.05.012.

Antoni, J. 2006. The spectral kurtosis: a useful tool for characterising non-stationary signals. Mechanical Systems and Signal Processing 20 (2), 282 - 307. doi:https://doi.org/10.1016/j.ymssp.2004.09.001. ⟨URL:http://www.sciencedirect.com/science/article/pii/S0888327004001517⟩.

Banjevic, D. & Jardine, A. 2014. Condition Monitoring. doi:10.1002/9781118445112.stat03643.

Baraldi, P., Cannarile, F., Maio, F. D. & Zio, E. 2016a. Hierarchical k-nearest neighbours classification and binary differential evolution for fault diagnostics of automotive bearings operating under variable conditions. Engineering Applications of Artificial Intelligence 56, 1 - 13. doi:10.1016/j.engappai.2016.08.011.

Baraldi, P., Cannarile, F., Maio, F. D. & Zio, E. 2016b. Hierarchical k-nearest neighbours classification and binary differential evolution for fault diagnostics of automotive bearings operating under variable conditions. Engineering Applications of Artificial Intelligence 56, 1 - 13. doi:10.1016/j.engappai.2016.08.011.

Barszcz, T. & Sawalhi, N. 2012. Fault detection enhancement in rolling element bearings using the minimum entropy deconvolution. Archives of Acoustics 37 (2). doi:10.2478/v10168-012-0019-2.

Bezdek, J. C. 1973. Fuzzy mathematics in pattern classification. Cornell University. Ph. D. Thesis.

Bezdek, J. C. 1981. Pattern Recognition with Fuzzy Objective Function Algorithms. Plenum. doi:10.1007/978-1-4757-0450-1.

Bishop, C. 2006. Pattern Recognition and Machine Learning. Springer-Verlag New York.

Bo, L. & Peng, C. 2016. Fault diagnosis of rolling element bearing using more robust spectral kurtosis and intrinsic time-scale decomposition. Journal of Vibration and Control 22 (12), 2921-2937. doi:10.1177/1077546314547727.

Bogert, B. P., Healy, J. R. & Tukey, J. W. 1963. The quefrency analysis of time series for echoes cepstrum,pseudo-autocovariance, cross-cepstrum, and saphe cracking. In Proceedings of the Symposium on Time Series Analysis, 209-243.

Borghesani, P., Pennacchi, P., Randall, R., Sawalhi, N. & Ricci, R. 2013. Application of cepstrum pre-whitening for the diagnosis of bearing faults under variable speed conditions. Mechanical Systems and Signal Processing 36 (2), 370 - 384. doi:10.1016/j.ymssp.2012.11.001.

Bosch, J., Molin, P., Mattsson, M. & Bengtsson, P. 2000. Object-oriented framework-based software development: Problems and experiences. ACM Computing Surveys 32 (1es). doi:10.1145/351936.351939.

Bozchalooi, I. S. & Liang, M. 2009. Oil debris signal analysis based on empirical mode decomposition for machinery condition monitoring. In 2009 American Control Conference, 4310-4315. doi:10.1109/ACC.2009.5160417.

CWRU s. a. Bearing Data Centre, Case Western Reserve University. (data retrieved from, https://csegroups.case.edu/bearingdatacenter/pages/download-data-file).

Caesarendra, W. & Tjahjowidodo, T. 2017. A review of feature extraction methods in vibration-based condition monitoring and its application for degradation trend estimation of low-speed slew bearing. Machines 5, 21. doi:10.3390/machines5040021.

Carlson, B. 1975. Communication systems: an introduction to signals and noise in electrical communication. McGraw-Hill.

Chegini, S. N., Bagheri, A. & Najafi, F. 2019. Application of a new ewt-based denoising technique in bearing fault diagnosis. Measurement 144, 275 - 297. doi:10.1016/j.measurement.2019.05.049.

Christer, A. H. & Wang, W. 1995. A simple condition monitoring model for a direct monitoring process. European Journal of Operational Research 82 (2), 258 - 269. doi:10.1016/0377-2217(94)00262-B.

Cooley, J. W. & Tukey, J. W. 1965. An Algorithm for the Machine Calculation of Complex Fourier Series. Mathematics of Computation 19, 297-301. doi:10.1090/S0025-5718-1965-0178586-1.

Cover, T. & Hart, P. 1967. Nearest neighbor pattern classification. IEEE Transactions on Information Theory 13 (1), 21-27. doi:10.1109/TIT.1967.1053964.

Cui, L., Wu, N., Ma, C. & Wang, H. 2016a. Quantitative fault analysis of roller bearings based on a novel matching pursuit method with a new step-impulse dictionary. Mechanical Systems and Signal Processing 68-69, 34 - 43. doi:10.1016/j.ymssp.2015.05.032.

Cui, L., Zhang, Y., Zhang, F., Zhang, J. & Lee, S. 2016b. Vibration response mechanism of faulty outer race rolling element bearings for quantitative analysis. Journal of Sound and Vibration 364, 67 - 76. doi:10.1016/j.jsv.2015.10.015.

Dempsey, P. J., Bolander, N., Haynes, C. & Toms, A. M. 2011. Investigation of bearing fatigue damage life prediction using oil debris monitoring. NASA/TM 2011-217117, 1-17.

Dietterich, T. G. & Bakiri, G. 1995. Solving multiclass learning problems via error-correcting output codes. Journal of Artificial Intelligence Research 2 (1), 263–286.

Domingos, P. & Pazzani, M. 1997. On the optimality of the simple bayesian classifier under zero-one loss. Machine Learning 29 (2), 103-130. doi:10.1023/A:1007413511361.

Dong, S. & Luo, T. 2013. Bearing degradation process prediction based on the pca and optimized ls-svm model. Measurement 46 (9), 3143 - 3152. doi:10.1016/j.measurement.2013.06.038.

Dongre, P. R., Chiddarwar, S. S. & Deshpande, V. S. 2013. Tool condition monitoring in various machining operations and use of acoustic signature analysis. International Journal on Mechanical Engineering and Robotics (IJMER) 1 (1), 2321–5747.

Du, W., Tao, J., Li, Y. & Liu, C. 2014. Wavelet leaders multifractal features based fault diagnosis of rotating mechanism. Mechanical Systems and Signal Processing 43 (1), 57 - 75. doi:10.1016/j.ymssp.2013.09.003.

Dunn, J. 1973. A fuzzy relative of the isodata process and its use in detecting compact well-separated clusters. Journal of Cybernetics 3 (3), 32-57. doi:10.1080/01969727308546046.

Dupuis, R. 2010. Application of oil debris monitoring for wind turbine gearbox prognostics and health management. In PHM (Ed.) Annual Conference of the Prognostics and Health Management Society.

Dwyer, R. 1983. Detection of non-gaussian signals by frequency domain kurtosis estimation. In ICASSP '83. IEEE International Conference on Acoustics, Speech, and Signal Processing, Vol. 8, 607-610. doi:10.1109/ICASSP.1983.1172264.

El-Thalji, I. & Jantunen, E. 2014. A descriptive model of wear evolution in rolling bearings. Engineering Failure Analysis 45, 204-224. doi:10.1016/j.engfailanal.2014.06.004.

Escalera, S., Pujol, O. & Radeva, P. 2010. On the decoding process in ternary error-correcting output codes. IEEE Transactions on Pattern Analysis and Machine Intelligence 32 (1), 120-134. doi:10.1109/TPAMI.2008.266.

Estupiñan, E., White, P. & Martin, C. S. 2007. A cyclostationary analysis applied to detection and diagnosis of faults in helicopter gearboxes. In L. Rueda, D. Mery & J. Kittler (Eds.) Progress in Pattern Recognition, Image Analysis and Applications. Berlin, Heidelberg: Springer Berlin Heidelberg, 61–70.

Feldman, M. 2011. Hilbert transform in vibration analysis. Mechanical Systems and Signal Processing 25 (3), 735 - 802. doi:10.1016/j.ymssp.2010.07.018.

Fernández-Francos, D., Martínez-Rego, D., Fontenla-Romero, O. & Alonso-Betanzos, A. 2013. Automatic bearing fault diagnosis based on one-class v-svm. Computers and Industrial Engineering 64 (1), 357 - 365. doi:10.1016/j.cie.2012.10.013.

Fyfe, K. & Munck, E. 1997. Analysis of computed order tracking. Mechanical Systems and Signal Processing 11 (2), 187 - 205. doi:10.1006/mssp.1996.0056.

Gallager, R. G. 2008. Principles of Digital Communication. Cambridge University Press. doi:10.1017/CBO9780511813498.

Gao, Y., Randall, R. & Ford, R. 1998. Estimation of envelope spectra using maximum entropy spectral analysis and spectrum interpolation. International Journal of COMADEM 1, 15-22.

Ghissoni, S., Costa, E., Lazzari, C., Monteiro, J., Aksoy, L. & Reis, R. 2010. Radix-2 decimation in time (dit) fft implementation based on a matrix-multiple constant multiplication approach. In Radix-2 Decimation in Time (DIT) FFT implementation based on a Matrix-Multiple Constant multiplication approach, 859-862. doi:10.1109/ICECS.2010.5724648.

Gilles, J. 2013. Empirical wavelet transform. IEEE Transactions on Signal Processing 61 (16), 3999-4010. doi:10.1109/TSP.2013.2265222.

Glavatskih, S. & Hoglund, E. 2008. Tribotronics towards active tribology. Tribology International 41 (9), 934 - 939. doi:10.1016/j.triboint.2007.03.001. (Nordtrib 2006).

Gong, T., Yuan, X., Lei, X., Yuan, Y. & Zhang, B. 2018. Fault detection for rolling element bearing based on repeated single-scale morphology and simplified sensitive factor algorithm. Measurement 127, 348 - 355. doi:10.1016/j.measurement.2018.05.082.

Gong, T., Yuan, X., Yuan, Y., Lei, X. & Wang, X. 2019. Application of tentative variational mode decomposition in fault feature detection of rolling element bearing. Measurement 135, 481 - 492. doi:10.1016/j.measurement.2018.11.083.

Gonzales, C. 2015. What is the difference between bearings? (https://www.machinedesign.com/whats-difference-between/what-s-difference-between-bearings-1).

Gonzalez, R. C. & Woods, R. E. 2008. Digital Image Processing. Pearson.

Grami, A. 2019. Introduction to Digital Communications. Academic Press.

Group, S. 2012. the Railway technical handbook. SKF Group.

Gryllias, K. & Antoniadis, I. 2012. A support vector machine approach based on physical model training for rolling element bearing fault detection in industrial environments. Engineering Applications of Artificial Intelligence 25 (2), 326 - 344. doi:10.1016/j.engappai.2011.09.010. (Special Section: Local Search Algorithms for Real-World Scheduling and Planning).

Gröchenig, K. 2001. Foundations of Time-Frequency Analysis. Birkhäuser Basel. doi:10.1007/978-1-4612-0003-1.

Guo, J., Zhen, D., Li, H., Shi, Z., Gu, F. & Ball, A. D. 2019. Fault feature extraction for rolling element bearing diagnosis based on a multi-stage noise reduction method. Measurement 139, 226 - 235. doi:10.1016/j.measurement.2019.02.072.

Guyon, I. & Elisseeff, A. 2003. An introduction to variable and feature selection. Journal of Machine Learning Research 3, 1157–1182.

Hamrock, B. J. & Anderson, W. J. 1983. Rolling element bearings. NASA.

Han, T., Liu, Q., Zhang, L. & Tan, A. C. 2019. Fault feature extraction of low speed roller bearing based on teager energy operator and ceemd. Measurement 138, 400 - 408. doi:10.1016/j.measurement.2019.02.053.

Harris, F. J. 1978. On the use of windows for harmonic analysis with the discrete fourier transform. Proceedings of the IEEE 66 (1), 51-83. doi:10.1109/PROC.1978.10837.

Harvey, T. J., Wood, R. J. K. & Powrie, H. E. G. 2007. Electrostatic wear monitoring of rolling element bearings. Wear 263 (7), 1492-1501. doi:10.1016/j.wear.2006.12.073. (16th International Conference on Wear of Materials).

He, C., Niu, P., Yang, R., Wang, C., Li, Z. & Li, H. 2019. Incipient rolling element bearing weak fault feature extraction based on adaptive second-order stochastic resonance incorporated by mode decomposition. Measurement 145, 687 - 701. doi:10.1016/j.measurement.2019.05.052.

Heng, A., Tan, A. C., Mathew, J., Montgomery, N., Banjevic, D. & Jardine, A. K. 2009. Intelligent condition-based prediction of machinery reliability. Mechanical Systems and Signal Processing 23 (5), 1600 - 1614. doi:10.1016/j.ymssp.2008.12.006.

Ho, D. & Randall, R. B. 2000. Optimisation of bearing diagnostic techniques using simulated and actual bearing fault signals. Mechanical Systems and Signal Processing 14 (5), 763 - 788. doi:10.1006/mssp.2000.1304.

Hoang, D.-T. & Kang, H.-J. 2019. A survey on deep learning based bearing fault diagnosis. Neurocomputing 335, 327 - 335. doi:10.1016/j.neucom.2018.06.078.

Hu, Q., He, Z., Zhang, Z. & Zi, Y. 2007. Fault diagnosis of rotating machinery based on improved wavelet package transform and svms ensemble. Mechanical Systems and Signal Processing 21 (2), 688 - 705. doi:10.1016/j.ymssp.2006.01.007.

Huang, D., Gan, Z. & Chow, T. W. 2008. Enhanced feature selection models using gradient-based and point injection techniques. Neurocomputing 71, 3114–3123.

Huang, N. E., Shen, Z., Long, S. R., Wu, M. C., Shih, H. H., Zheng, Q., Yen, N.-C., Tung, C. C. & Liu, H. H. 1998. The empirical mode decomposition and the hilbert spectrum for nonlinear and non-stationary time series analysis. Proceedings of the Royal Society of London. Series A: Mathematical, Physical and Engineering Sciences 454 (1971), 903-995. doi:10.1098/rspa.1998.0193.

Ismail, M. & Sawalhi, N. 2017. Vibration response characterisation and fault-size estimation of spalled ball bearings. Insight - Non-Destructive Testing and Condition Monitoring 59, 149-154. doi:10.1784/insi.2017.59.3.149.

Ismail, M. A., Bierig, A. & Sawalhi, N. 2018. Automated vibration-based fault size estimation for ball bearings using savitzky–golay differentiators. Journal of Vibration and Control 24 (18), 4297-4315. doi:10.1177/1077546317723227.

Jain, A. K., Murty, M. N. & Flynn, P. J. 1999. Data clustering: A review. ACM Comput. Surv. 31 (3), 264-323. doi:10.1145/331499.331504.

Jain, A. K. 2010. Data clustering: 50 years beyond k-means. Pattern recognition letters 31 (8), 651-666.

James, G., Witten, D., Hastie, T. & Tibshirani, R. 2013. An Introduction to Statistical Learning with Applications in R. Springer New York Heidelberg Dordrecht London. doi:10.1007/978-1-4614-7138-7.

Jantunen, E. 2002. A summary of methods applied to tool condition monitoring in drilling. International Journal of Machine Tools and Manufacture 42 (9), 997 - 1010. doi:10.1016/S0890-6955(02)00040-8.

Jantunen, E. 2006. How to diagnose the wear of rolling element bearings based on indirect condition monitoring methods. International Journal of COMADEM 9, 24-38.

Jayaswal, P., Verma, S. N. & Wadhwani, A. K. 2011. Development of ebp artificial neural network expert system for rolling element bearing fault diagnosis. Journal of Vibration and Control 17 (8), 1131-1148. doi:10.1177/1077546310361858.

John, G. H., Kohavi, R. & Pfleger, K. 1994. Irrelevant features and the subset selection problem. In W. W. Cohen & H. Hirsh (Eds.) Machine Learning Proceedings 1994. San Francisco (CA): Morgan Kaufmann, 121 - 129. doi:10.1016/B978-1-55860-335-6.50023-4.

Johnson, R. E. & Foote, B. 1988. Designing reuseable classes. Journal of Object-Oriented Programming.

Kang, S., Ma, D., Wang, Y., Lan, C., Chen, Q. & Mikulovich, V. 2017. Method of assessing the state of a rolling bearing based on the relative compensation distance of multiple-domain features and locally linear embedding. Mechanical Systems and Signal Processing 86, 40 - 57. doi:doi.org/10.1016/j.ymssp.2016.10.006.

Kankar, P., Sharma, S. C. & Harsha, S. 2011. Rolling element bearing fault diagnosis using autocorrelation and continuous wavelet transform. Journal of Vibration and Control 17 (14), 2081-2094. doi:10.1177/1077546310395970.

Kedadouche, M., Thomas, M. & Tahan, A. 2016. A comparative study between empirical wavelet transforms and empirical mode decomposition methods: Application to bearing defect diagnosis. Mechanical Systems and Signal Processing 81, 88 - 107. doi:10.1016/j.ymssp.2016.02.049.

Keller, J., Gray, M. & Givens, J. 1985. A fuzzy k-nearest neighbor algorithm. IEEE Transactions on Systems, Man, and Cybernetics - TSMC SMC-15.

Khanam, S., Tandon, N. & Dutt, J. K. 2014. Fault size estimation in the outer race of ball bearing using discrete wavelet transform of the vibration signal. Procedia Technology 14, 12 - 19. doi:10.1016/j.protcy.2014.08.003. (2nd International Conference on Innovations in Automation and Mechatronics Engineering, ICIAME 2014).

Kiral, Z. & Karagülle, H. 2003. Simulation and analysis of vibration signals generated by rolling element bearing with defects. Tribology International 36 (9), 667 - 678. doi:10.1016/S0301-679X(03)00010-0.

Kohavi, R. & John, G. H. 1997. Wrappers for feature subset selection. Artificial Intelligence 97 (1), 273 - 324. doi:10.1016/S0004-3702(97)00043-X. (Relevance).

Koskimies, K. & Mikkonen, T. 2005. Ohjelmistoarkkitehtuurit. Talentum Media Oy.

Kovacevic, J. & Vetterli, M. 1995. Wavelets and Subband Coding. Prentice Hall.

Kumar, H. S., P, P., Vijay, G. & Rao, R. 2013. Wavelet transform for bearing condition monitoring and fault diagnosis: A review. International Journal of COMADEM 17.

Laha, S. K. 2017. Enhancement of fault diagnosis of rolling element bearing using maximum kurtosis fast nonlocal means denoising. Measurement 100, 157 - 163. doi:10.1016/j.measurement.2016.12.058.

Li, F., Chen, Y., Wang, J., Zhou, X. & Tang, B. 2019. A reinforcement learning unit matching recurrent neural network for the state trend prediction of rolling bearings. Measurement 145, 191 - 203. doi:10.1016/j.measurement.2019.05.093.

Li, Y., Xu, M., Wang, R. & Huang, W. 2016a. A fault diagnosis scheme for rolling bearing based on local mean decomposition and improved multiscale fuzzy entropy. Journal of Sound and Vibration 360, 277 - 299. doi:10.1016/j.jsv.2015.09.016.

Li, Y., Xu, M., Zhao, H. & Huang, W. 2016b. Hierarchical fuzzy entropy and improved support vector machine based binary tree approach for rolling bearing fault diagnosis. Mechanism and Machine Theory 98, 114 - 132. doi:10.1016/j.mechmachtheory.2015.11.010.

Li, Y., Billington, S., Zhang, C., Kurfess, T., Danyluk, S. & Liang, S. 1999. Dynamic prognostic prediction of defect propagation on rolling element bearings. Tribology Transactions 42 (2), 385-392. doi:10.1080/10402009908982232.

Li, Y., Kurfess, T. R. & Liang, S. Y. 2000. Stochastic prognostics for rolling element bearings. Mechanical Systems and Signal Processing 14 (5), 747 - 762. doi:10.1006/mssp.2000.1301.

Liang, M. & Faghidi, H. 2014. Intelligent bearing fault detection by enhanced energy operator. Expert Systems with Applications 41 (16), 7223 - 7234. doi:10.1016/j.eswa.2014.05.026.

Liang, Y., Zhang, M. & Browne, W. N. 2017. Image feature selection using genetic programming for figure-ground segmentation. Engineering Applications of Artificial Intelligence 62, 96–108.

Liu, H. & Motoda, H. 1998. Feature Selection for Knowledge Discovery and Data Mining. Norwell, MA: Kluwer.

Liu, T., Chen, J. & Dong, G. 2015. Singular spectrum analysis and continuous hidden markov model for rolling element bearing fault diagnosis. Journal of Vibration and Control 21 (8), 1506-1521. doi:10.1177/1077546313496833.

Lou, X. & Loparo, K. A. 2004. Bearing fault diagnosis based on wavelet transform and fuzzy inference. Mechanical Systems and Signal Processing 18 (5), 1077 - 1095. doi:10.1016/S0888-3270(03)00077-3.

Luo, G. Y., Osypiw, D. & Irle, M. 2003a. On-line vibration analysis with fast continuous wavelet algorithm for condition monitoring of bearing. Journal of Vibration and Control 9 (8), 931-947. doi:10.1177/10775463030098002.

Luo, J., Bixby, A., Pattipati, K., Qiao, L., Kawamoto, M. & Chigusa, S. 2003b. An interacting multiple model approach to model-based prognostics. In SMC03 Conference Proceedings. 2003 IEEE International Conference on Systems, Man and Cybernetics., Vol. 1, 189-194 vol.1. doi:10.1109/ICSMC.2003.1243813.

McFadden, P. & Smith, J. 1984. Model for the vibration produced by a single point defect in a rolling element bearing. Journal of Sound and Vibration 96 (1), 69 - 82. doi:10.1016/0022-460X(84)90595-9.

McFadden, P. & Smith, J. 1985. The vibration produced by multiple point defects in a rolling element bearing. Journal of Sound and Vibration 98 (2), 263 - 273. doi:10.1016/0022-460X(85)90390-6.

Miller, A. J. 1990. Subset Selection in Regression. Chapman and Hall.

Mitchell, T. M. 1997. Machine Learning. McGraw-Hill Science/Engineering/Math.

Mitra, S. K. 2005. Digital Signal Processing. McGraw-Hill Science/Engineering/Math.

Momono, T. & Noda, B. 1999. Sound and vibration in rolling bearings. Motion and Control 6, 29–37.

Moradi, P. & Rostami, M. 2015. A graph theoretic approach for unsupervised feature selection. Engineering Applications of Artificial Intelligence 44, 33 - 45. doi:10.1016/j.engappai.2015.05.005.

Moshrefzadeh, A., Fasana, A. & Antoni, J. 2019. The spectral amplitude modulation: A nonlinear filtering process for diagnosis of rolling element bearings. Mechanical Systems and Signal Processing 132, 253 - 276. doi:10.1016/j.ymssp.2019.06.030.

Moubray, J. 1999. Reliability-centered Maintenance.

NTN 2019. Rolling bearings handbook. NTN.

Nikias, C. L. & Mendel, J. M. 1993. Signal processing with higher-order spectra. IEEE Signal Processing Magazine 10 (3), 10-37. doi:10.1109/79.221324.

Nyquist, H. 1928. Certain topics in telegraph transmission theory. Transactions of the American Institute of Electrical Engineers 47 (2), 617-644. doi:10.1109/T-AIEE.1928.5055024.

Oppenheim, A. V., Willsky, A. S. & Young, I. T. 1983. Signals and systems. Prentice-Hall.

Paliwal, D., Choudhury, A. & Tingarikar, G. 2014. Wavelet and scalar indicator based fault assessment approach for rolling element bearings. Procedia Materials Science 5, 2347-2355. doi:10.1016/j.mspro.2014.07.478.

Peng, Z. K. & Chu, F. L. 2004. Application of the wavelet transform in machine condition monitoring and fault diagnostics: a review with bibliography. Mechanical Systems and Signal Processing 18 (2), 199 - 221. doi:10.1016/S0888-3270(03)00075-X.

Peng, Z. K., Tse, P. W. & Chu, F. L. 2005. A comparison study of improved hilbert–huang transform and wavelet transform: Application to fault diagnosis for rolling bearing. Mechanical Systems and Signal Processing 19 (5), 974 - 988. doi:10.1016/j.ymssp.2004.01.006.

Philipps, J. & Rumped, B. 1999. Refinement of pipe-and-filter architectures. In J. M. Wing, J. Woodcock & J. Davies (Eds.) FM99 Formal Methods. Berlin, Heidelberg: Springer Berlin Heidelberg, 96–115.

Prabhakar, S., Mohanty, A. R. & Sekhar, A. S. 2002. Application of discrete wavelet transform for detection of ball bearing race faults. Tribology International 35 (12), 793 - 800. doi:10.1016/S0301-679X(02)00063-4.

Qiu, H., Lee, J., Lin, J. & Yu, G. 2006. Wavelet filter-based weak signature detection method and its application on rolling element bearing prognostics. Journal of Sound and Vibration 289 (4), 1066 - 1090. doi:10.1016/j.jsv.2005.03.007.

Rai, A. & Upadhyay, S. 2016. A review on signal processing techniques utilized in the fault diagnosis of rolling element bearings. Tribology International 96. doi:10.1016/j.triboint.2015.12.037.

Randall, R. B., Antoni, J. & Chobsaard, S. 2001. The relationship between spectral correlation and envelope analysis in the diagnostics of bearing faults and other cyclostationary machine signals. Mechanical Systems and Signal Processing 15 (5), 945 - 962. doi:10.1006/mssp.2001.1415.

Randall, R. B. 2010. Vibration based Condition Monitoring: Industrial, Aerospace and Automotive Applications. doi:10.1002/9780470977668.

Randall, R. B. 2008. Noise and Vibration Data Analysis. doi:10.1002/9780470209707.ch46.

Randall, R. B. & Antoni, J. 2011. Rolling element bearing diagnostics a tutorial. Mechanical Systems and Signal Processing 25 (2), 485 - 520. doi:10.1016/j.ymssp.2010.07.017.

Rehab, I., Tian, X., Gu, F. & Ball, A. 2014. The fault detection and severity diagnosis of rolling element bearings using modulation signal bispectrum. In 11th International Conference on Condition Monitoring and Machinery Failure Prevention Technologies - CM 2014 MFPT 2014. British Institute of Non-Destructive Testing.

Rohani, A. & Mba, D. 2011. A new model for estimating vibrations generated in the defective rolling element bearings. Journal of Vibration and Acoustics 133, 041011. doi:10.1115/1.4003595ÍŤ.

Ruhm, K. H. 2010. Sensoren der Schwingungsmesstechnik.

Ruspini, E. 1969. A new approach to clustering. Information and Control 15 (1), 22-32. doi:10.1016/S0019-9958(69)90591-9.

Saari, J., Strömbergsson, D., Lundberg, J. & Thomson, A. 2019. Detection and identification of windmill bearing faults using a one-class support vector machine (svm). Measurement 137, 287 - 301. doi:10.1016/j.measurement.2019.01.020.

Saidi, L., Ali, J. B. & Fnaiech, F. 2015. Application of higher order spectral features and support vector machines for bearing faults classification. ISA Transactions 54, 193 - 206. doi:10.1016/j.isatra.2014.08.007.

Sawalhi, N. & Randall, R. B. 2011. Vibration response of spalled rolling element bearings: Observations, simulations and signal processing techniques to track the spall size. Mechanical Systems and Signal Processing 25 (3), 846 - 870. doi:10.1016/j.ymssp.2010.09.009.

Schwach, D. & Guo, Y. 2006. A fundamental study on the impact of surface integrity by hard turning on rolling contact fatigue. International Journal of Fatigue 28 (12), 1838-1844. doi:10.1016/j.ijfatigue.2005.12.002.

Seker, S. & Ayaz, E. 2003. Feature extraction related to bearing damage in electric motors by wavelet analysis. Journal of the Franklin Institute 340 (2), 125 - 134. doi:10.1016/S0016-0032(03)00015-2.

Sheng, Y. 2000. Wavelet transform. In A. D. Poularikas (Ed.) The Transforms and Applications Handbook. Oxford: CRC Press LLC.

Siegel, D., Al-Atat, H., Shauche, V., Liao, L., Snyder, J. & Lee, J. 2012. Novel method for rolling element bearing health assessment a tachometer-less synchronously averaged envelope feature extraction technique. Mechanical Systems and Signal Processing 29, 362 - 376. doi:10.1016/j.ymssp.2012.01.003.

Siemens 2016. Selection and Installation of Vibration Sensors. ⟨URL:https://cache.industry.siemens.com/dl/files/202/109740202/att_890764/v6/109740202_Sensors_DOC_V10_en.pdf⟩.

Sikorska, J., Hodkiewicz, M. & Ma, L. 2011. Prognostic modelling options for remaining useful life estimation by industry. Mechanical Systems and Signal Processing 25 (5), 1803 - 1836. doi:10.1016/j.ymssp.2010.11.018.

Silberwolf 2006. Radial deep groove ball bearings. ⟨URL:https://commons.wikimedia.org/wiki/File:Radial-deep-groove-ball-bearing_din625-t1_2rs_120.png⟩. (This file is licensed under the Creative Commons Attribution 2.5 Generic license.).

Sovilj, D. 2014. Learning Methods for Variable Selection and Time Series Prediction. Aalto University. Ph. D. Thesis.

Tan, L. 2008. Digital Signal Processing: Fundamentals and Applications. Academic Press.

Tandon, N. & Choudhury, A. 1999. A review of vibration and acoustic measurement methods for the detection of defects in rolling element bearings. Tribology International 32 (8), 469 - 480. doi:10.1016/S0301-679X(99)00077-8.

Tang, H., Chen, J. & Dong, G. 2011. Signal complexity analysis for fault diagnosis of rolling element bearings based on matching pursuit. Journal of Vibration and Control 18 (5), 671-683. doi:10.1177/1077546311405369.

Tian, J., Morillo, C., Azarian, M. H. & Pecht, M. 2016. Motor bearing fault detection using spectral kurtosis-based feature extraction coupled with k-nearest neighbor distance analysis. IEEE Transactions on Industrial Electronics 63 (3), 1793-1803. doi:10.1109/TIE.2015.2509913.

Tretter, S. A. 2008. Communication System Design Using DSP Algorithms. Springer.

Tse, P. W. & Wang, D. 2011. The sparsogram a new and effective method for extracting bearing fault features. In 2011 Prognostics and System Health Managment Confernece, 1-6. doi:10.1109/PHM.2011.5939587.

Tse, P. W. & Wang, D. 2013. The automatic selection of an optimal wavelet filter and its enhancement by the new sparsogram for bearing fault detection part 2 of the two related manuscripts that have a joint title as two automatic vibration-based fault diagnostic methods using the novel sparsity measurement parts 1 and 2. Mechanical Systems and Signal Processing 40 (2), 520 - 544. doi:10.1016/j.ymssp.2013.05.018.

Vapnik, V. N. 2000. The Nature of Statistical Learning Theory. New York, US: Springer-Verlag. doi:10.1007/978-1-4757-3264-1.

Vetterli, M. & Herley, C. 1992. Wavelets and filter banks: theory and design. IEEE Transactions on Signal Processing 40 (9), 2207-2232. doi:10.1109/78.157221.

Wagh, S., Neelwarna, G. & Kolhe, S. 2012. A comprehensive analysis and study in intrusion detection system using k-nn algorithm. In C. Sombattheera, N. K. Loi, R. Wankar & T. Quan (Eds.) Multi-disciplinary Trends in Artificial Intelligence. Berlin, Heidelberg: Springer Berlin Heidelberg, 143–154.

Wang, H. 2016. Fault diagnosis of rolling element bearing compound faults based on sparse no-negative matrix factorization-support vector data description. Journal of Vibration and Control 24 (2), 272-282. doi:10.1177/1077546316637979.

Wang, J. J., Zheng, Y. H., Zhang, L. B., Duan, L. X. & Zhao, R. 2017. Virtual sensing for gearbox condition monitoring based on kernel factor analysis. Petroleum Science 14 (3), 539–548. doi:10.1007/s12182-017-0163-4.

Wang, Q., Liu, Y. B., He, X., Liu, S. Y. & Liu, J. H. 2014a. Fault diagnosis of bearing based on kpca and knn method. Advanced Materials Research 986-987 (1), 1491-1496. doi:10.4028/www.scientific.net/AMR.986-987.1491.

Wang, Q., Liu, Y. B., He, X., Liu, S. Y. & Liu, J. H. 2014b. Fault diagnosis of bearing based on kpca and knn method. Advanced Materials Research 986-987 (1), 1491-1496. doi:10.4028/www.scientific.net/AMR.986-987.1491.

Wang, Y., Xiang, J., Markert, R. & Liang, M. 2016. Spectral kurtosis for fault detection, diagnosis and prognostics of rotating machines a review with applications. Mechanical Systems and Signal Processing 66-67, 679 - 698. doi:https://doi.org/10.1016/j.ymssp.2015.04.039. ⟨URL:http://www.sciencedirect.com/science/article/pii/S0888327015002897⟩.

Wang, Y., Kang, S., Jiang, Y., Yang, G., Song, L. & Mikulovich, V. 2012. Classification of fault location and the degree of performance degradation of a rolling bearing based on an improved hyper-sphere-structured multi-class support vector machine. Mechanical Systems and Signal Processing 29, 404 - 414. doi:10.1016/j.ymssp.2011.11.015.

Wen, J., Gao, H., Li, S., Zhang, L., He, X. & Liu, W. 2015a. Fault diagnosis of ball bearings using synchrosqueezed wavelet transforms and svm. In 2015 Prognostics and System Health Management Conference (PHM), 1-6. doi:10.1109/PHM.2015.7380084.

Wen, J., Gao, H., Li, S., Zhang, L., He, X. & Liu, W. 2015b. Fault diagnosis of ball bearings using synchrosqueezed wavelet transforms and svm. In 2015 Prognostics and System Health Management Conference (PHM), 1-6. doi:10.1109/PHM.2015.7380084.

Xiang, J., Zhong, Y. & Gao, H. 2015. Rolling element bearing fault detection using ppca and spectral kurtosis. Measurement 75, 180 - 191. doi:10.1016/j.measurement.2015.07.045.

Xu, Y., Zhang, K., Ma, C., Cui, L. & Tian, W. 2019. Adaptive kurtogram and its applications in rolling bearing fault diagnosis. Mechanical Systems and Signal Processing 130, 87 - 107. doi:10.1016/j.ymssp.2019.05.003.

Yang, B.-S., Han, T. & Hwang, W.-W. 2005. Fault diagnosis of rotating machinery based on multi-class support vector machines. Journal of Mechanical Science and Technology 19, 846-859. doi:10.1007/BF02916133.

Yang, Y., Yu, D. & Cheng, J. 2007. A fault diagnosis approach for roller bearing based on imf envelope spectrum and svm. Measurement 40 (9), 943 - 950. doi:doi.org/10.1016/j.measurement.2006.10.010.

Yiakopoulos, C. T. & Antoniadis, I. A. 2005. Cyclic bispectrum patterns of defective rolling element bearing vibration response. Forschung im Ingenieurwesen 70 (2), 90–104. doi:10.1007/s10010-005-0018-9.

Yoshioka, T. & Shimizu, S. 2009. Monitoring of ball bearing operation under grease lubrication using a new compound diagnostic system detecting vibration and acoustic emission. Tribology Transactions 52 (6), 725-730. doi:10.1080/10402000902913345.

Yu, D., Cheng, J. & Yang, Y. 2005. Application of emd method and hilbert spectrum to the fault diagnosis of roller bearings. Mechanical Systems and Signal Processing 19 (2), 259 - 270. doi:10.1016/S0888-3270(03)00099-2.

Zaki, M. J., Meira Jr, W. & Meira, W. 2014. Data mining and analysis: fundamental concepts and algorithms. Cambridge University Press.

Zare, H. & Niazi, M. 2016. Relevant based structure learning for feature selection. Engineering Applications of Artificial Intelligence 55, 93 - 102. doi:10.1016/j.engappai.2016.06.001.

Zhang, S., Zhang, S., Wang, B. & Habetler, T. G. 2019. Machine learning and deep learning algorithms for bearing fault diagnostics - A comprehensive review. CoRR abs1901.08247. ⟨URL:https://arxiv.org/abs/1901.08247⟩.

Zhang, X., Liang, Y., Zhou, J. & zang, Y. 2015. A novel bearing fault diagnosis model integrated permutation entropy, ensemble empirical mode decomposition and optimized svm. Measurement 69, 164 - 179. doi:10.1016/j.measurement.2015.03.017.

Zhang, Y., Zuo, H. & Bai, F. 2013. Classification of fault location and performance degradation of a roller bearing. Measurement 46 (3), 1178 - 1189. doi:10.1016/j.measurement.2012.11.025.

Zhao, M., Jin, X., Zhang, Z. & Li, B. 2014. Fault diagnosis of rolling element bearings via discriminative subspace learning: Visualization and classification. Expert Systems with Applications 41 (7), 3391 - 3401. doi:10.1016/j.eswa.2013.11.026.

Zhao, S., Liang, L., Xu, G., Wang, J. & Zhang, W. 2013. Quantitative diagnosis of a spall-like fault of a rolling element bearing by empirical mode decomposition and the approximate entropy method. Mechanical Systems and Signal Processing 40 (1), 154 - 177. doi:10.1016/j.ymssp.2013.04.006.

Ziegel, E. 1989. Kendall's Advanced Theory of Statistics, Vol. 1: Distribution Theory. Taylor and Francis.

APPENDIX 1 RESEARCH PAPERS ON BEARING DIAGNOSTICS

TABLE 3 Recently done research on bearing diagnostics and prognostics.

Title / Journal	Research interest / Methods	Data source / Bearing (Pitch diameter [mm])
The spectral amplitude modulation: A nonlinear filtering process for diagnosis of rolling element bearings (Moshrefzadeh et al., 2019) / MSSP	Fault diagnostics / SAM, CPW	Test rig (CWRU), Test rig (SpectralQuest) / SKF 6203-2RS JEM (28.5 mm), SKF 6205-SR2 JEM (39 mm), MB-ER-16K 1 (39.32 mm)
Adaptive Kurtogram and its applications in rolling bearing fault diagnosis (Xu et al., 2019) / MSSP	Fault diagnostics / AK, OSF, EWT	Test rig (XJU) / 6307 (49.56 mm?)
Application of a new EWT-based denoising technique in bearing fault diagnosis (Chegini et al., 2019) / Measurement	Fault diagnostics / EWT	Test rig (CWRU) / SKF 6205-SR2 JEM (39 mm)
Detection and identification of windmill bearing faults using a one-class support vector machine (SVM) (Saari et al., 2019) / Measurement	Fault diagnostics / SVM	Windmill bearing
A reinforcement learning unit matching recurrent neural network for the state trend prediction of rolling bearings (Li et al., 2019) / Measurement	Fault prognostics / RLUM-RNN	Test rig (IMS) / REXNORD ZA-2115 (71.5 mm)
Application of tentative variational mode decomposition in fault feature detection of rolling element bearing (Gong et al., 2019) / Measurement	Fault diagnostics / TVMD, DTW	Test rig (CWRU) / SKF 6203-2RS JEM (28.5 mm), SKF 6205-SR2 JEM (39 mm)
A statistical methodology for the design of condition indicators (Antoni and Borghesani, 2019) / MSSP	Fault diagnostics / Statistical methodology	Test rig (IMS) / REXNORD ZA-2115 (71.5 mm)
Fault feature extraction for rolling element bearing diagnosis based on a multi-stage noise reduction method (Guo et al., 2019) / Measurement	Fault diagnostics / EEMD, WT, MSB	Test rig (UHF) / 6206ZZ (46.4 mm), 6008 (54 mm)
Incipient rolling element bearing weak fault feature extraction based on adaptive second-order stochastic resonance incorporated by mode decomposition (He et al., 2019) / Measurement	Fault diagnostics / EMD, CEEMDAN, AUSR	Test rig (IMS), Gear test rig / REXNORD ZA-2115 (71.5 mm), Unknown (57 mm)
Fault feature extraction of low speed roller bearing based on Teager energy operator and CEEMD (Han et al., 2019) / Measurement	Fault diagnostics / TEO, CEEMD	Test rig (wind turbine) / 22208C (60 mm)
Fault detection for rolling element bearing based on repeated single-scale morphology and simplified sensitive factor algorithm (Gong et al., 2018) / Measurement	Fault diagnostics / RSSMF, SSF	Test rig (IMS) / REXNORD ZA-2115 (71.5 mm)
Automated vibration-based fault size estimation for ball bearings using Savitzky–Golay differentiators (Ismail et al., 2018) / JVC	Fault size estimation /Savitzky–Golay differentiator	Test rig (DLR) / FAG QJ212TVP (85.15 mm)
Vibration response characterisation and fault-size estimation of spalled ball bearings (Ismail and Sawalhi, 2017) / Insight	Fault size estimation / Numerical differentiator + RMS envelope	Test rig (DLR), Test rig (UNSW) / NACHI 2206GK (39 mm), FAG QJ212TVP (85.15 mm)
Method of assessing the state of a rolling bearing based on the relative compensation distance of multiple-domain features and locally linear embedding (Kang et al., 2017) / MSSP	Fault severity estimation / EEMD, SVD, KPCA, LLE, LPP, LTSA	Test rig (CWRU) / SKF 6205-SR2 JEM (39 mm)
Enhancement of fault diagnosis of rolling element bearing using maximum kurtosis fast nonlocal means denoising (Laha, 2017) / Measurement	Fault diagnostics / NL-means	Test rig (CWRU), Test rig (SpectraQuest) / SKF 6205-SR2 JEM (39 mm), REXNORD ER12K (30.2 mm)
Fault diagnosis of rolling element bearing compound faults based on sparse no-negative matrix factorization-support vector data description (Wang, 2016) / JVC	Fault Diagnostics / SNMF, SVDD	Test rig / NU205 (39 mm)

Vibration response mechanism of faulty outer race rolling element bearings for quantitative analysis (Cui et al., 2016b) / JSV	Fault size estimation / Dynamic modeling	Test rig / 6307 (57.5 mm)
Quantitative fault analysis of roller bearings based on a novel matching pursuit method with a new step-impulse dictionary (Cui et al., 2016a) / MSSP	Fault size estimation / Matching pursuit algorithm	Test rig (UNSW) / NACHI 2206GK (45.15 mm)
A fault diagnosis scheme for rolling bearing based on local mean decomposition and improved multiscale fuzzy entropy (Li et al., 2016a) / JSV	Fault diagnostics / LMD, IMFE, LS, ISVM-BT	Test rig (CWRU) / SKF 6205-SR2 JEM (39 mm)
Hierarchical k-nearest neighbours classification and binary differential evolution for fault diagnostics of automotive bearings operating under variable conditions (Baraldi et al., 2016b) / EAAI	Fault diagnostics / MO, BDE, k-NN	Test rig (CWRU) / SKF 6203-2RS JEM (28.5 mm), SKF 6205-SR2 JEM (39 mm)
Fault diagnosis of rolling element bearing using more robust spectral kurtosis and intrinsic time-scale decomposition (Bo and Peng, 2016) / JVC	Fault diagnostics / ITD, SK	Test rig (CWRU) / SKF 6205-SR2 JEM (39 mm)
Rolling element bearing fault detection using PPCA and spectral kurtosis (Xiang et al., 2015) / Measurement	Fault diagnostics / PPCA, SK	Test rig (Spectra Quest) / ER-12 K (33.48 mm)
Fault diagnosis of ball bearings using Synchrosqueezed wavelet transforms and SVM (Wen et al., 2015b) / PHM 2015	Fault diagnostics / DWT, SVM	Test rig (CWRU) / SKF 6203-2RS JEM (28.5 mm), SKF 6205-SR2 JEM (39 mm)
Application of higher order spectral features and support vector machines for bearing faults classification (Saidi et al., 2015) / ISA Trans.	Fault diagnostics / Bispectrum, SVM	Test rig (CWRU) / SKF 6205-SR2 JEM (39 mm)
Singular spectrum analysis and continuous hidden Markov model for rolling element bearing fault diagnosis (Liu et al., 2015) / JVC	Fault diagnostics / SSA, Bispectrum, CHMM	Test rig (CWRU), Test rig (HBRC) / SKF 6205-SR2 JEM (39 mm), 6307 (58.5 mm)
A novel bearing fault diagnosis model integrated permutation entropy, ensemble empirical mode decomposition and optimized SVM (Zhang et al., 2015) / Measurement	Fault diagnostics / PE, IMF, EEMD, SVM	Test rig (CWRU) / SKF 6205-SR2 JEM (39 mm)
Fault size estimation in the outer race of ball bearing using discrete wavelet transform of the vibration signal (Khanam et al., 2014) / Procedia Engineering	DWT	Test rig / SKF BB1B420204 (32.9 mm)
Fault Diagnosis of Bearing Based on KPCA and KNN Method (Wang et al., 2014b) / AMR	Fault diagnostics / KPCA, k-NN	Test rig (CWRU) / SKF 6205-SR2 JEM (39 mm)
Classification of fault location and performance degradation of a roller bearing (Zhang et al., 2013) / Measurement	Fault diagnostics / KPCA, PSO-SVM, EEMD	Test rig (CWRU) / SKF 6205-SR2 JEM (39 mm)
Quantitative diagnosis of a spall-like fault of a rolling element bearing by empirical mode decomposition and the approximate entropy method (Zhao et al., 2013) / MSSP	Fault size estimation / ApEn, EMD	Test rig (CWRU) / SKF 6205-SR2 JEM (39 mm)
Automatic bearing fault diagnosis based on one-class ν-SVM (Fernández-Francos et al., 2013) / CIE	Fault diagnostics / SVM	Test rig (CWRU), Test rig (IMS) / SKF 6203-2RS JEM (28.5 mm), SKF 6205-SR2 JEM (39 mm), REXNORD ZA-2115 (71.5 mm)
Bearing degradation process prediction based on the PCA and optimized LS-SVM model (Dong and Luo, 2013) / Measurement	Fault prognostics / PCA, PSO-SVM	Test rig (IMS) / REXNORD ZA-2115 (71.5 mm)
Classification of fault location and the degree of performance degradation of a rolling bearing based on an improved hyper-sphere-structured multi-class support vector machine (Wang et al., 2012) / MSSP	Fault diagnostics / EMD, HSS-SVM	Test rig (CWRU) / SKF 6205-SR2 JEM (39 mm)
A Support Vector Machine approach based on physical model training for rolling element bearing fault detection in industrial environments (Gryllias and Antoniadis, 2012) / EAAI	Fault diagnostics / SVM	Test rig (CWRU), Industrial pump / SKF 6205-SR2 JEM (39 mm), SKF 22205 EK (41.2 mm)
Signal complexity analysis for fault diagnosis of rolling element bearings based on matching pursuit (Tang et al., 2011) / JVC	Fault diagnostics / Complexity spectrum entropy, Matching pursuit	Test rig / GB203 (28.5 mm)

Rolling element bearing fault diagnosis using autocorrelation and continuous wavelet transform (Kankar et al., 2011) / JVC	Fault diagnostics / Autocorrelation, CWT	Test rig / Ball bearing (25.88 mm)
Development of EBP–Artificial neural network expert system for rolling element bearing (Jayaswal et al., 2011) / JVC	Fault diagnostics / DWT, ANN, Fuzzy rules	Test rig / SKF 1205EKTN9/C3 (33.3 mm)

ORIGINAL PAPERS

I

FLEXIBLE SIMULATOR FOR THE VIBRATION ANALYSIS OF ROLLING ELEMENT BEARINGS

by

Jarno Kansanaho, Kari Saarinen and Tommi Kärkkäinen 2017

International journal of COMADEM

International journal of COMADEM
Vol 20 No 2 (April 2017) 17-22

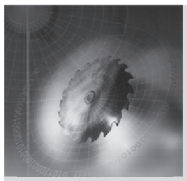

COMADEM
International Journal of Condition Monitoring and Diagnostic Engineering Management

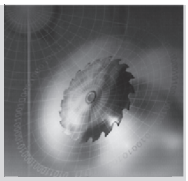

Flexible Simulator for the Vibration Analysis of Rolling Element Bearings

Jarno Kansanaho[a] *, Kari Saarinen[b], and Tommi Kärkkäinen[c]

[a]University of Jyväskylä, Department of Mathematical Information Technology, PO Box 35, FI-40014 University of Jyväskylä, Finland
[b]ABB AB, Corporate Research, Forskargränd 8, SE-721 78, Västerås, Sweden
[c]University of Jyväskylä, Department of Mathematical Information Technology, PO Box 35, FI-40014 University of Jyväskylä, Finland
* Jarno Kansanaho. Tel.: +358-400-248-111; e-mail: jarno.m.kansanaho@jyu.fi

ABSTRACT

The detection of incipient faults as early as possible has great economic value in the monitoring of the rolling element bearings in industrial applications. In the early stage, a local fault in the bearing element produces a series of weak impacts at a rate dependent on the bearing geometry. These impacts in turn excite a special type of vibration that is, in principle, possible to detect using various condition monitoring methods. However, the analysis of vibration measurements taken from a real industrial environment can be challenging because measurements are noisy and periodic phenomena from other external, known and unknown sources may overlap the known behavior of interest, for example, in the spectral representation. In this paper, we present a flexible simulator for advancing early bearing fault detection. In the simulator, the vibration signals are generated by parametric models of the impulse responses for different vibrating components, with adjustable noise and jitter effects included. The possibility to adjust models and parameters during the simulation allows a more realistic exploration of changes, for example, in different operating conditions. This includes the generation of non-stationary components into the vibration signals, which are not suitable per se for frequency domain methods. It is possible to load measured vibration signals to verify the simulation model. The main purpose of the versatile simulation environment is to enable the rigorous testing of analysis tools consisting of digital filters, frequency domain methods (FFT, HFRT), time-frequency methods (STFT, WT) etc. In turn, improved knowledge on the behavior of analysis methods and approaches can be reflected back to the simulation when searching the limits of the early fault detection methods.

Keywords: Rolling element bearings, Early fault detection, Vibration measurements, Spectral analysis, Simulation model

1. Introduction

Rolling element bearings (REBs) are widely used in various machines, motors, wheels, cooling fans etc., to support rotating shafts. Failures of bearings are the most common reason for machine breakdowns. The most common cause of failure is fatigue in REBs [1]. In terms of condition monitoring and system maintenance, research on REB vibrations is essential. An ideal method is a condition-based maintenance that is able to detect incipient faults so early that it is possible to perform the maintenance actions before the bearing fails. Compared to the planned maintenance actions, unplanned stoppages are very expensive.

Generally, REB defects are classified into distributed and localized effects. The distributed effects are surface roughness, waviness, misaligned races, and off-size rolling elements. The localized defects include cracks, pits, and spalls caused by fatigue on the rolling surfaces [2]. The resonances of the bearing parts and housing structure emerge when a rolling element strikes a localized defect; an exponentially decaying ringing is generated [2] [3]. These vibrations in the 2 – 20 kHz range, are commonly measured by acceleration sensors. Ultrasound and acoustic emission measurements cover considerably higher frequencies.

The main motivation for this work is that the weak bearing fault signatures experience interference from noise from different external sources and internal mechanical components, which makes bearing fault detection from real measurements a very challenging task. In this paper, we present a vibration signal simulation approach to improve bearing fault detection analysis.

In the simulator, the vibration signals are generated by parametric models of the impulse responses for different vibrating components, with adjustable noise and jitter effects included. The possibility to adjust models and parameters during the simulation allows a more realistic exploration of changes, for example, in different operating conditions. This includes the generation of non-stationary components into the vibration signals, which are not suitable per se for frequency domain methods. As known, the Fourier transformation does not work very well on vibration signals that contain short and high-frequency pulses, which very important in nonstationary signals [4]. In the time-frequency domain methods, the signal decomposition is performed to split the spectrum into sequential sub-spectral components that are processed individually. The sinusoidal and phase information of local sections of the signal are determined by Short-Time Fourier transform (STFT). Weakness of the STFT is that the constant window size does not provide sufficient frequency and time resolution at the same time [5]. Lately, the wavelet transform has been applied for signal demodulation and optimal band-pass filter design [6]. Wavelet transform has been successfully applied to bearing fault detection [7][8]. However, there is no standard method to select the wavelet function for different purposes, so that the wavelets do not have a standard status in fault diagnostics [9]. Breakdown points, trends and discon-

tinuities in higher derivatives are detectable by using wavelet analysis [10]. Verma and Sreejith introduced a Morlet wavelet based filtering method that efficiently detects weak bearing fault impulses even the signal to noise ratio is very low [11]. In the simulator, the disturbance pulses can be simulated by using wavelet filter constructions. It is possible to load measured vibration signals to verify the simulation model. The simulator is being developed with LabVIEW™ and MATLAB software products.

The nature of the vibrations generated by the REBs, a parametric model of the impulse response and the information about the disturbances, are explained in the second chapter (theoretical background). The flexible simulator and its demonstration in two different scenarios of the vibration signal simulation and analysis are introduced in the third chapter (simulator). Conclusions and ideas for future development are summarized in the fourth chapter.

2. Theoretical background

Vibrations generated by REBs are the vibration of the raceway ring, the vibration of the cage, rolling element passage vibration, vibration due to waviness, vibration due to flaw, vibration due to contamination, and seal vibration [12]. Other than flaw vibrations, the presented vibrations of the REBs can be considered normal. Bearing fault signals have a deterministic part and a stochastic part. The stochastic part is quasi-cyclostationary and very often small because of the low-pass filtering effect of random jitter, combined with the band-pass filtering effect of resonances that are excited [13]. In some cases, the REB signals are modeled as cyclostationary [14].

The local fault in the bearing element produces a series of weak impacts at a rate dependent on the bearing geometry. These impulses occur when the defective part hits other elements of the bearing. If the shaft is rotating at a constant speed, these impacts will occur periodically with a certain frequency, which can be calculated based on the location of the fault, the bearing geometry, and the shaft speed. These frequencies are known as the bearing fault frequencies and can be determined for a fault on: the outer race (Ball Pass Frequency Outer, BPFO), the inner race (Ball Pass Frequency Inner, BPFI), the ball or roller, (Ball Spin Frequency, BSF), and the gage (Fundamental Train Frequency, FTF) [14]. A ratio of the length to width of the localized defects has a remarkable effect on the generated pulse waveform [15].

The dynamic behavior and features of the rolling element bearings are studied using different dynamic simulation models. Jantunen et al. [16] classified dynamic simulation models into the following categories: bearing contact, clearances, EHL contact, distributed defect, and localised defect. Further, the dynamic simulation of the localised defects is divided into geometrical defect, force defect, and defect function.

In the simulations, we need a model for the impulses generated by the defects that is simple to parametrize and at the same time realistic enough. Randall et al. [1] provided a useful analytical equation for a single degree of freedom impulse response:

$$r(t) = Ae^{\left(\frac{-t}{\tau}\right)}\sin(\omega_r t), \quad (1)$$

where ω_r is the frequency of the excited resonance and τ is the damping time constant(s).

Liang and Faghidi evaluated the signal-to-interference ratio when the fault-bearing signal contains multiple interferences. They present a vibration signal model [17] of the form:

$$r(t) = \mathrm{x}(t) + v(t) = Ae^{-\beta t}\cos(\omega_r t + \varphi) + \sum_{k=1}^{A} L_k \cos(\omega_{lk} t), \quad (2)$$

where A is the amplitude of the fault signal, β is the structural damping characteristic, L_k represents the frequency of the k^{th} interference component, x(t) is the vibration signal containing fault generated impulse, and v(t) contains multiple vibration interferences. Instead of the constant amplitude in equations 1 and 2, we have added the possibility to modulate the amplitude based on rotation speed:

$$A(t) = A_0 + A_1 \sin(\omega_{rotation} t), \quad (3)$$

where $\omega_{rotation}$ is the rotation frequency. The modulation term is added into bearing model equation (eq.2):

$$r(t) = \mathrm{x}(t) + v(t) = A(t)e^{-\beta t}\cos(\omega_r t + \varphi) + \sum_{k=1}^{A} L_k \cos(\omega_{lk} t). \quad (4)$$

The occurrences of the impacts in faulty bearing never reproduce exactly at the same position due to the slip of the rolling elements [13]. This random variation is modeled with jitter. Jitter, a measure of uncertainty, is the deviation from the true periodicity of a presumed periodic signal. Jitter can be deterministic, random, or both. Randal et al. presented a model for jitter [14] where the random variable ΔT_i is defined as the difference:

$$\Delta T_i = T_{i+1} - T_i, \quad (5)$$

where T_i is the i^{th} time of occurrence.

The possibility to adjust models and parameters during the simulation allows a more realistic exploration of changes, for example, in different operating conditions. This includes the generation of non-stationary components into the vibration signals, which are not suitable per se for frequency domain methods. Certain components in the rotary machinery, such as rotary blades, frequency converter etc., create vibrations that disturb the analysis. The disturbances can be modeled with a sinusoidal pulse, a parametric pulse model, or a wavelet in the simulator.

Unlike the Short Time Fourier Transform (SFFT), the wavelet transform provides multi-scale analysis. By using dilation and translation, the wavelet transform can extract time-frequency features of a signal efficiently [6]. The frequency resolution increases and the time resolution decreases when the wavelet transform is done at sequentially wide scales. Like Fourier transform the wavelet-transform concludes the basis-function called wavelet. The wavelet family is derived from the mother wavelet by scaling and translation:

$$\psi_{(a,b)}(t) = \frac{1}{\sqrt{a}}\psi\left(\frac{t-b}{a}\right), \quad (6)$$

where ψ is the mother wavelet, a is the scaling (dilation) parameter, and b if the translation parameter. The parameter a controls the window length and effects the frequency resolution; large a for better frequency resolution. As one weakness, the wavelet transform does not maintain the absolute phase of the signal components. A wavelet is orthogonal when the corresponding wavelet transform is orthogonal. When the wavelet transform is invertible the corresponding wavelet is biorthogonal (not necessarily orthogonal). The number of degrees of freedom increases when biorthogonal wavelets are used. For biorthogonal wavelets there are two scaling functions and the scaling sequences may differ. Designing biorthogonal wavelets allows more degrees of freedom than orthogonal wavelets. More flexible wavelets than basic wavelet basis are spline wavelets that are constructed with a spline function. Spline wavelets are cathegorized to interpolatory spline wavelets, B-spline wavelets, cardinal B-spline wavelets, and Battle-Lemarie wavelets. The polynomial and discrete splines are a source for a family of filters, which generate biorthogonal wavelets [18].

The construction of wavelet filter banks concludes the analysis and synthesis functions that perform composition of the original spectrum using sub-spectral components. The wavelet transform is orthogonal when the analysis and the synthesis function sets are the same. For the biorthogonal transform, these function sets are different. A common technique for computing wavelet transform is to use two-channel perfect reconstruction (PR) filter banks: low pass filter $G_0(z)$ and high pass filter $G_1(z)$ form an analysis filter bank and low pass filter $H_0(z)$ and high pass filter $H_1(z)$ form a synthesis filter bank (Figure 1).

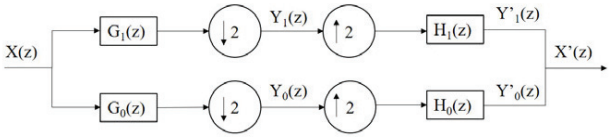

Figure 1. Two-channel filter-bank

The signal X(z) is first filtered by a filter bank constituted by $G_0(z)$ and $G_1(z)$. Then $G_0(z)$ and $G_1(z)$ are down-sampled by two (2) to obtain $Y_0(z)$ and $Y_1(z)$. The desired modifications are done for $Y_0(z)$ and $Y_1(z)$ to process filtering. Filter bank constructed by $H_0(z)$ and $H_1(z)$ is applied for up-sampled $Y_0(z)$ and $Y_1(z)$. The wavelet transformations are special cases of two-channel PR filter banks. Consequently, two-channel PR filter banks do not necessary correspond to the wavelet transform. Biorthogonal filter banks are defined by the equation(s):

$$\sum_n g_i[n-2k]h_i[n] = \delta(k) \text{ and } \sum_n g_i[n-2k]h_l[n] = 0, \quad i \neq l, \forall k \qquad (7)$$

where g and h are finite impulse response (FIR) digital filters (low or high-pass depending of i), δ is the scaling function. For the orthogonal filter bank (special case of biorthogonal), simply set h as g.

3. Simulator

Understanding the nature of the disturbances in complicated vibration signal analysis scenarios will lead to accurate conclusions when selecting and developing vibration signal analysis methods. The flexible simulator offers an interactive tool for the vibration signal simulation and analysis for hard-to-analyze scenarios. The main parts of the simulator are the pulse generator, the vibration signal generator and, the vibration signal analysis module. The simulation and analysis process is described in Figure 2. The pulse generator produces a (shock) pulse based on the parametric model of the impulse response. The model parameters are adjustable. In addition, the white noise can be added to the pulse signal. A real measured pulse can be loaded and plotted into the same window with the simulated signal. This makes it possible to adjust the simulated pulse to match with the true pulse. The vibration signal generator produces the simulated vibration signal. The simulated shock pulses are added to the base signal, based on the adjustable frequency and the first pulse start position. The length of the base signal is given and white noise is added to it. There is often a slight misalignment on the shaft and the rolling element bearings. To simulate this, a sinusoidal low-frequency component is added to the base signal. Signal pre-processing is done with digital filters such as linear continuous-time filter (elliptic), finite impulse response filter (FIR), and wavelet filter. Standard statistical measures, including the root mean square (RMS), peak-to-peak value, crest factor, and kurtosis, are calculated in the analysis module. Mainly frequency domain methods (FFT, HFRT) and time-frequency methods (STFT, WT) are used in the analysis of the vibrations. In addition, with the simulator, it is easy to compare algorithms developed earlier [19] with the newer development (Early SPD) [20]. Improved understanding on the behaviour of the analysis methods and approaches can be reflected back to the simulation, for example, when searching the limitations of the early

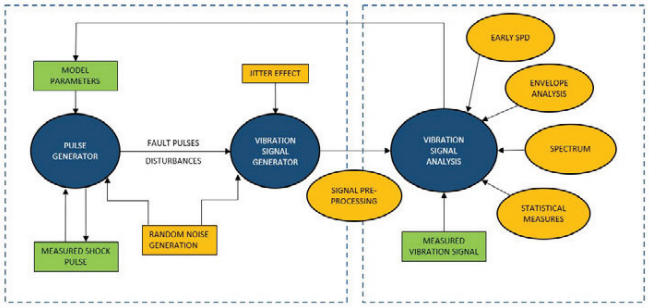

Figure 2. Process flow of the flexible simulator fault detection methods.

The disturbance pulse can be simulated by using wavelet filter constructions. The type of wavelet can be orthogonal or bi-orthogonal for the discrete wavelet analysis and reconstruction. A customized wavelet for the discrete wavelet analysis and reconstruction is designed with the following parameters: product of low pass ($P_0 = G_0 * H_0$) and factorization (type of G_0). P_0 is the product of the low pass analysis filter G_0 and the low pass synthesis filter H_0. $P_0(z)$ satisfies the equation [21]:

$$p_0[n] = \begin{cases} 0 & n \text{ odd and } n \neq l \\ 2 & n = 1 \\ arbitrary & n \text{ even} \end{cases} \qquad (8)$$

Wavelet and filter bank configuration according to the National Instrument's Wavelet and Filter bank design toolkit manual [21] is presented next. The process is divided into the following steps:

1. Design $P_0(z) = G_0(z)H_0(z)$ with $P_0(z)-P_0(-z) = 2z^{-1}$
2. Factorize $P_0(z)$ into $G_0(z)$ and $H_0(z)$
3. Compute $G(-z) = H_1(z)$ and $H_1(z) = -G_0(-z)$

The product of the low pass ($P_0 = G_0 * H_0$) can be max flat, positive equiripple, or general equiripple (biorthogonal). Factorization (type of G_0) contains configuration options for filter type, and zeros at pi (G_0). $P_0(z)$, $G_0(z)$ and $H_0(z)$ are real-valued finite impulse response (FIR) filters. The zeros of these filters are mirror-symmetric about the x-axis in the z-plane. The corresponding wavelet is smoother if there are more zeros at pi. The filter type factorizes P_0 to G_0 and H_0. The filter type is configured with the following options:

- Arbitrary. When the parameter is set, there exists no restriction on the placement of zeros.
- Minimum phase. The parameter defines which zeros of G_0 are located inside the unit circle.
- Linear phase. The parameter defines whether one zero belongs to $G_0(H_0)$
- B-Spline. The parameter defines that except for some zeros at pi, all the zeros of P_0 belong to H_0.

Selecting different values for Filter type puts different constraints on the selections of zeros. For example, if you select Linear Phase for Filter type and select a zero for one filter, the filter automatically contains the reciprocal of the zero. Figure 3 shows the wavelet filter constructions parameters in the user interface [21].

4. Results

The goal of the demonstration of the simulator is to show how the vibrations generated by machine components other than rolling element bearings may create false alarms on defects. Two case studies are introduced. The first simulated signal, as depicted on the top of Figure 4, contains bearing fault pulses, sinusoidal disturbance, and noise. The fault pulse is modeled using equation 4 with the resonant frequency of 2500 Hz. The pulse repetition frequency of the fault, i.e., bearing fault frequency is 10.2 Hz and frequency of sinusoidal disturbance is 7.0 Hz. In the second case, we model disturbances generated by blade and electric motors using pulses with resonant frequencies of 171 Hz (blade) and 4500 Hz (electric motor). The pulse repetition frequencies of the blade and motor disturbance are 5.0 Hz and 12.0 Hz, respectively. There are no fault pulses in the second case; the rolling element bearing is healthy. In the third case, the disturbance (pump) is modeled using biorthogonal wavelet filter construction with b-spline factorization. The pulse repetition frequency of the pump is 10 Hz. There is the same bearing fault pulse (10.2 Hz) in the third as it was in the first case. The simulated vibration signals of the presented cases are shown in the Figure 4; case 1 on the top, case 2 in the middle, and case 3 on the bottom.

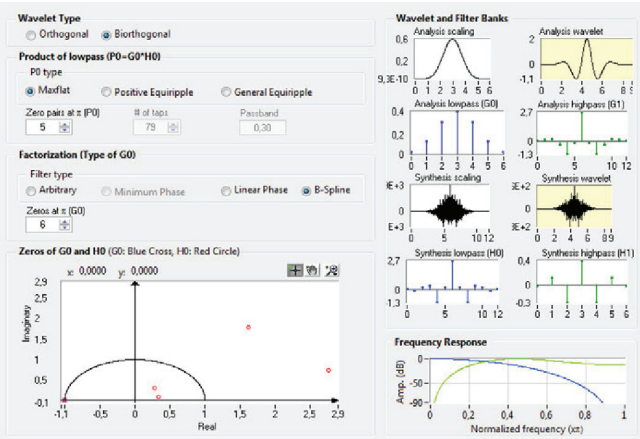

Figure 3. Disturbance modeling using wavelet filter banks

Frequency domain methods, spectrum and envelope spectrum are used in the vibration signal analysis. Like in common envelope analysis, we use the high-pass filter (1500 Hz cut-off-frequency) before calculating the envelope signal and the envelope spectrum. The top most images in Figure 5 incorporate spectra of the first case. The sinusoidal disturbance frequency (1000 Hz) and resonant area exited by fault pulses (2500 Hz) appear in the left hand side. The envelope spectrum reveals clearly the fault frequencies of the simulated vibration signal of a faulty bearing. The frequency axis of the envelope spectrum is normalized according to the rotation speed.

The images in the middle in Figure 5 incorporate the spectra of the second case. The resonant frequencies of the disturbing components are seen in the spectrum. In addition, there are some leakages to lower frequencies. Harmonics of blade- and motor-generated frequencies appear in the spectrum of the enveloped signal (right hand side). Despite the usage of the high-pass filter (1500 Hz), attenuation on the amplitudes of the blade frequency and its harmonics is small in the envelope spectrum. The second harmonic of the blade frequency (10 RPM order) is very close to the bearing fault frequency (10.2 RPM order) that may lead to a false alarm.

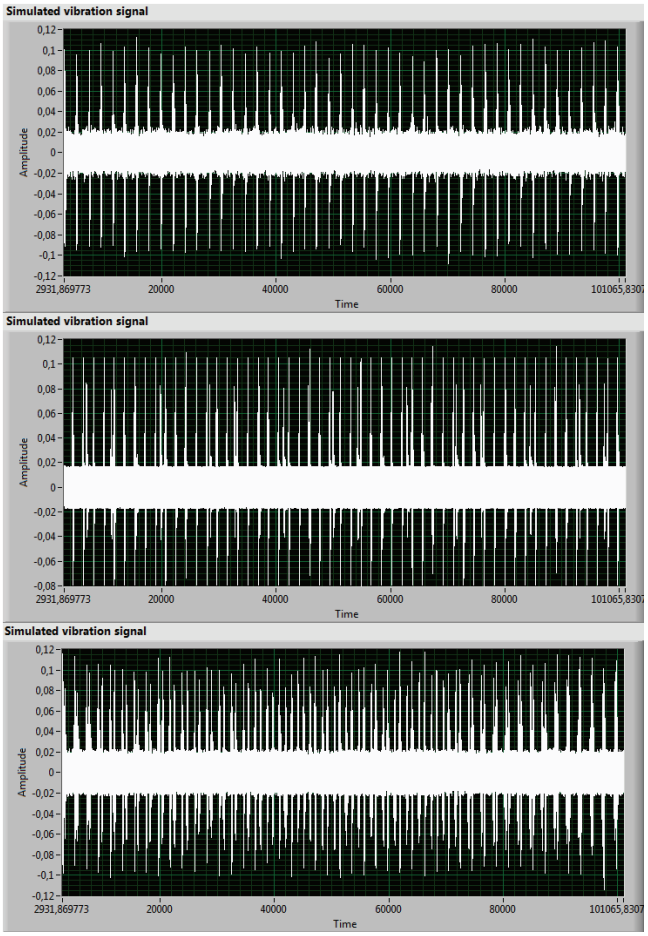

Figure 4. Simulated vibration signals of the case study

The images in the bottom of figure 5 shows spectra of the case 3. The resonant frequencies exited by fault pulses (2500 Hz) and by the disturbance component (pump) are seen in multiple frequency ranges. The spectrum of the enveloped signal reveals the repetition frequency of the pulses (10 RPM order). Since the bearing fault frequency and the pulse repetition frequency of the disturbance are the same, it is impossible to say whether there is a bearing fault or not based on the envelope analysis. The results of the case study are summarized in Table 1.

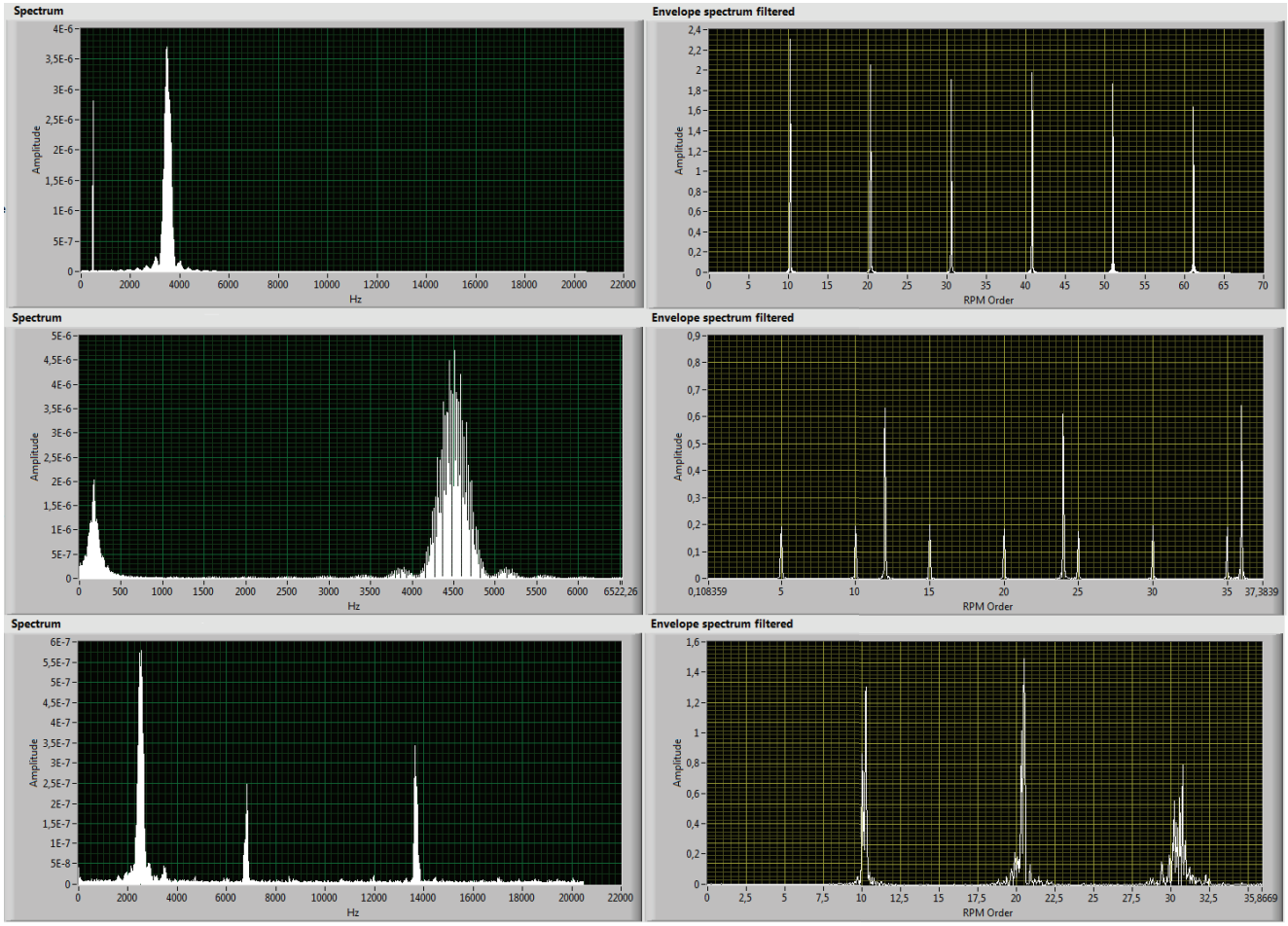

Figure 5. Frequency analysis of the simulated vibration signals

Table 1. Summary of the case study

	Pulse I	**Pulse II**	**Analysis method**	**Result**
Case I	Bearing fault pulse (eq. 4) Resonant frequency 2500 Hz Pulse repetition 10.2 Hz	Sinusoidal disturbance Pulse repetition 1000 Hz	Envelope spectrum	The envelope spectrum reveals clearly the fault frequencies of the simulated vibration signal of a faulty bearing.
Case II	Blade disturbance (eq. 4) Resonant frequency 171 Hz Pulse repetition 5 Hz	Electric motor disturbance (eq. 4) Resonant frequency 4500 Hz Pulse repetition 12 Hz	Envelope spectrum	The second harmonic of the blade frequency (10 RPM order) is very close to the bearing fault frequency (10.2 RPM order) that may lead to a false alarm.
Case III	Bearing fault pulse (eq. 4) Resonant frequency 2500 Hz Pulse repetition 10.2 Hz	Pump disturbance (eq. 7) Pulse repetition 10 Hz	Envelope spectrum	The bearing fault frequency and the disturbance frequencies overlap each other. It is impossible to say whether there is a fault or not by using envelope analysis as only analysis method.

5. Discussion and conclusions

The developed flexible simulator offers a new approach to study vibration signals that are complicated to analyze. The basic idea was to simulate bearing fault pulses and disturbances as they appear in the measured signals. In a perfect simulation scenario, the analysis results should be the same for the simulated and the measured signals. The simulator advances the analysis, especially in the cases when there are disturbing non-stationary components in the vibration signals that create false alarms.

The power of the simulator was demonstrated in the case study. The results of the case study show how the vibrations of the other known machine components disturb the analysis of the vibrations produced by REB faults and the weakness of the used high-pass filter on removing pulsating low-frequency disturbances from the envelope spectrum. Disturbances simulation using complex wavelet modeling is demonstrated with the simulator. With the flexible simulator vibrations of different machinery scenarios can be easily investigated. Further development of the simulator will concentrate on the modeling of disturbances in REB study and the development of an advanced wavelet analysis module.

References

1. Sawalhi, N. and Randall, R.B. (2011). Vibration response of spalled rolling element bearings: Observations, simulations and signal processing techniques to track the spall size, Mechanical Systems and Signal Processing, 25, 846–870
2. Tandon, N. and Choudhury, A. (1997). An analytical model for the predition of the vibration response of rolling element bearings due to a localized defect, Journal of Sound and Vibration, 205(3), 275–292
3. Kiral, Z. and Karagulle, H. (2003). Simulation and analysis of vibration signals generated by rolling element bearing with defects, Tribology International, 36, 667–678
4. Sejdic, E., Djurovic, I., and Jiang, J. (2009). Time–frequency feature representation using energy concentration: An overview of recent advances Digital Signal Processing, 19, 153–183
5. James Li, C. and Ma, J. (1997). Wavelet decomposition of vibrations for detection of bearing-localized defects NDT&E International, Vol. 30, No. 3, 143-149
6. Qiua, H., Leea, J., Linb, J., and, Yuc, G. (2006). Wavelet filter-based weak signature detection method and its application on rolling element bearing prognostics, Journal of Sound and Vibration, 289, 1066–1090
7. Rubini, R. (2001). Application of the envelope and wavelet transform analyses for the diagnosis of incipient faults in ball bearings, Mechanical Systems and Signal Processing, 15(2), 287-302
8. Luo, G. Y., Osypiw, D., and Irle, M. (2003). On-line vibration analysis with fast continuous wavelet algorithm for condition monitoring of bearing, Journal of Vibration and Control, 9, 931-947
9. Peng, Z. K. and Chu, F. L. (2004). Application of the wavelet transform in machine condition monitoring and fault diagnostics: a review with bibliography, Mechanical Systems and Signal Processing, 18,199–221
10. Kumar, H.S., Srinivasa Pai, P., Vijay, G.S. & Raj B.K.N. Rao (2014). Wavelet Transform for Bearing Condition Monitoring and Fault Diagnosis: A Review, 17(1), 9-23
11. Verma, A. K. and Sreejith, B. (2009), Rolling element bearing fault diagnosis using adaptive Morlet wavelet filter, International Journal of COMADEM, 12(4), 25-32
12. Momono, T. and Noda, B. (1999). Sound and Vibration in Rolling Bearings, Motion & Control No. 6
13. Randall, R. B., Antoni, J., and Chobsaard, S. (2001). The relationship between spectral correlation and envelope analysis in the diagnostics of bearing faults and other cyclostationary machine signals, Mechanical Systems and Signal Processing, 15(5), 945–962
14. Randall, R. B. and Antoni, J. (2011). Rolling element bearing diagnostics — A tutorial, Mechanical Systems and Signal Processing, 25, 485–520
15. Liu, J., Shao, Y., and Lim, T. C. (2012). Vibration analysis of ball bearings with a localized defect applying piecewise response function, Mechanism and Machine Theory, 56, 156–169
16. El-Thalji, I. and Jantunen, E. (2015). A summary of fault modelling and predictive health monitoring of rolling element bearings, Mechanical Systems and Signal Processing, 60-61, 252–272
17. Liang, M. and Faghidi, H. (2014). Intelligent bearing fault detection by enhanced energy operator, Expert Systems with Applications, 41, 7223–7234
18. Averbuch, A. Z., Neittaanmäki, P., and Zheludev, V. A. (2014). Spline and Spline Wavelet Methods with Applications to Signal and Image Processing, Volume I: Periodic Splines
19. Toukonen, J., Orkisz, M., Wnek, M., Saarinen, K., and Korendo, Z. (2001). ARMADA – Advanced Rotating Machines Diagnostics Analysis tool for added service productivity. Proceedings of COMADEM2001 conference, (2001) 717–724
20. Saarinen, K. and Nowak, J., A method for detection and automatic identification of damage to rolling bearings. EP 2053375
21. National Instruments Corporation, Wavelet and Filter Bank Design Toolkit Reference Manual, Part Number 321380A-01, January 1997 Edition

II

SPLINE WAVELET BASED FILTERING FOR DENOISING FOR VIBRATION SIGNALS GENERATED BY ROLLING ELEMENT BEARINGS

by

Jarno Kansanaho, Kari Saarinen and Tommi Kärkkäinen 2018

International journal of COMADEM

International journal of COMADEM
Vol # No # (April 2018) p.##-##

COMADEM

International Journal of Condition Monitoring and Diagnostic Engineering Management

Spline wavelet based filtering for denoising vibration signals generated by rolling element bearings

Jarno Kansanaho[a]*, Kari Saarinen[b], and Tommi Kärkkäinen[c]

[a]*University of Jyväskylä, Department of Mathematical Information Technology, PO Box 35, FI-40014 University of Jyväskylä, Finland*
[b]*ABB AB, Corporate Research, Forskargränd 8, SE-721 78, Västerås, Sweden*
[c]*University of Jyväskylä, Department of Mathematical Information Technology, PO Box 35, FI-40014 University of Jyväskylä, Finland*
∗*Jarno Kansanaho. Tel.: +358-400-248-111; e-mail: jarno.m.kansanaho@jyu.fi*

ABSTRACT

In this paper, we study biorthogonal spline wavelet decomposition to extract fault features from vibration signals generated by rolling element bearings. Common challenges in the analysis of vibration measurements taken from a real industrial environment is that non-stationary components, generated by other machine components, disturb the analysis. Vibration signals generated by non-faulty and faulty rolling element bearings are studied. As known, the Fourier transformation does not work very well on non-stationary signals because their spectral content changes over time. In the time-frequency domain methods, signal decomposition is performed to split spectrum into sequential sub-spectral components that are processed individually. The weakness of the short-time Fourier transform is that the constant window size does not provide sufficient frequency and time resolution at the same time. Lately, the wavelet transform has been applied on signal demodulation and optimal band-pass filter design. More flexible than basic wavelet basis are spline wavelets that are constructed with a spline function. Spline wavelets are linear combination of B-splines and they can be defined explicitly. Biorthogonal spline wavelets are regular, compactly supported and have finite impulse response implementation. Computer simulated vibration signals and vibration signals acquired from a real-world application are used in our study.

Keywords: Rolling element bearings, Vibration analysis, Advanced signal processing, Spline wavelets
Corresponding author: Jarno Kansanaho (jarno.m.kansanaho@jyu.fi)

1. Introduction

Rolling element bearing (REB) is one of the most common and the most vulnerable component in machinery. Rolling element bearings, that support rotating shafts, are often installed in extremely hard conditions. A machine becomes inoperable when a rolling element bearing breaks down. Sudden breakdowns can be very expensive. Consequently, detection of the bearing fault as early as possible is very valuable.

Signal processing methods are continuously developed for bearing fault detection. Signal processing methods focus to extract characteristic features from vibration signals generated by REBs. The decision-making based on these extracted features can be considered as the second step in signal processing approaches [1]. Removal of the speed fluctuations, the smearing effect of signal transfer path and the background noise are common challenges in feature extraction from vibration signals [2].

The main motivation for this work is that the weak bearing fault signatures experience interference from noise from different external sources and internal mechanical components, which makes bearing fault detection from real measurements a very challenging task. De-noising (noise reduction) is the key technique to reduce the effect of the disturbing components in the analysis.

Random signals are categorized as stationary and non-stationary. Cyclostationary processes are non-stationary processes whose statistics are periodically varying [3]. Vibration signals generated by rolling element bearings can be modelled as pseudo-cyclostationary [4]. These vibration signals contain short and high frequency pulses that are difficult to identify by the Fourier transform [5]. In the time-frequency domain methods, the signal decomposition is performed to split the spectrum into sequential sub-spectral components that are processed individually. The sinusoidal and phase information of local sections of the signal are determined by Short-Time Fourier transform (STFT). Weakness of the STFT is that the constant window size does not provide sufficient frequency and time resolution at the same time [6].

Lately, the wavelet transform has been used for signal demodulation and optimal band-pass filter design [7]. The wavelet transform has been successfully applied to bearing fault detection [9, 10, 11, 12, 13]. Fault features extracted by wavelet transform can be classified as wavelet coefficients based, wavelet energy

based, singularity based, and wavelet function based [13]. However, there is no standard method to select the wavelet function for different purposes, so that the wavelets do not have a standard status in fault diagnostics [13]. Breakdown points, trends and discontinuities in higher derivatives are detectable by using wavelet analysis [14].

Verma and Sreejith introduced a Morlet wavelet based filtering method that efficiently detects weak bearing fault impulses even if the signal to noise ratio is very low [15]. Yumona et. al. used a Morlet wavelet bank for denoising and obtained the resonance band of interest from the wavelet kurtogram [16]. It has been shown that the discrete wavelet transform (DWT) can be used to detect single and multiple faults in the ball bearings [11]. Mori et.al. used a trend of the wavelet coefficients maximum values, acquired with the DWT analysis, to predict spalling of rolling element bearings [20]. The wavelet packet transform has been utilized often in the condition monitoring of the rolling element bearings [17, 18, 19]. It has been noticed that the Wavelet packet transform (WPTT) has better de-noising ability on non-stationary signals because the frequency resolution of the DWT may not be enough to extract important features from the decomposed part of the signal [18]. The Haar wavelet transform has been applied to transient detection [21]. Tse et. al. introduced exact wavelet analysis that used genetic algorithm to generate an adaptive daughter wavelet to match the inspected signal as exactly as possible [22]. Frequency B-spline wavelets have been applied to bearing fault detection by selecting the spline wavelet based on the prior knowledge of the impulse responses [23].

2. Theoretical background

The wavelet transform enables multiresolution analysis with dilated windows. In other words, the wavelet transform is a constant relative bandwidth analysis [24]. By using dilation and translation, the wavelet transform can extract time-frequency features of a signal efficiently [15]. It is an excellent tool to analyze non-stationary signals. The frequency resolution increases and the time resolution decreases when the wavelet transform is done at sequentially wide scales. Like Fourier transform the wavelet-transform concludes the basis-function called mother wavelet.

The continuous wavelet transform (CWT) transforms signal to a two-dimensional time-scale joint representation. The idea of the CWT is to calculate continuously scalable function by moving this function continuously over a signal. As result, the wavelet coefficients are acquired. However, the bases of the scalable functions become non-orthogonal that makes wavelet coefficients redundant [25]. The definition of the CWT as the function of time is:

$$T(a,b) = \int_{-\infty}^{\infty} f(t)\,\psi^{*}_{(a,b)}(\mathrm{t})\mathrm{dt}, \qquad (1)$$

where ψ is the mother wavelet and * refers to complex conjugation. Here, the transformation of mother wavelet reads as:

$$\psi_{(a,b)}(t) = \frac{1}{\sqrt{a}}\psi\left(\frac{t-b}{a}\right) \quad (a,b \in R, a \neq 0), \qquad (2)$$

where a is the scaling (dilation) parameter, and b if the translation parameter. The parameter a controls the window length and effects the frequency resolution; large a for better frequency resolution.

The time-scale joint representation of a discrete wavelet transform (DWT) is a grid along the scale and time axes. The discrete wavelet is a piecewise continuous function. The discretization of the wavelet is done by sampling the time-scale axis at discrete intervals. Usually dyadic sampling is used with a geometric sequence of ratio two. The DWT as a function of time:

$$\psi_{(i,j)}(t) = \frac{1}{\sqrt{2^i}}\left(\frac{t-2^i j}{2^i}\right), \qquad (3)$$

where the dilation term is 2^i and translation term is 2^ij.

As one weakness, the wavelet transform does not maintain the absolute phase of the signal components. A wavelet is orthogonal when the corresponding wavelet transform is orthogonal. When the wavelet transform is invertible the corresponding wavelet is biorthogonal (not necessarily orthogonal). The number of degrees of freedom increases when biorthogonal wavelets are used. For biorthogonal wavelets, there are two scaling functions whose scaling sequences may differ. Designing biorthogonal wavelets allows more degrees of freedom than orthogonal wavelets. The semi-orthogonal wavelets were introduced when relaxation of the intra-scale orthogonality constraint was founded [26]. Wavelets are categorized into families based on their properties. Some of the important properties of the wavelets are regularity, symmetry or anti-symmetry, a number of vanishing moments and existence of a scaling function. In practice, for example a greater number of vanishing moments provide sharper frequency resolution.

More flexible wavelets compared to the basic forms are obtained by using spline wavelets that are constructed with a spline function. Spline wavelets are categorized to interpolatory spline wavelets, B-spline wavelets, cardinal B-spline wavelets, and Battle-Lemarie wavelets. The polynomial and discrete splines are a source for a family of filters, which generate biorthogonal wavelets [27]. The greatest benefits of using spline wavelets are [28]:

- Polynomial spline bases have a simple and explicit analytic form that is easy to manipulate; differentiation and integration.
- The B-splines have compact support.
- Any degree of regularity is achieved by increasing the order of the polynomial splines.
- Polynomial splines are piecewise constant functions in the simplest case.

A polynomial spline function of degree n is defined by a linear combination of shifted B-splines [28]:

$$g^n(x) = \sum_{k=-\infty}^{+\infty} c(k)\beta^n(x-k), \qquad (4)$$

where c(k) is the sequence of B-spline coefficients and $\beta^n(x)$is the central B-spline of order n which definition is:

$$\beta^n(x) = \beta^n * \beta^{n-1}(x), \qquad (5)$$

where $\beta^0(x)$is the characteristics function and * is the convolution operator. B-spline is visualized in the Figure 1.

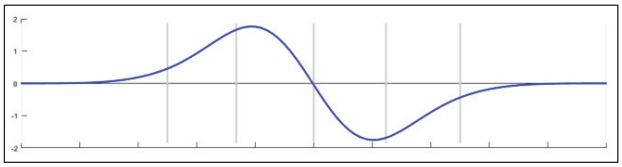

Figure 1B-spline of order 6 contains six polynomial pieces of order 5

The compactly supported B-spline wavelet of order m is defined by the equation [29]:

$$\psi_m(x) = \frac{1}{2^{m-1}}\sum_{j=0}^{2m-2}(-1)^j N_{2m}(j+1)N_{2m}^{(m)}(2\mathrm{x}-\mathrm{j}). \qquad (6)$$

When m is set to 1, the equation 6 defines the Haar wavelet [29]:

$$\psi_1(x) = \begin{cases} 1, when\ 0 < x < 1/2 \\ -1, when\ 1/2 < x < 1 \\ 0, otherwise\,. \end{cases} \qquad (7)$$

Biorthogonal spline wavelets are regular, compactly supported and have FIR (finite impulse response) implementation. The simplest B-spline biorthogonal wavelet is bior1.1 that contain reconstruction and decomposing filters with one vanishing moment each. Figure 2 shows decomposing (analysis) and reconstructing (synthesis) filters of bior1.1.

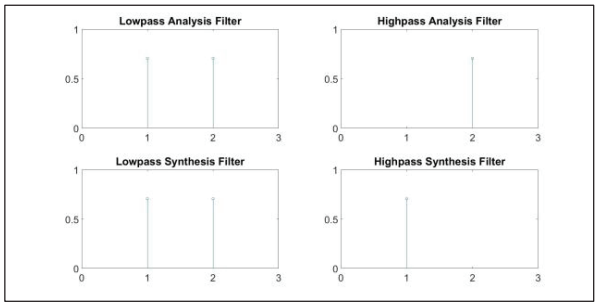

Figure 2 Decomposing and reconstructing filters of bior1.1

When the number of vanishing moments are increased, complex function can be represented with a sparser set of wavelet coefficients. Figure 3 incorporates decomposing and reconstructing scaling filters of bior6.8.

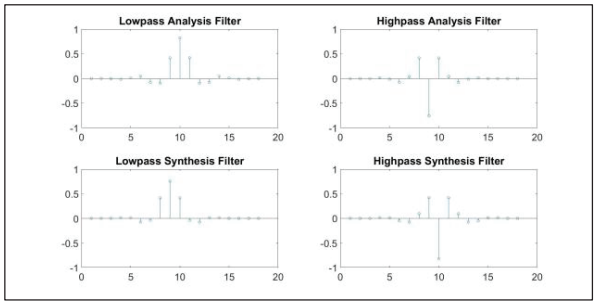

Figure 3 Decomposing and reconstructing filters of bior6.8

Biorthogonal spline wavelet filtering is applied to de-noising of the vibration signals in the experimental part of this work. The construction of wavelet filter banks concludes the analysis and synthesis functions that perform composition of the original spectrum using sub-spectral components.

3. Experimental part and results

Biorthogonal spline wavelet based filtering for denoising of vibration signals is presented in this case study. Simulated and real-world measured vibration signals are analyzed. Decomposition of vibration signals was done with biorthogonal spline wavelets: bior1.1, bior1.3, bior1.5, bior2.2, bior2.4, bior2.6, bior2.8, bior3.1, bior3.3, bior3.5, bior3.7, bior3.9, bior4.4, bior5.5, and bior6.8. These common wavelets provide versatile set of filters for de-noising. Reconstruction of vibration signal is done separately for each decomposition level. Simultaneously other levels are filtered by using soft thresholding. Hilbert transform based envelope spectrum is calculated for reconstructed signals. Finally, peak detection based on local maxima and thresholding is applied for fault frequency peak detection.

The process of the experimental work is the following:

- Vibration signal preparation
  - Simulation of background noise, disturbing pulses and bearing fault pulses
  - Import measured vibration signal data
- The CWT study of the vibration signal using biorthogonal spline wavelets
- Vibration signal decomposition using biorthogonal spline wavelets
- Envelope analysis of the original signal and the wavelet filtered signal
- Fault frequency peaks detection from the envelope spectrum

The first case incorporates the analysis of the simulated vibration signal. The disturbance pulse is modeled using a wavelet function and it's repetition frequency is 5.0 Hz. Addition to, white noise is added to signal by signal to noise ratio of 5.0. The top most image in Figure 4 incorporate the vibration signal of the first case. The CWT is performed on the vibration signal by using biorthogonal spline wavelet (bior1.3). The bottom image in Figure 4 show the scaleogram of the signal. The envelope spectrum of the simulated signal shows the assumed disturbance frequency (Figure 5). The envelope spectrum of the raw simulated signal and the wavelet filtered signal (bior1.3) are plotted blue and brown colors respectively.

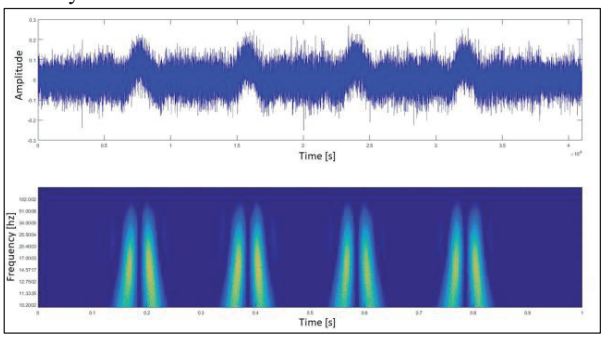

Figure 4 Case 1: The CWT analysis (bior1.3)

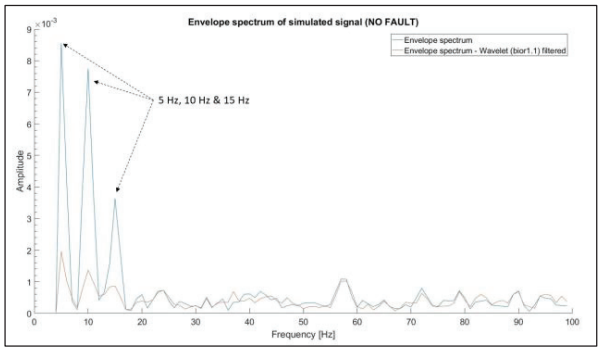

Figure 5 Case 1: Envelope spectrum

In the second case the vibration signal model presented by Kansanaho et.al. is applied in the simulation [30]. The resonant frequency of the bearing fault pulse is 500 Hz and the bearing fault frequency is 11.0 Hz. The same disturbance pulse with repetition frequency of 5.0 Hz as in the first case, is simulated in the second case. Figures 6 and 7 include different frequency bands of the scaleograph that stand out the modelled pulses. Figure 8 show the envelope spectra of the raw simulated signal (blue) and the wavelet filtered signal (bior1.3, brown). The envelope spectrum of the simulated vibration signal includes high amplitudes of disturbance pulse and it's harmonics (5 Hz, 10 Hz, 15 Hz). The wavelet-filtered signal does not contain the low frequency disturbance. The bearing fault frequency and its harmonics are clearly seen (11 Hz, 22 Hz, 33 Hz).

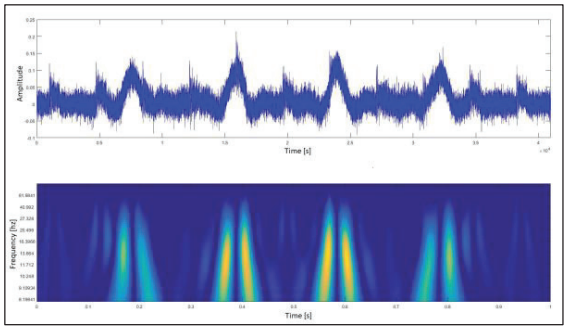

Figure 6 Case 2: The CWT analysis, the disturbance pulse

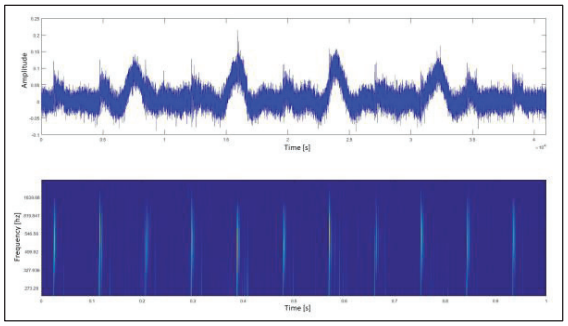

Figure 7 Case 2: The CWT analysis, the fault pulse

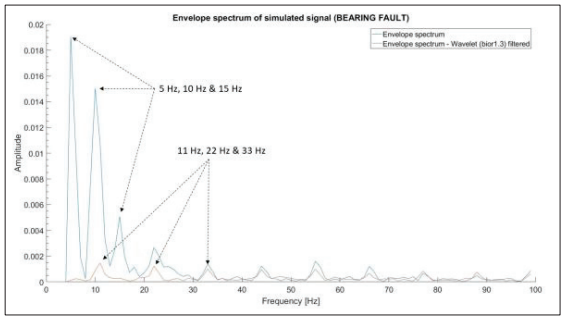

Figure 8 Case 2: Envelope spectra of the simulated and the filtered signal

Case 3 consists of analysis of vibration signals acquired from a real-world application. The first sample includes a clear inner race bearing fault. Biorthogonal spline wavelets bior3.5 and bior6.8, emerged as the most appropriate filters to detect the characteristic bearing fault frequencies from the measured signal. Figure 9 shows the CWT analysis of decomposition of the frequency band (approximately 2000 Hz). Envelope spectra of the high-pass filtered signal (1000 Hz) and the wavelet filtered signal show high intensity bearing fault frequency peaks in Figure 10. One of the shock pulses produced by the bearing fault is zoomed in Figure 11. Note that Sawalhi and Randall observed a low frequency step response before a broader impulse response in the acceleration signals and used this particular information for spall size estimation [31]. In our data, there exists no similar step response before the impulse response.

Figure 12 introduces a vibration signal that does not contain a bearing fault. The CWT analysis by using bior3.5 and bior6.8 reveals resonating frequencies between 200 Hz and 400 Hz. These impulses are indigenous from different surrounding components.

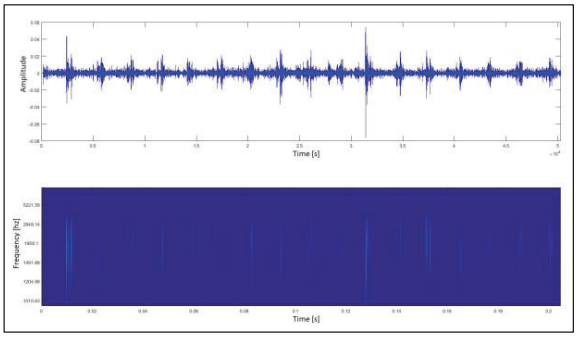

Figure 9 Case 3: The CWT analysis, a measured signal with bearing fault

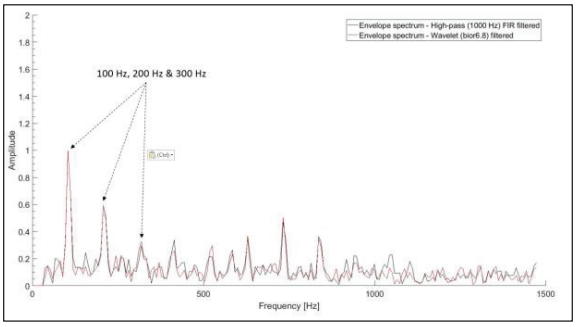

Figure 10 Case 3: Envelope spectra of the high-pass filtered and the wavelet filtered signal (BPFI fault)

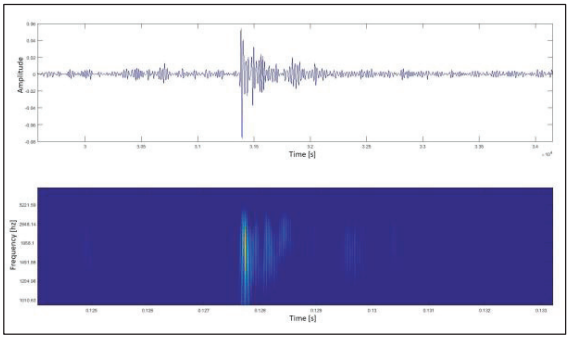

Figure 11 Case 3: Individual bearing fault pulse zoomed in

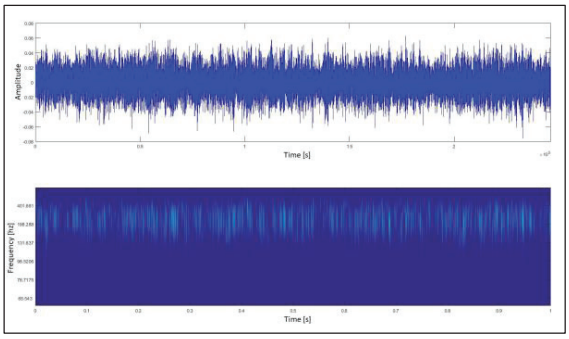

Figure 12 Case 3: Measured signal, no bearing fault

Lastly, a measured vibration signal with weak bearing fault signature is analyzed. The bearing fault is at early stage. The CWT analysis (Figure 13) with bior3.5 and bior6.8 reveal the bearing fault pulses with approximate a resonant frequency of 2000 Hz. Characteristic frequency of inner race fault (BPFI) and it's harmonics appear clearly in the envelope spectrum (Figure 14); plotted with brown. For comparison the envelope spectrum of the high-pass filtered signal (1000 Hz), plotted with black color, is included in the Figure 14. An individual shock pulse is more fragmented than in the previous signal.

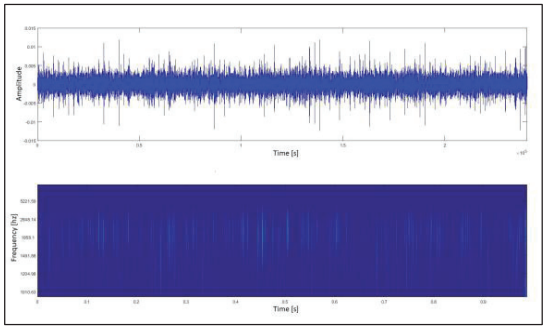

Figure 13 Case 3: The CWT analysis, a measured signal; a bearing fault with weak signature

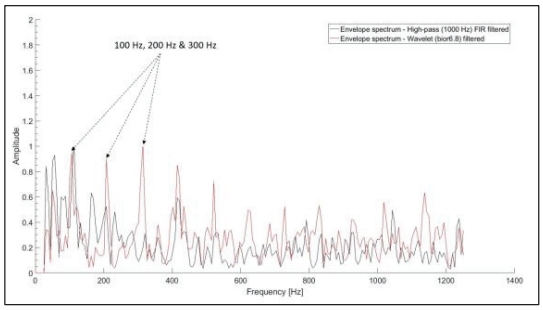

Figure 14 Case 3: Envelope spectra of the high-pass filtered and the wavelet filtered signal (BPFI fault)

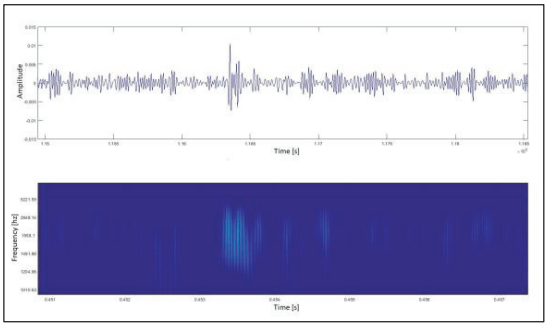

Figure 15 Case 3: Invidual bearing fault pulse zoomed in

We presented a set of case studies with biorthogonal spline wavelet based identification of bearing faults. It was shown that there exists a (not always the same) biorthogonal spline wavelet, which can be used to process the vibration signal.

4. Conclusions and discussion

Biorthogonal spline wavelet decomposition is an efficient method to extract weak bearing fault signatures from vibration signals. Non-stationary components of the vibration signal can be extracted and, if necessary, they can be filtered. It has been remarked earlier that Hilbert transform together with the wavelet transform wherein Morlet wavelet is used as mother wavelet, do not successfully address how to enhance the weak signature from a noisy signal and how to detect early stage defects [8]. However, by using our approach fault frequencies can be detected in early stage in the presented case study. The decomposition was done by using 14 different biorthogonal wavelets with increasing complexity. Biorthogonal wavelets bior3.5 and bior6.8 proved to be the best for fault signature extraction when the measured vibration signals were analyzed. There exists no unified method to select the wavelet function for different purposes, so this part of the proposed approach needs manual elaboration. The implementation to fast algorithm is possible with efficient implementations available. Previously developed flexible simulator offered a new way to study complicated vibration signals [31]. The simulator incorporates generation of vibration signals and analysis of them and then the reflection back to parameters of the simulation model. Moreover, the flexible simulation of the vibration signals is a great tool when developing and testing denoising filters.

Acknowledgments

References

1. Akhand Rai and S.H. Upadhyay, A review on signal processing techniques utilized in the fault diagnosis of rolling element bearings, Tribology International 96 (2016) 289–306
2. I. El-Thalji and E. Jantunen, A summary of fault modelling and predictive health monitoring of rolling element bearings, Mechanical Systems and Signal Processing 60-61 (2015) 252–272
3. J. Antoni (2006), The spectral kurtosis: a useful tool for characterising non-stationary signals, Mechanical Systems and Signal Processing 20, 282–307
4. R. B. Randall, and Jerome Antoni (2011), Rolling element bearing diagnostics — A tutorial, Mechanical Systems and Signal Processing 25, 485–520
5. Sejdic, E., Djurovic, I., and Jiang, J. (2009). Time–frequency feature representation using energy concentration: An over-view of recent advances Digital Signal Processing, 19, 153–183
6. James Li, C. and Ma, J. (1997). Wavelet decomposition of vibrations for detection of bearing-localized defects NDT&E International, Vol. 30, No. 3, 143-149
7. Qiua, H., Leea, J., Linb, J. and, Yuc, G. (2006), Wavelet filter-based weak signature detection method and its application on rolling element bearing prognostics, Journal of Sound and Vibration 289, 1066–1090
8. Rubini, R. (2001). Application of the envelope and wavelet transform analyses for the diagnosis of incipient faults in ball bearings, Mechanical Systems and Signal Processing, 15(2), 287-302
9. Xinsheng, L. and Loparo, A. K. (2004), Bearing fault diagnosis based on wavelet transform and fuzzy inference, Mechanical Systems and Signal Processing 18 (2004) 1077–1095
10. Seker, S. and Ayaz, E. (2003), Feature extraction related to bearing damage in electric motors by wavelet analysis. Journal of the Franklin Institute 340 125–134
11. Prabhakar, S., Mohanty, A.R. and A.S. Sekhar, Application of discrete wavelet transform for detection of ball bearing race faults, Tribology International 2002; 35(12): 793–800.
12. Luo, G. Y., Osypiw, D., and Irle, M. (2003). On-line vibration analysis with fast continuous wavelet algorithm for condition monitoring of bearing, Journal of Vibration and Control, 9, 931-947
13. Peng, Z. K. and Chu, F. L. (2004). Application of the wavelet transform in machine condition monitoring and fault diagnostics: a review with bibliography, Mechanical Systems and Signal Processing, 18,199–221

14. Kumar, H.S., Srinivasa Pai, P., Vijay, G.S. & Raj B.K.N. Rao (2014). Wavelet Transform for Bearing Condition Monitoring and Fault Diagnosis: A Review, 17(1), 9-23

15. Verma, A. K. and Sreejith, B. (2009), Rolling element bearing fault diagnosis using adaptive Morlet wavelet filter, International Journal of COMADEM, 12(4), 25-32

16. M. Yuwono, Y. Qin, J. Zhou, Y. Guo, B. G. Celler, S. W. Su (2016), Automatic bearing fault diagnosis using particle swarm clustering and Hidden Markov Model, Engineering Applications of Artificial Intelligence 47, 88-100
17. N. G. Nikolaou and I. A. Antoniadis (2002), Rolling element bearing fault diagnosis using wavelet packets, NDT&E International 35, pp. 197-205

18. J. L. F. Chacon, V. Kappatos, W. Balachandran, and T. H. Gan (2015), A novel approach for incipient defect detection in rolling bearings using acoustic emission technique. Applied Acoustics 89, pp. 88–100

19. F. Sloukia, M. El Aroussi, H. Medromi, M. Wahbi (2013), Bearings prognostic using mixture of Gaussians hidden Markov model and support vector machine, Proceedings of IEEE ACS international conference on computer systems and applications (AICCSA), p. 1–4.

20. K. Mori, N. Kasashima, T. Yoshioka, and Y. Ueno (1996), Prediction of spalling on a ball bearing by applying the discrete wavelet transform to vibration signals, Wear, 195(1):162–8.

21. J. Pineyro, A. Klempnow, and V. Lescano, Effectiveness of new spectral tools in the anomaly detection of rolling element bearings, Journal of Alloys and Compounds 310 (2000) 276–279

22. Tse, P. W., Yang, W-X. and Tam H.Y. (2004), Machine fault diagnosis through an effective exact wavelet analysis. Journal of Sound and Vibration 277 (2004) 1005–1024

23. D. Paliwal, A. Choudhury, G. Tingarikar, Wavelet and scalar indicator based fault assessment approach for rolling element bearings. Procedia Materials Science 5 (2014) 2347 – 2355.

24. J. Kovacevic and M. Vetterli (1995), Wavelets and Subband Coding, Prentice Hall PTR

25. Y. Sheng (2000), “Wavelet Transform.”, The Transforms and Applications Handbook: Second Edition, Ed. Alexander D. Poularikas, Boca Raton: CRC Press LLC

26. M. Unser, P. Thenenaz, and Akram Aldroubi (1996), Shift-Orthogonal Wavelet Bases Using Splines, IEEE Signal Processing Letters, Vol. 3, No. 3

27. A. Z. Averbuch, P. Neittaanmäki, and V. A. Zheludev (2014), Spline and Spline Wavelet Methods with Applications to Signal and Image Processing, Volume I: Periodic Splines

28. M. Unser, P. Thenenaz, and Akram Aldroubi (1992), “Polynomial Splines and Wavelets – A Signal Processing Perspective”, Wavelets – A tutorial in Theory and Applications, Ed. C. K. Chui, pp. 91-122

29. C. K. Chui and J.-Z. Wang (1992), On Compactly Supported Spline Wavelets and a Duality Principle, Transactions of the American Mathematical Society, Volume 330, Issue 2, pp. 903-915

30. J. Kansanaho, K. Saarinen, and T. Karkkainen (2017), Flexible Simulator for the Vibration Analysis of Rolling Element Bearings, International Journal of COMADEM, Vol 20,No 2

31. Sawalhi, N. and Randall, R.B. (2011). Vibration response of spalled rolling element bearings: Observations, simulations and signal processing techniques to track the spall size, Mechanical Systems and Signal Processing, 25, 846–870

III

HYBRID VIBRATION SIGNAL MONITORING APPROACHFOR ROLLING ELEMENT BEARINGS

by

Jarno Kansanaho and Tommi Kärkkäinen 2019

In Proceedings of European Symposium on Artificial Neural Networks, Computational Intelligence and Machine Learning (ESANN 2019)

Hybrid vibration signal monitoring approach for rolling element bearings

Jarno Kansanaho[1] and Tommi Kärkkäinen[1*]

1- University of Jyvaskyla - Faculty of Information Technology
Jyvaskyla - Finland

Abstract. New approach to identify different lifetime stages of rolling element bearings, to improve early bearing fault detection, is presented. We extract characteristic features from vibration signals generated by rolling element bearings. This data is first pre-labelled with an unsupervised clustering method. Then, supervised methods are used to improve the labelling. Moreover, we assess feature importance with each classifier. From the practical point of view, the classifiers are compared on how early emergence of a bearing fault is being suggested. The results show that all of the classifiers are usable for bearing fault detection and the importance of the features was consistent.

1 Introduction

In general terms, rolling-element bearings (REBs) are common elements in various rotating machines and the failure of a bearing is a common cause of machine breakdowns. Economical and human losses due to an unexpected failure of a critical bearing can be extensive [1]. They can be prevented and significantly reduced by applying a proper maintenance strategy [2]. Vibration measurements are the most widely used method for detection and diagnosis of bearing faults [3]. Signal processing methods are continuously developed for bearing fault detection. These methods focus to extract characteristic features from vibration signals.

Wear, a measure of condition, accumulates over time and the cumulative wear is measured at chosen times in the machine condition monitoring systems [4]. Presentation of the wear evolution process as a time series describes the wear interaction and evolution at different lifetime stages. El-Thalji et al. introduced a five-stage descriptive model of wear evolution including: running-in, steady-state, defect initiation, defect propagation, and damage growth [5]. The main period of interest is between the steady state and the defect initiation and the propagation stages. Hence, in general we try to identify the time-instance of the occurrence of such a concept drift [6].

In doing so, the feature data is pre-labelled with an unsupervised method for a preliminary identification of the defect initiation. A similar time-series clustering approach was also used in[7]. Then, three popular supervised classification techniques [8], also central for the determination of concept drift [6], are applied and tested to sharpen the unsupervised result. Note that recently a combination of unsupervised fuzzy clustering and supervised learning to improve a machine

*The work supported by the Academy of Finland from grants 311877 and 315550.

learning method referred as minimum learning machine was proposed in [9]. Our study confirms that the proposed novel, hybrid combination of methods is useful, real-time applicable, and reliable for early bearing fault detection.

2 Methodological Background

As described above, condition monitoring and preventive maintenance are based on proper processing of measurement data [10, 2]. We describe next the basics of those methods that will be applied as part of the proposed approach.

2.1 Unsupervised learning

Fuzzy clustering algorithms, especially the fuzzy c-means (FCM) which was originally developed by Ruspini [11], generalize the k-means by allowing data points to belong to multiple clusters. This relation is represented with a membership function. Such an approach is appealing especially in the condition monitoring setting, where we have no fixed change-points but a gradual evolution of different lifetime stages [5]. The FCM algorithm was further developed by Dunn and Bezdek [12, 13].

We use FCM clustering to identify the different REB lifetime-stages. The number of centroids corresponds to number different life-time stages. Our techniques are different but the basic idea is similar to [7]. Transition states between lifecycle stages are not characterized by sudden changes in the characteristic features of vibration signals. Consequently, FCM clustering produces overlapping clusters. Yiakopoulos et al. introduced a k-means clustering approach for the diagnosis of the bearing faults [14]. They used a set of features based on vibration energies in the frequency domain and statistical time-domain indices [14].

2.2 Supervised learning

In this experimental study, we examine different supervised classification methods, namely K-nearest-neighbors (KNN), Naive Bayes (NB), and Support Vector Machine (SVM), in terms of how well they are able to generalize the lifetime stage labelling from characteristic features of vibration signals. Previously, performance of various supervised classifiers (including the techniques here) on acoustic emission measurements of REBs were compated in [8]. The KNN classifier was found as the best suited there.

The K-nearest neighbor classification rule was originally introduced by Cover and Hart [15]. The KNN rule is applicable on data that is in the metric space and it does not make assumptions on the distribution of data. Support vector machine (SVM) is a supervised machine learning algorithm that can be used for both classification and regression problems. General review of the use of SVM in condition monitoring and fault diagnostics was given in [16]. The naive Bayes (NB) classifier is a probabilistic classifier that is based on the Bayes theorem.

The NB classifier considers prior probability of the predicted class when the likelihood of that class is calculated [17].

Quality of the classifiers was assessed using ten-fold cross-validation with misclassification in percentages (MCP) as error measure. We used Distribution Optimally Balanced Stratified Cross Validation (10-DOB-SCV), which tries to keep data distribution as similar as possible between the training and test data by minimizing the covariate shift [18, 19]. Analysis of feature saliency (importance) was carried out with each classifier, to identify the most informative features. It was estimated using backward elimination of individual features one-by-one [20, 21]. All MCP errors $\{e_i\}_{i=1}^{n}$ are sorted to the descend order in order to identify the ranking of features, where n is the number of features. Moreover, relative importance of each feature in percentages, MCP order, is estimated simply by taking $100\frac{e_i}{\sum_{i=1}^{n} e_i}$.

3 Experimental results

Vibration data were generated by the NSF I/UCR Center for Intelligent Maintenance Systems (IMS) with support from Rexnord Corp. in Milwaukee, WI [22]. The vibration data was collected from the IMS bearing test rig. Total of four bearings (Rexnord ZA-2115) were installed on a shaft. All the tests were "run-to-a-failure" tests. We use vibration signals from two test runs. The first case includes an inner race fault in the bearing. The second case includes an outer race fault in the bearing. The sampling rate of the vibration measurements was 20 kHz and the measurements were recorded every ten minutes. The total number of vibration measurements were 2156 and 4448 in these two datasets.

Commonly used statistical time-domain degradation features are used: 1.Root mean square 2.Crest factor, 3.Shape factor, 4.Impulse factor, 5.Mean frequency, 6.Skewness, 7.Kurtosis and 8.Entropy [23, 24]. The ninth (9.) feature, which is the only frequency-domain feature, refers to the amplitude of the characteristic bearing fault frequency in envelope spectrum. Later in the results, the features are referred to by order number.

3.1 Unsupervised clustering

FCM clustering is performed with four centroids for the unsupervised vibration features data. The moving median of 50 samples is used to smoothen the feature data before the fuzzy c-means. Length of the median window is c. 8.3 hours that gives good resolution for life-time stage identification. Vibration data covers almost the entire lifetime of the investigated bearings. Figure 1 presents the FCM clustering results for both cases. The classification indicator is a floating point value between zero and one. The first indication of a bearing fault is seen as an increment in the indicator values of the first class (1) in both cases. This change point is interpreted as the beginning of the defect initiation stage (the first black dotted line). When the defect initiation stage shifts to the propagation stage, changes are seen in the second class (2). The assumed beginning of the damage growth stage begins when the indicator value of the third class (3) increases.

The defect initiation, the defect propagation and the damage growth stages are clearly separated by fuzzy c-means clustering.

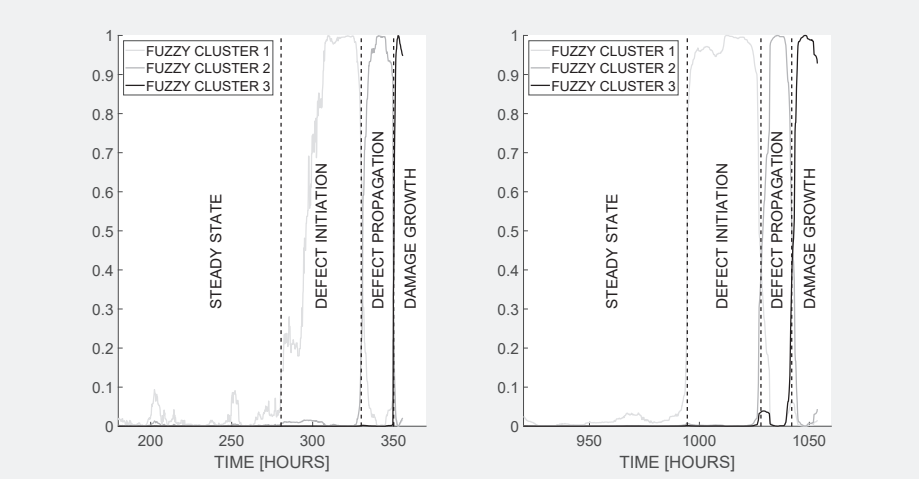

Fig. 1: Lifetime stage identification using c-means fuzzy clustering (Case 1 on the left side, Case 2 on the right side)

3.2 Supervised classification

The evaluation of the classifiers is done for the merged data of both cases, containing 4481 feature data points. Moreover, results from the unsupervised processing were used to introduce binary labelling of the time-series, where the label changes corresponded to the unsupervised identification of the time instances for the emergence of the defect initiation stage. The feature data split by 10-DOB-SCV and the bearing fault detection is done for the partitioned data. Hence, the start time of the defect initiation state was set as a zero point to compare how early different classifiers detect the bearing fault.

The quantified results of the evaluation of the classifiers and the bearing fault detection estimations are listed in Table 1. First, the optimal number of nearest neighbors (k) for the KNN classifier is estimated by using 10-DOB-SCV, i.e., by seeking the minimal CV-error. As a result k=5 was fixed. In each experiment, the CV-errors were calculated separately for all classifiers. All the calculations were repeated for 15 times. Average of the CV-errors for the KNN, SVM and NB classifiers are roughly equal 3.5%, 3.3% and 3.3%, respectively. The standard deviation of the CV-errors are fairly unobtrusive. The MCP order (%) range is between 9.3% - 11.1% for all features (1-9), which means that every feature is important in the classification for all classifiers. The KNN classifier detected the bearing fault about 51 hours before the zero point, i.e., before the first suggestion of the unsupervised FCM. The SVM- and NB-classifiers also detected the bearing fault c. 31 hours and c. 46 hours before the zero point, respectively.

	KNN	SVM	NB
CV-error mean	0.035	0.033	0.033
CV-error std	0.006	0.006	0.006
Earlier fault detection mean [hours]	51	33	46
Earlier fault detection std	2.7	3.7	1.8

Table 1: Supervised classification results (15 runs).

4 Conclusions

Our experiments confirmed that the results from FCM clustering can be used for the initial identification of different lifetime stages of rolling element bearings. Identification of the defect initiation, the defect propagation and the damage growth stages succeeded quite well. Utilization of the FCM clustering was straightforward. However, the feature data were smoothen by median averaging.

The studied supervised classification methods were not easy to implement with the presented feature data of vibration signals. The affecting parameters of the classifiers need to be configured properly and the sensitivity of the classifiers must be evaluated for reliable results. Our case studies showed that all the classifiers gave reliable results in bearing fault detection. The KNN classifier gave slightly the earliest fault detection for the presented vibration signal features. The importance of the features was consistent and none of the features needed to be discarded. As a result, several classifiers with different models were obtained. Future research will focus how to find the best of these models and apply it to separate case studies to detect bearing faults.

References

[1] I. Salam, A. Tauqir, A. U. Haq, and A. Q. Khan. An air crash due to fatigue failure of a ball bearing. In D.R.H. Jones, editor, *Failure Analysis Case Studies II*, pages 415–423. Elsevier, 2001.

[2] E. Jantunen. A summary of methods applied to tool condition monitoring in drilling. *International Journal of Machine Tools and Manufacture*, 42(9):997 – 1010, 2002.

[3] N. Tandon and A. Choudhury. A review of vibration and acoustic measurement methods for the detection of defects in rolling element bearings. *Tribology International*, 32(8):469 – 480, 1999.

[4] A. H. Christer and W. Wang. A simple condition monitoring model for a direct monitoring process. *European Journal of Operational Research*, 82(2):258 – 269, 1995.

[5] I. El-Thalji and E. Jantunen. A descriptive model of wear evolution in rolling bearings. *Engineering Failure Analysis*, 45:204–224, 2014.

[6] J. Gama, I. Žliobaitė, A. Bifet, M. Pechenizkiy, and A. Bouchachia. A survey on concept drift adaptation. *ACM computing surveys (CSUR)*, 46(4):44, 2014.

[7] X. Wang, J. Wu, C. Liu, S. Wang, T. Wang, and W. Niu. Improving failures prediction by exploring weighted shape-based time-series clustering. *Quality and Reliability Engineering International*, 34(2):138–160, 2018.

[8] D. H. Pandya, S. H. Upadhyay, and S. P. Harsha. Fault diagnosis of rolling element bearing with intrinsic mode function of acoustic emission data using apf-knn. *Expert Systems with Applications*, 40(10):4137 – 4145, 2013.

[9] J. A. V. Florêncio, M. L. D. Dias, A. R. da R. Neto, and A. H. de Souza Júnior. A fuzzy c-means-based approach for selecting reference points in minimal learning machines. In *Fuzzy Information Processing - 37th Conference of the North American Fuzzy Information Processing Society, NAFIPS 2018, Fortaleza, Brazil, July 4-6, 2018, Proceedings*, pages 398–407, 2018.

[10] D. Banjevic and A. K. S. Jardine. *Condition Monitoring*. American Cancer Society, 2008.

[11] E. H. Ruspini. A new approach to clustering. *Information and Control*, 15(1):22–32, 1969.

[12] J. C. Dunn. A fuzzy relative of the isodata process and its use in detecting compact well-separated clusters. *Journal of Cybernetics*, 3(3):32–57, 1973.

[13] J. C. Bezdek. *Fuzzy mathematics in pattern classification*. PhD thesis, , Cornell University, , 1973.

[14] C. T. Yiakopoulos, K. C. Gryllias, and I. A. Antoniadis. Rolling element bearing fault detection in industrial environments based on a k-means clustering approach. *Expert Systems with Applications*, 38(3):2888 – 2911, 2011.

[15] T. Cover and P. Hart. Nearest neighbor pattern classification. *IEEE Transactions on Information Theory*, 13(1):21–27, September 2006.

[16] A. Widodo and B-S. Yang. Support vector machine in machine condition monitoring and fault diagnosis. *Mechanical systems and signal processing*, 21(6):2560–2574, 2007.

[17] M. J. Zaki and W. Meira Jr. *Data Mining and Analysis: Fundamental Concepts and Algorithms*. Cambridge University Press, 2014.

[18] J. G. Moreno-Torres, J. A. Saez, and F. Herrera. Study on the impact of partition-induced dataset shift on k-fold cross-validation. *IEEE Transactions on Neural Networks and Learning Systems*, 23(8):1304–1312, Aug 2012.

[19] T. Kärkkäinen. Assessment of feature saliency of mlp using analytic sensitivity. *ESANN 2015 proceedings, European Symposium on Artificial Neural Networks, Computational Intelligence and Machine Learning*, pages 22–24, 2015.

[20] I. Guyon and A. Elisseeff. An introduction to variable and feature selection. *J. Mach. Learn. Res.*, 3:1157–1182, March 2003.

[21] J. Loughrey and P. Cunningham. Overfitting in wrapper-based feature subset selection: The harder you try the worse it gets. In Max Bramer, Frans Coenen, and Tony Allen, editors, *Research and Development in Intelligent Systems XXI*, pages 33–43, London, 2005. Springer London.

[22] University of Cincinnati the Center for Intelligent Maintenance Systems (IMS). Ims bearing data, 2007.

[23] B. Zhang, L. Zhang, and J. Xu. Degradation feature selection for remaining useful life prediction of rolling element bearings. *Quality and Reliability Engineering International*, 32(2):547–554, 2016.

[24] W. Caesarendra and T. Tjahjowidodo. A review of feature extraction methods in vibration-based condition monitoring and its application for degradation trend estimation of low-speed slew bearing. *Machines*, 5:21, 09 2017.

IV

FEATURE RANKING FOR FAULT SIZE ESTIMATION OF ROLLING ELEMENT BEARINGS

by

Jarno Kansanaho, Tommi Kärkkäinen, Pietro Borghesani,Wade A. Smith, Robert B. Randall, Zhongxiao Peng 2019

Submitted to: Measurement

Feature ranking for fault size estimation of rolling element bearings

Jarno Kansanaho[a,*], Tommi Kärkkäinen[a], Pietro Borghesani[b], Wade A. Smith[b], Robert B. Randall[b], Zhongxiao Peng[b]

[a] *Faculty of Information Technology, University of Jyväskylä, Finland*
[b] *School of Mechanical and Manufacturing Engineering, New South Wales University, Sydney, Australia*

Abstract

Fault size estimation of defected rolling element bearings is one of the main challenges in diagnostics and prognostics, especially when vibration measurements are used to determine the health state. In this paper, a novel feature integration and ranking process for the vibration signals is presented to improve the fault size estimation. First, multiplicative feature scaling is applied to the vibration signal features when using the k-Nearest Neighbour (k-NN) and the Support Vector Machine (SVM) classifiers as predictors. Then, relevance ranking based on the feature importance analysis is used to identify the most important features to estimate the bearing fault size. A versatile set of vibration data of rolling element bearings gathered from different laboratory experiments with different operation parameters are exploited to evaluate the methodology. The multi-class SVM is concluded to be applicable and reliable method for the fault size estimation of the rolling element bearings.

Keywords: Rolling element bearing, Fault severity estimation, Vibration analysis, Feature selection, Supervised learning

1. Introduction

Rolling element bearings (REB) are widely used components in rotating machinery. Bearing failure is a common cause of machine breakdowns. An unexpected failure of a critical bearing can lead to significant economical or even human losses. Fault detection, diagnostics and prognostics methods are frequently developed to improve condition based maintenance.

Condition monitoring, a part of condition based maintenance (CBM), includes data acquisition, data processing and maintenance decision making [1]. Fault detection, fault diagnostics and fault prognostics produce inputs for condition based maintenance (Figure 1). Diagnostics covers identification and quantification of an occurred fault of machine component, while prognostics covers prediction of component′s future condition, remaining operational life, or risk to complete operation [2, 3]. In other words, diagnostics is posterior event analysis while prognostics is prior event analysis [1]. Prognostics is dependent on diagnostics that provides valuable inputs for prediction; fault indicators and degradation rates [2]. Engel [4] has stated: "Prognostics is the capability to provide early detection

*Corresponding author
Email address: jarno.m.kansanaho@jyu.fi (Jarno Kansanaho)

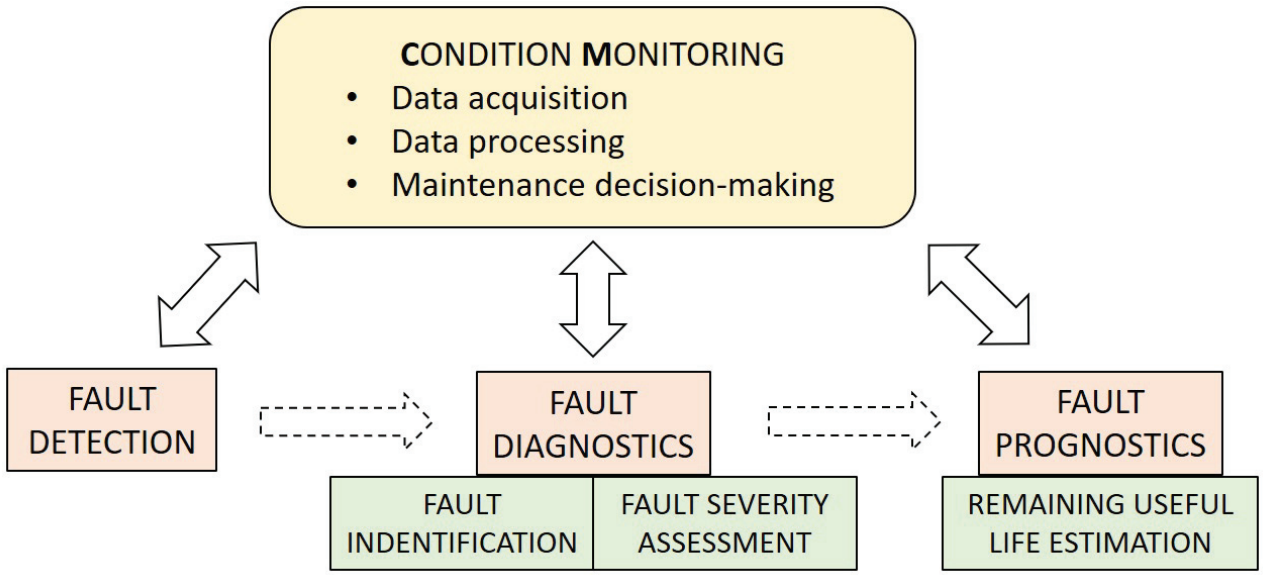

Figure 1: Key elements of condition monitoring.

of the precursor and/or incipient fault condition of a component, and to have the technology and means to manage and predict the progression of this fault condition to component failure". Hence, the fault severity assessment and the fault size estimation are important stages of diagnostics.

Vibration measurements are the most widely used basis for detection and diagnosis of bearing faults [5]. Signal processing and time-series analysis methods are typically used for the necessary pre-processing of the vibration measurements and these methods focus on extracting characteristic features from vibration signals generated by REBs [6]. Recently, also deep autoencoders to gradually reduce the dimension of a large-scale signal representation have been used [7]. Vibration signals generated by REBs can be modelled as cyclostationary [8]. Statistics of cyclostationary processes are periodically varying [9]. A series of impulses are produced when the defective part (local fault) hits other elements of the bearing. The spacing between these impulses usually varies between 1-2% due to slippage resulting from the variation of the load angle of the rolling element [10].

Methods and experiments related to the vibration-based REB fault diagnostics are multifaceted. The analysis can be based on a direct formulae [11], a special fault-sensitive characteristics [12–14], or dedicated processing sequence with the selected techniques to reveal the fault characteristics frequencies [15, 16]. The experimental data can originate from simulated, analytical signals [12, 14, 17–19], the most popular Case Western dataset [14, 17, 19–21], or from own, dedicated test rig [15, 15, 21, 22]. A recent review paper by Cerrada et al. [23] reveals that the topic of fault size estimation is less addressed compared to the general fault severity estimation using vibration signals. However, many studies of the fault size estimation using vibration measurements have been published recently [24–30]. Also most of these studies are based on the data acquired from one test rig and bearing tests for one single bearing.

The proposed methodology for the fault size estimation starts from a set of a priori selected features with a novel, multiplication-based transformation for integrating the scaling and behavior oriented features. Then, we test two popular, instance-based predictive models—k-NN (e.g., [21]) and SVM (e.g., [31–33])—and identify the most important features for the fault size estimation using feature relevance ranking.

The contents of this article are as follows. Section 2 explains methodological background including: supervised methods, essentials for feature extraction and selection, processing of vibration signals, and experimental details. Results are presented in Section 3. Conclusions and ideas for future research are summarised in Section 4.

2. Methodological background

Proper processing of measurement data is a key element in condition monitoring and preventive maintenance [34, 35]. This kind of data processing can be unsupervised or supervised [36]. Machine learning algorithms exploit supervised and predictive-like data processing [36, 37]. The target function, training (teaching) data and an algorithm for learning the target from the training data need to be chosen when designing a machine learning approach [38]. Next the basics of those methods, that will be applied as part of the proposed approach, are described.

Supervised learning refers to training a predictive model, or its parameters, by using a labelled data. The predictor is then used to evaluate labels for new, unseen data. Supervised learning algorithms try to approximate the mapping function between input variables and output variables. Classification and regression problems are typical supervised learning problems. Classification algorithms attempt to assign new data points to pre-defined categories. Regression algorithms attempt to predict numeric values for new data points. We deploy well-known instance-based learning methods, namely the k-Nearest Neighbour (k-NN) algorithm and the multi-class Support Vector Machine (SVM), to estimate the fault size of REBs using vibration signals.

2.1. k-Nearest Neighbour algorithm

The k-Nearest Neighbour (k-NN) classification rule was originally introduced by Cover and Hart [39]. The k-NN rule is a sub-optimal non-parametric procedure for the assignment of a class label to the input pattern based on the class labels represented by the k closest neighbours [40]. The k-NN rule is applicable on data that is in the metric space and it does not make assumptions on the distribution of data. K is the number of the closest data points used in the classification. An example of the principle of the k-NN classifier is shown on the left side of Figure 2. A triangle is classified into the group of rectangles when k is three. If k is five, the triangle is classified into the group of stars. Euclidean distance, used as a dissimilarity measure, satisfies the three properties: positivity, symmetry, and triangle inequality. The k-NN is an instance based learning method. Unlike the inductive learning methods, instance-based learning methods do not include an explicit description of the target function [38]. Instance-based learning approximate real-valued or discrete-valued target functions [38]. The k-NN "on-line" trains the examples and finds out the k-nearest neighbours of the new instance [41].

There are a number of research papers where the k-NN classifiers have been applied to bearing diagnostics using vibration measurements (e.g., [42–44]). Pandya et al. [37] studied performance of various supervised classifiers in

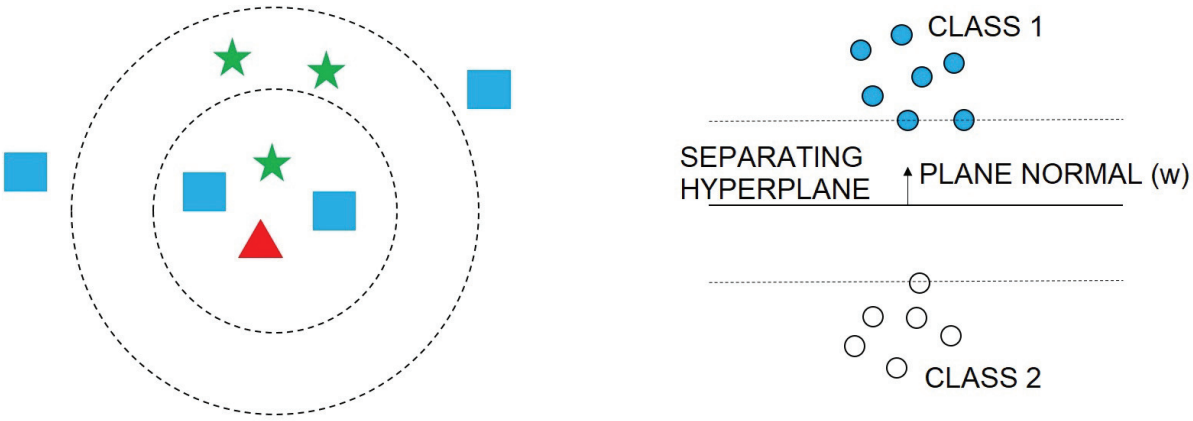

Figure 2: Examples of the k-NN classifier (left) and the SVM classifier (right).

bearing diagnostics using acoustic emission measurements. They compared Bayesian, Naive Bayes, Multi Layer Perceptron, k-NN, weighted k-NN, J48 and Random forest classifiers. The k-NN classifier was found to be the best suited classifier for their data.

2.2. Support vector machine

Support Vector Machine (SVM) is a supervised machine learning algorithm that can be used for both classification and regression problems. SVM is a binary classifier. An SVM algorithm tries to find an optimal separating hyperplane that separates classes from each other [45]. A "hard-margin" classifier is the simplest SVM classifier. It is applicable when the training data is linearly separable, meaning that the two hyperplanes clearly separate the data (on the right side of Figure 2). The SVM algorithm can solve optimisation problem to minimise the length of w that is orthogonal to two hyperplanes. In practice, non-linear kernel transformation is performed because the patterns are not linearly separable [46]. Nonlinearity of the SVM and the corresponding class boundaries is obtained from the famous kernel-trick, by using nonlinear transformation through a high-dimensional feature space [47].

The multi-class problem is reduced to multiple binary classification problems that can be solved separately. SVMs use Error-Correcting Output Codes (ECOC) framework to combine binary problems to address the multi-class problem [48]. The ECOC framework uses different decoding strategies which are implemented by the coding design [49]. The most commonly used coding designs are one-vs-all and one-vs-one. The one-vs-one coding design considers all possible pairs of classes while the one-vs-all discriminates a given class from all other classes. Disadvantages of the one-vs-all coding design is that the binary classifiers might have different scales and the training sets are not balanced (antisymmetric) [50].

General review of the use of SVM in condition monitoring and fault diagnostics was given in [51]. Since, methods

based on SVMs using vibration measurements have been frequently applied in bearing fault diagnostics [46, 52–58]. Usually, a number of fault samples in condition monitoring domain is limited. Unlike Artifical Neural Networks (ANN), SVM does not require a large number of training samples to be accurate [52, 59]. Further, SVMs have been utilised in fault severity estimation of REBs using vibration signals [60–65]. Repeatedly, most of these studies are based on tests acquired from one test rig.

2.3. Feature extraction and selection

Features are inputs for a model in data-driven approaches. Feature extraction refers to the case where a new, smaller-dimensional set of features is created from the original set of variables (e.g., [7]). The process of selecting a subset of relevant features is called feature selection or variable selection. The objective of feature selection can be three-fold [66]: to improve the performance of the model, to provide faster and more cost-effective models, and to improve understanding of the data generation process. John, Kohavi, and Pfleger [67, 68] proposed the division of a set of features into *irrelevant, weakly relevant,* and *strongly relevant*. Identification of such a division is a search problem, and many techniques and approaches exist for this purpose, for example, exhaustive search, branch-and-bound, evolutionary approaches etc. (see, e.g., [69, 70]). Forward search means adding new features one-by-one or group-by-group to the model, whereas backward elimination refers to the removal of individual or sets of features during the search process.

The intrinsic assumption behind feature selection is that there is some redundancy among the features. Liu et al. [69] divide feature selection criteria measuring the redundancy into five groups: information measures, distance measures, dependency measures, consistency measures, and accuracy measures. Depending on the constituents when constructing a criterion, two basic approaches for feature selection can be defined: the filter approach and the wrapper approach [67]. In the filter mode, one does not utilise the model, e.g. a classifier, in the feature selection process whereas the wrapper approach involves the model as black-box. Usually this means that a filter approach is faster and a wrapper approach more accurate [68]. Hybrid e.g., [71] or embedded methods [72, 73] perform feature selection by using another model or not fully trained actual classification model for assessing feature relevance. Special techniques ranking and selecting features during the construction of the predictive model are the hierarchical models, most prominently random forests [74].

The wrapper based feature selection is tightly linked to the variable selection in the statistical regression. For feature selection in classification problems [75], information on classes could be used to improve feature selection without actual model building, e.g., by comparing the feature-class correlations or mutual information (MI) in the joint densities of features and classes (e.g., [76]). Such methods could be referred to as warm filter methods or cold hybrid methods, because only the information on the classes without building any classifier is being utilised.

The misclassification rate and the training time in REB fault diagnostics can be reduced by feature selection [77]. The features calculated from the vibration signals are usually high-dimensional and non-Gaussian leading to a pattern recognition problem [78]. It is typical that dimension reduction methods such as Principal Component Analysis (PCA), Kernel Principal Component Analysis (KPCA), and Linear Discriminant Analysis (LDA) are

Table 1: Features of vibration signal.

No.	Feature	Description
	SCALING PARAMETERS	
1.	Root mean square	The power content
2.	Scale parameter: mean(abs(x))	Mean of absolute amplitudes
3.	Scale parameter: mean(log(x^2))	Mean of logaritmic power
4.	Scale parameter: median(abs(x))	Median of absolute amplitudes
5.	Scale parameter: median(log(x^2))	Median of logaritmic power
	AFTER PRE-WHITENING	
6.	Skewness	Asymmetry of distribution of signal
7.	Kurtosis	Impulsiveness of signal
	ENVELOPE SPECTRUM (normalization with the DC value)	
8.	BPFI peak amplitude	Amplitude of characteristic defect frequency (1. harmonic) of inner race in envelope spectrum
9.	BPFI 2. harmonic peak amplitude	Amplitude of characteristic defect frequency (2. harmonic) of inner race in envelope spectrum
10.	BPFI 1. + 2.	Sum of features 8 and 9
	ENVELOPE SPECTRUM (DC bias removal and normalization with spectrum median)	
11.	BPFI peak amplitude	Amplitude of characteristic defect frequency (1. harmonic) of inner race in envelope spectrum
12.	BPFI 2. harmonic peak amplitude	Amplitude of characteristic defect frequency (2. harmonic) of inner race in envelope spectrum
13.	BPFI 1. + 2.	Sum of features 11 and 12
	GAUSSIAN AND NON-GAUSSIAN SYMPTOMS	
14.	GGS $\hat{\beta}_0$	Measure of stationarity
15.	GGS $\hat{\eta}_0$	Measure of stationarity
16.	GGCS $\hat{\beta}_1$	Measure of cyclostationarity
17.	GGCS mean $\hat{\eta}_1$	Measure of impulsiveness (cyclostationary signal)
18.	GGCS std $\hat{\eta}_1$	Measure of cyclostationarity

applied when processing vibration signal features [53, 63, 78].

2.4. Vibration signal processing

Basic features representing vibration signals can be separated into six categories: *i) time-domain features*; *ii) frequency-domain features*; *iii) time-frequency-domain features*; *iv) phase-space dissimilarity measurements*; *v) complexity measurements*; *vi) other features* [6]. However, El-Thalji et al. [79] stated that the whole wear evalution process in rolling element bearings cannot be tracked with indicators that are based on the statistical time domain parameters and amplitude at bearing defect frequency.

Here, a special set of vibration features were selected for analysis, as shown in Table 1 and Figure 3. The features were carefully chosen to describe different characteristics of the signal, such as the signal power level, the statistical moments, the cyclic impulsiveness, the gaussian and non-gaussian properties of vibration signals. Features are selected to describe as versatile as possible the properties of vibration signals.

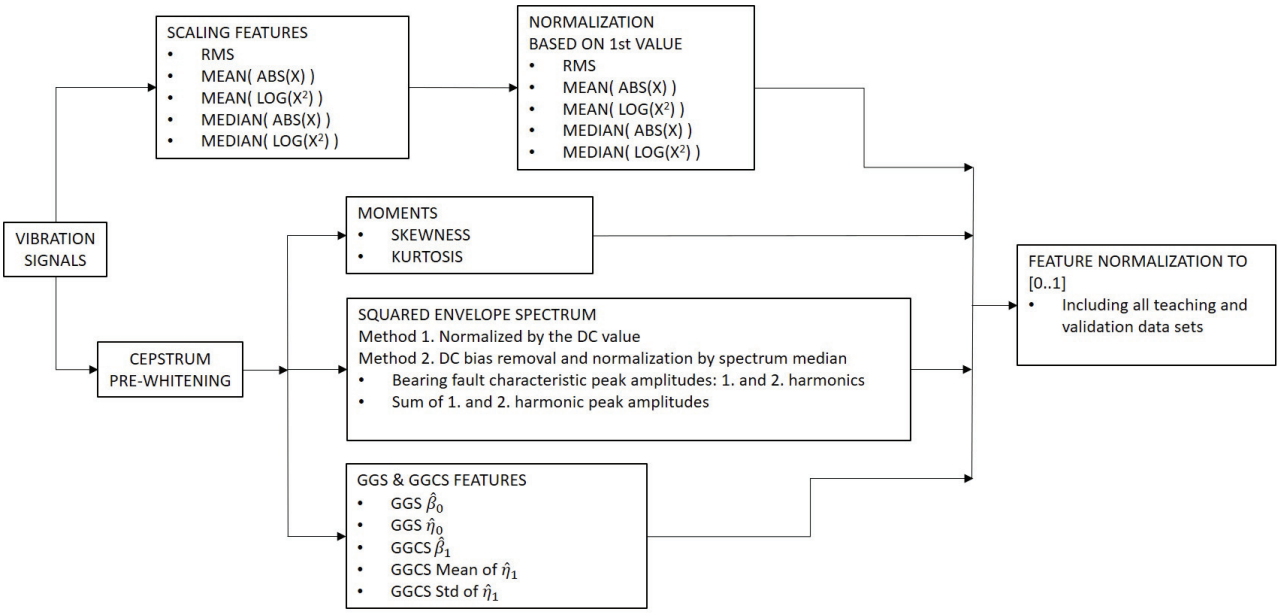

Figure 3: Feature extraction from vibration signals.

Statistical moments, skewness and kurtosis, are commonly used time-domain features in bearing diagnostics and prognostics. The skewness (third moment) describes the asymmetry of the probability density function (PDF) of vibration signal. The skewness value will shift to either negative or positive when the PDF of a vibration signal changes due to bearing faults [6]. The kurtosis (fourth moment) describes the "tailedness" of the PDF of vibration signal and it indicates if the vibration signal is impulsive [6]. However, the skewness and the kurtosis are sensitive to variations of the rotation speed of the shafts, band-pass filtering, resonance of the sensor, or background noise [80].

The amplitude modulation of vibration signals is studied with envelope analysis. A series of impulses are generated by a bearing fault, when bearing elements hit the defective part of the bearing. These impulses excite high frequency resonances and the resulting signal appears as a sequence of transient impulsive vibrations [81]. The characteristic frequencies of these impulses can be detected from the envelope spectrum of a vibration signal. The squared envelope spectrum [82] was used to detect the amplitudes of characteristic bearing fault frequencies. The envelope spectra were normalized by two strategies: 1. normalisation by the DC value, 2. normalisation by median of the spectrum.

Recently Antoni et al. [83] introduced indicators that are used to track, separately, Gaussianity (GGS) and cyclostationarity (GGCS) of vibration signals. This fresh methodology is based on the generalised likelihood ratio and it provides a statistical threshold that can be used to develop robust condition indicators. It extracts features that separate non-Gaussianity and non-stationarity properties of vibration signals.

All the selected features are listed in Table 1. The root mean square (RMS), the mean and median of absolute amplitudes, the power and the logaritmic power are referred as scaling parameters. The scaling parameters were calculated for raw vibration signals without any pre-processing for all the tests. Vibration signals were processed with Cepstrum pre-whitening [84] before calculating statistical moments, envelope spectra, and the GGS/GCCS features. The pre-processing were done because the vibration signals included unknown disturbing components that weakened the bearing fault signatures. Figure 3 presents the feature extraction from vibration signals and the data normalization process.

2.5. Experimental details

Vibration data of three different bearing models were acquired. Table 2 presents the bearing specifications and test numbers in which the bearings were used. Vibration data were collected from three different test stands / rigs : a Bearing Prognostics Simulator (SpectralQuest) at the University of New South Wales, a FAG test rig facility and a test stand of Case Western Reserve University Bearing Data Center. Seven different bearing tests were acquired to evaluate the performance of the k-NN and the multi-class SVM classifiers in bearing fault size estimation.

Table 2: Bearing information.

Bearing type	Bearing index	N.of rollers	Ball diameter [mm]	Pitch diameter [mm]	BPFI [RPM order]	Tests
Deep groove ball bearing	1	9	7.94	39.04	5.412	1-5
Angular contact bearing	2	12	8.0	38.5	7.310	6
Deep groove ball bearing	3	8	6.7	28.2	4.947	7

The bearing tests 1-5 were run on the Bearing Prognostics Simulator [85]. Single-row deep groove ball bearing was studied in the tests with a nominal shaft speed of 6 Hz. Vibration signals were captured for ten seconds with

the sampling rate of 131072 Hz. A single notch of width 0.4 mm was artificially made in the inner race of bearing to initiate spalling using an electrical discharge machining. The bearing was then run and allowed to degrade over time, during which vibration measurements were frequently taken and the bearing was periodically dismantled and the size of the actual fault was determined using a laser microscope.

The bearing test 6 [86] was performed on a FAG bearing rig that runs at 196 Hz. Single row angular contact bearing was used in this test. Small indentations were created on the circumference of the inner race to initiate the spall. Bearings were run for one minute with a contaminated lubricant, before being cleaned and run again with clean oil. Vibration signals were collected for four seconds with the sampling rate of 50000 Hz. The fault size of the inner race fault (BPFI 1397.5 Hz) was measured at certain time intervals.

The bearing test 7 was selected from the Case Western Reserve University's Fan-End bearing fault data [87]. The bearing test 7 was performed with nominal shaft speed of 30 Hz. Electro-discharge machining was used to produce artificial bearing fault to the inner race of a deep groove ball bearing. Vibration signals were collected for four seconds with the sampling rate of 12000 Hz. The Case Western bearing data have been recently analysed carefully by [88].

Progressive degradation of bearings were examined in the bearing tests 1-6. Differently, in the bearing test 7, the size of the bearing fault was manually enlarged and then studied.

3. Results

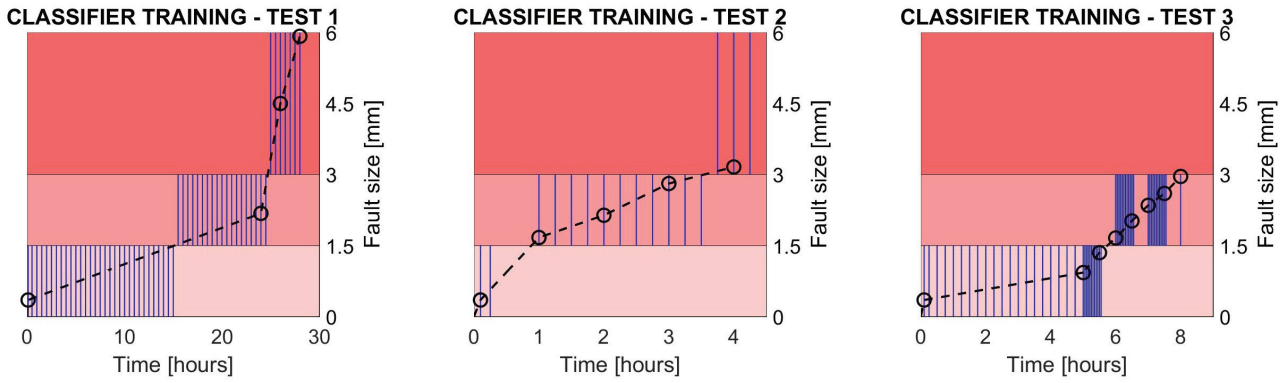

Figure 4: Classifier training using three bearing tests (1-3).

The k-NN and the multi-class SVM classifiers were trained by using the selected features of vibration signals collected from tests 1-3 (see Figure 4). Initially, a total number of 130 vibration signals were used in the training. The black circles represent the actual measured fault size, the blue lines represent the vibration signal features and the red tones represent the classified fault size ranges in Figure 4. In the supervised labeling each class (label) corresponds to a certain fault size range (red tones in the Figure 4): Class 0 = No bearing fault, Class 1 = 0 mm $<\sim$ Fault size $<\sim$ 1.5 mm, Class 2 = 1.5 mm $<\sim$ Fault size $<\sim$ 3.0 mm, Class 3 = 3.0 mm $<\sim$ Fault size $<\sim$ 6.0 mm.

Figure 5: Improved classifier training using three bearing tests (1-3).

Initial training lead to significant classification errors in the fault size estimation, because there was not actual fault size measurements in the beginning and the end of the classification ranges 4. The training was changed that the classification ranges were enclosed by the fault size measurements as shown in Figure 5. However, the number training samples decreased to 85 vibration signals.

Correlation analysis was performed in order to find the best features that linearly correlate with the measured fault size. The results of the correlation analysis are listed in Table 3. It is evident that the scaling parameters correlate the most with the fault size. Further, the mean of the logaritmic power is the most strongly correlated feature with the fault size. However, the scaling parameters are very similar so their usage as features leads to the curse of dimensionality. The conclusion was to use the best scaling parameter together with other features. Correlation analysis can only detect linear dependencies between variable and target [66]. Hence, the approach here concerning the feature selection is a hybrid one (see Section 2): the correlation-based filter approach is used to identify the single most relevant feature. This seed feature is then augmented using the most relevant features from the wrapper-approach with the exhaustive forward search. Feature ranking process is the following:

1. Feature extraction
2. Filter based feature selection -> Correlation analysis
3. Wrapper based feature selection -> Exhaustive forward search
4. Misclassification score
5. Feature relevance rank

Two approaches were established for usage of the scaling parameters. In the first approach the best scaling parameter was used as feature among the other features; additive feature scaling. In the second approach the best scaling parameter was used as a multiplier for other features; multiplicative scaling. The multiplicative scaling is a simplified version of the product kernel approach used with the SVM [89].

The fault size estimation was done for the tests 4-7 that contain 66 vibration signals. Exhaustive search was used for the feature subset selection [90]. Exhaustive search produces a total number $\binom{n}{m} = \frac{n!}{m!(n-m)!}$ subsets, where n is the total number of features and m is the number of features in a subset [90]. Exhaustive search was processed

Table 3: Correlation betweeen measured fault sizes and vibration signal features.

No.	Feature name	Correlation: Feature value vs. Fault size
	SCALING PARAMETERS	
1.	Root mean square	0.5812
2.	Scale parameter: mean(abs(x))	0.8387
3.	Scale parameter: mean(log(x^2))	0.9352
4.	Scale parameter: median(abs(x))	0.8775
5.	Scale parameter: median(log(x^2))	0.8803
	AFTER PRE-WHITENING	
6	Skewness	0.2922
7.	Kurtosis	0.1124
	ENVELOPE SPECTRUM (normalization by the DC value)	
8.	BPFI peak amplitude	0.2187
9.	BPFI 2. harmonic peak amplitude	-0.0356
10.	BPFI 1. + 2.	0.1127
	ENVELOPE SPECTRUM (DC bias removal and normalization by spectrum median)	
11.	BPFI peak amplitude	0.1410
12.	BPFI 2. harmonic peak amplitude	-0.0192
13.	BPFI 1. + 2.	0.1051
	GGS/GGCS	
14.	GGS $\hat{\beta}_0$	-0.0187
15.	GGS $\hat{\eta_0}$	-0.1405
16.	GGCS $\hat{\beta}_1$	0.0263
17.	GGCS mean $\hat{\eta_1}$	-0.0951
18.	GGCS std $\hat{\eta_1}$	0.0277

to produce all the possible feature combinations. However, due the limited number of features the algorithm is applicable in this research; the maximum number of combinations is 3432. Exhaustive feature search was processed for both classifiers using additive and multiplicative feature scaling.

Figure 6 shows misclassification percentages for both classifiers with the best feature combinations using multiplicative feature scaling (on the left side) and additive feature scaling (on the right side). The best feature combination refers to a combination of features that produces fault estimation results with least misclassifications. Misclassification was 6.1 % (4 of 66 samples) for the best combinations. Addivitive feature scaling is not usable due to the very high misclassication percentages through all feature combinations. The fault size estimation using multiplicative feature scaling leads to better results with noticeably smaller misclassification percentages. Among the classifiers the multiclass SVM works better with all feature combinations.

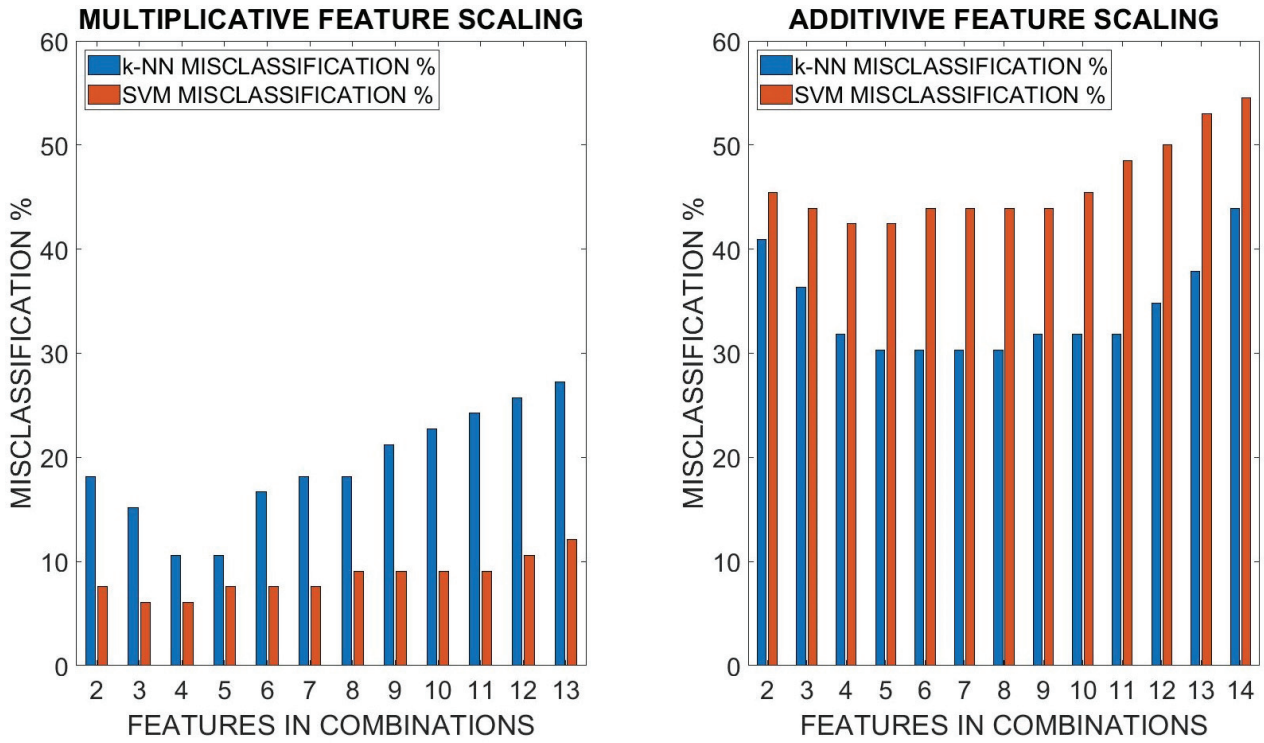

Figure 6: Misclassification of fault size estimation.

Feature ranking results are shown in Table 4. Individual counts for each feature in the best feature combination(s) were calculated. Then individual counts were normalised by the maximum feature count in the combination in question. Normalised counts are reported for each feature (6-18) starting from the second column. Total score for each feature, a sum of normalised counts, are listed in the last row of the Table 4. The most strongly relevant features were the sum of the first and second harmonic BPFI amplitudes (10) in the envelope spectrum and the GGS $\hat{\eta_0}$ (15) when the mean of the logaritmic power was used as the scaling parameter. Features 11-13 acquired from the envelope spectrum (DC bias removal and spectrum median normalisation) are less relevant than features 8-10 acquired from the envelope spectrum (the DC value normalisation). As a consequence, features 11-13 could be discarded. It is also seen that the GGCS features mean $\hat{\eta_1}$ (17) and std $\hat{\eta_1}$ (18) are irrelevant features that do not improve the fault size estimation result.

It appears the best metrics for basic diagnostics are not necessarily the best for the fault size estimation. Many research studies try to explain how the individual features extracted from vibration signals explain the health state of REBs. Further, this leads to research and development of new and "better" features to describe the health state of REBs. Utilised instance-based classifiers provide a combination of features that are the most relevant for the fault size estimation.

The multi-class SVM performs convincingly in the fault size estimation. The fault size estimation results are plotted in Figure 7 for the both classifiers.

Table 4: Feature relevance evalution for multi-class SVM using multiplicative feature scaling

	Feature number (Table 3)												
Combs	6	7	8	9	10	11	12	13	14	15	16	17	18
2	0.0	0.0	0.0	0.0	1.0	0.0	0.0	0.0	0.0	1.0	0.0	0.0	0.0
3	0.5	0.0	0.0	0.5	1.0	0.0	0.0	0.0	0.0	1.0	0.0	0.0	0.0
4	0.5	0.5	0.0	0.5	1.0	0.0	0.5	0.0	0.5	0.5	0.0	0.0	0.0
5	0.7	0.4	0.4	0.8	0.8	0.0	0.6	0.0	1.0	1.0	0.4	0.0	0.0
6	0.3	0.8	0.8	0.6	0.6	0.0	0.4	0.0	1.0	0.9	0.6	0.1	0.0
7	0.5	1.0	1.0	0.5	1.0	0.0	0.0	0.0	1.0	1.0	0.5	0.5	0.0
8	0.6	0.5	1.0	0.8	1.0	0.3	0.6	0.4	1.0	0.9	0.7	0.3	0.1
9	0.6	0.6	1.0	0.9	1.0	0.5	0.6	0.5	1.0	1.0	0.9	0.1	0.4
10	0.8	0.8	1.0	1.0	1.0	0.6	0.8	0.6	1.0	1.0	1.0	0.2	0.2
11	1.0	1.0	1.0	1.0	1.0	1.0	1.0	1.0	1.0	1.0	1.0	0.0	0.0
12	1.0	1.0	1.0	1.0	1.0	1.0	1.0	1.0	1.0	1.0	1.0	0.0	1.0
13	1.0	1.0	1.0	1.0	1.0	1.0	1.0	1.0	1.0	1.0	1.0	1.0	1.0
Score	7.5	7.6	8.2	8.5	11.3*	4.4	6.5	4.5	9.5	11.3*	7.0	2.3	2.7

4. Conclusions

This paper studied the use of a number of different vibration features, and combinations thereof, in combination with two established classification methods for the estimation of fault severity (size) in rolling element bearings. The experimental data were collected from three different testing environments with most datasets involving gradual fault degradation from a known starting spall size (an artificially seeded slot). Selected tests were performed with different shaft rotation speeds and the measurements were done with different vibration sensors. However, the size of the bearings were roughly the same.

The k-NN and the multi-class classifiers SVM were selected to perform estimation of the fault size because the classifiers are suitable for smaller data sets. It was discovered that the training phase needs to be done in a way that there exists fault size measurements at the beginning and at the end of the chosen fault size class ranges. Otherwise, the chosen fault size range might include wrong fault size measurements.

Vibration signal features were selected to represent the power level, the impulsiveness, the cyclic impulsiveness and the non-gaussian and gaussian properties. Exhaustive search was performed for the feature subset selection that covered all possible feature combinations. Also studied was multiplicative feature scaling which was found to work better than additive feature scaling. The multiplicative feature scaling emphasises the effect of the most correlating feature on other features. However, the scaling parameters are very similar so their usage as features leads to the curse of dimensionality. Particularly, the classifiers can detect non-linear relations between the features. Relevance analysis of the features reveal the most relevant features to estimate the bearing fault size when the chosen classifiers are used. Presented feature ranking process of features of vibration signals is completely novel and it is

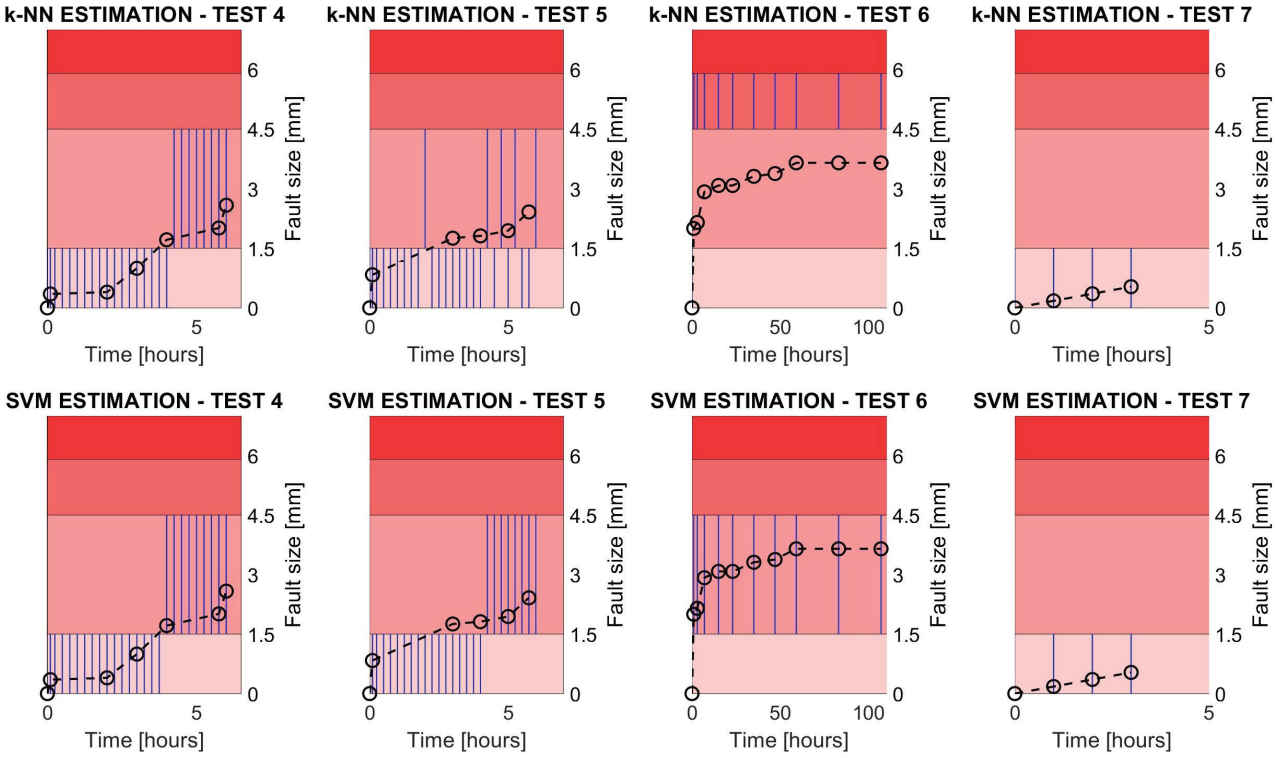

Figure 7: Fault size estimation (tests 4-7).

reproducible.

The multi-class SVM classifier was found to work convincingly for the fault size estimation with these available data sets. The one-vs-one coding design in the multi-class SVM design provided more accurate results than the one-vs-all coding design. The multi-class SVM detects the class boundaries more accurately than the k-NN classifier. The k-NN classifier was found not to be reliable for fault size estimation with these available data sets.

Still more data is needed to better test the features; in particular under different operating environments and for larger bearings. This research included only inner race faults. Moreover, different types of the bearing faults are needed for future studies (outer race, rolling element). It is not exception that other machine components produce noise that makes extraction of bearing fault features more difficult. In such cases, preprocessing is required to filter out the disturbing components. Further, the physical link between fault severity and the best found features is not clear. We would need to focus to develop features that are able to describe the time span between events linked to the spall size.

Acknowledgements

Many thanks to Win Sum Siew, Bo Peng and Nader Sawalhi who provided very valuable bearing vibration data for the research. The research (prof. T.K.) was supported by the Academy of Finland (grants no 315550 and

311877).

References

[1] A. K. Jardine, D. Lin, D. Banjevic, A review on machinery diagnostics and prognostics implementing condition-based maintenance, Mechanical Systems and Signal Processing 20 (7) (2006) 1483 – 1510. doi:10.1016/j.ymssp.2005.09.012.

[2] J. Sikorska, M. Hodkiewicz, L. Ma, Prognostic modelling options for remaining useful life estimation by industry, Mechanical Systems and Signal Processing 25 (5) (2011) 1803 – 1836. doi:10.1016/j.ymssp.2010.11.018.

[3] A. Heng, A. C. Tan, J. Mathew, N. Montgomery, D. Banjevic, A. K. Jardine, Intelligent condition-based prediction of machinery reliability, Mechanical Systems and Signal Processing 23 (5) (2009) 1600 – 1614. doi:10.1016/j.ymssp.2008.12.006.

[4] S. J. Engel, B. J. Gilmartin, K. Bongort, A. Hess, Prognostics, the real issues involved with predicting life remaining, in: 2000 IEEE Aerospace Conference. Proceedings (Cat. No.00TH8484), Vol. 6, 2000, pp. 457–469 vol.6. doi:10.1109/AERO.2000.877920.

[5] N. Tandon, A. Choudhury, A review of vibration and acoustic measurement methods for the detection of defects in rolling element bearings, Tribology International 32 (8) (1999) 469 – 480. doi:10.1016/S0301-679X(99)00077-8.

[6] W. Caesarendra, T. Tjahjowidodo, A review of feature extraction methods in vibration-based condition monitoring and its application for degradation trend estimation of low-speed slew bearing, Machines 5 (2017) 21. doi:10.3390/machines5040021.

[7] Z. Xiang, X. Zhang, W. Zhang, X. Xia, Fault diagnosis of rolling bearing under fluctuating speed and variable load based on tco spectrum and stacking auto-encoder, Measurement 138 (2019) 162–174. doi:10.1016/j.measurement.2019.01.063.

[8] R. B. Randall, J. Antoni, Rolling element bearing diagnostics—a tutorial, Mechanical Systems and Signal Processing 25 (2) (2011) 485 – 520. doi:10.1016/j.ymssp.2010.07.017.

[9] J. Antoni, The spectral kurtosis: a useful tool for characterising non-stationary signals, Mechanical Systems and Signal Processing 20 (2) (2006) 282 – 307. doi:10.1016/j.ymssp.2004.09.001.

[10] T. Barszcz, N. Sawalhi, Fault detection enhancement in rolling element bearings using the minimum entropy deconvolution, Archives of Acoustics 37 (2). doi:10.2478/v10168-012-0019-2.

[11] A. Chen, T. R. Kurfess, A new model for rolling element bearing defect size estimation, Measurement 114 (2018) 144–149. doi:10.1016/j.measurement.2017.09.018.

[12] S. Liu, S. Hou, K. He, W. Yang, L-kurtosis and its application for fault detection of rolling element bearings, Measurement 116 (2018) 523–532. doi:10.1016/j.measurement.2017.11.049.

[13] S. Kass, A. Raad, J. Antoni, Self-running bearing diagnosis based on scalar indicator using fast order frequency spectral coherence, Measurement 138 (2019) 467–484. doi:10.1016/j.measurement.2019.02.046.

[14] J. Yin, M. Xu, H. Zheng, Fault diagnosis of bearing based on symbolic aggregate approximation and lempel-ziv, Measurement 138 (2019) 206–216. doi:10.1016/j.measurement.2019.02.011.

[15] J. Guo, D. Zhen, H. Li, Z. Shi, F. Gu, A. D. Ball, Fault feature extraction for rolling element bearing diagnosis based on a multi-stage noise reduction method, Measurement 139 (2019) 226–235. doi:10.1016/j.measurement.2019.02.072.

[16] C. He, P. Niu, R. Yang, C. Wang, Z. Li, H. Li, Incipient rolling element bearing weak fault feature extraction based on adaptive second-order stochastic resonance incorporated by mode decomposition, Measurement 145 (2019) 687–701. doi:10.1016/j.measurement.2019.05.052.

[17] T. Gong, X. Yuan, Y. Yuan, X. Lei, X. Wang, Application of tentative variational mode decomposition in fault feature detection of rolling element bearing, Measurement 135 (2019) 481 – 492. doi:10.1016/j.measurement.2018.11.083.

[18] Y. Chi, S. Yang, W. Jiao, J. He, X. Gu, E. Papatheou, Spectral dcs-based feature extraction method for rolling element bearing pseudo-fault in rotor-bearing system, Measurement 132 (2019) 22–34. doi:10.1016/j.measurement.2018.09.006.

[19] T. Gong, X. Yuan, Y. Yuan, X. Lei, X. Wang, Application of tentative variational mode decomposition in fault feature detection of rolling element bearing, Measurement 135 (2019) 481–492. doi:10.1016/j.measurement.2018.11.083.

[20] J. Zheng, Z. Dong, H. Pan, Q. Ni, T. Liu, J. Zhang, Composite multi-scale weighted permutation entropy and extreme learning machine based intelligent fault diagnosis for rolling bearing, Measurement 143 (2019) 69–80. doi:10.1016/j.measurement.2019.05.002.

[21] X. Yan, M. Jia, Z. Zhao, A novel intelligent detection method for rolling bearing based on ivmd and instantaneous energy distribution-permutation entropy, Measurement 130 (2018) 435–447. doi:10.1016/j.measurement.2018.08.038.

[22] B. Chen, B. Shen, F. Chen, H. Tian, W. Xiao, F. Zhang, C. Zhao, Fault diagnosis method based on integration of rssd and wavelet transform to rolling bearing, Measurement 131 (2019) 400–411. doi:10.1016/j.measurement.2018.07.043.

[23] M. Cerrada, R.-V. Sánchez, C. Li, F. Pacheco, D. Cabrera, J. V. de Oliveira, R. E. Vásquez, A review on data-driven fault severity assessment in rolling bearings, Mechanical Systems and Signal Processing 99 (2018) 169 – 196. doi:10.1016/j.ymssp.2017.06.012.

[24] S. Zhao, L. Liang, G. Xu, J. Wang, W. Zhang, Quantitative diagnosis of a spall-like fault of a rolling element bearing by empirical mode decomposition and the approximate entropy method, Mechanical Systems and Signal Processing 40 (1) (2013) 154 – 177. doi:10.1016/j.ymssp.2013.04.006.

[25] S. Khanam, N. Tandon, J. Dutt, Fault size estimation in the outer race of ball bearing using discrete wavelet transform of the vibration signal, Procedia Technology 14 (2014) 12 – 19, 2nd International Conference on Innovations in Automation and Mechatronics Engineering, ICIAME 2014. doi:10.1016/j.protcy.2014.08.003.

[26] W. A. Smith, C. Hu, R. B. Randall, Z. Peng, Vibration-based spall size tracking in rolling element bearings, in: P. Pennacchi (Ed.), Proceedings of the 9th IFToMM International Conference on Rotor Dynamics, Springer International Publishing, Cham, 2015, pp. 587–597.

[27] L. Cui, N. Wu, C. Ma, H. Wang, Quantitative fault analysis of roller bearings based on a novel matching pursuit method with a new step-impulse dictionary, Mechanical Systems and Signal Processing 68-69 (2016) 34 – 43. doi:10.1016/j.ymssp.2015.05.032.

[28] L. Cui, Y. Zhang, F. Zhang, J. Zhang, S. Lee, Vibration response mechanism of faulty outer race rolling element bearings for quantitative analysis, Journal of Sound and Vibration 364 (2016) 67 – 76. doi:10.1016/j.jsv.2015.10.015.

[29] M. Ismail, N. Sawalhi, Vibration response characterisation and fault-size estimation of spalled ball bearings, Insight - Non-Destructive Testing and Condition Monitoring 59 (2017) 149–154. doi:10.1784/insi.2017.59.3.149.

[30] M. A. Ismail, A. Bierig, N. Sawalhi, Automated vibration-based fault size estimation for ball bearings using savitzky–golay differentiators, Journal of Vibration and Control 24 (18) (2018) 4297–4315. doi:10.1177/1077546317723227.

[31] X. Li, X. Zhang, C. Li, L. Zhang, et al., Rolling element bearing fault detection using support vector machine with improved ant colony optimization, Measurement 46 (8) (2013) 2726–2734. doi:10.1016/j.measurement.2013.04.081.

[32] Y. Li, M. Xu, Y. Wei, W. Huang, A new rolling bearing fault diagnosis method based on multiscale permutation entropy and improved support vector machine based binary tree, Measurement 77 (2016) 80–94. doi:10.1016/j.measurement.2015.08.034.

[33] Y. Fu, L. Jia, Y. Qin, J. Yang, Product function correntropy and its application in rolling bearing fault identification, Measurement 97 (2017) 88–99. doi:10.1016/j.measurement.2016.10.037.

[34] E. Jantunen, A summary of methods applied to tool condition monitoring in drilling, International Journal of Machine Tools and Manufacture 42 (9) (2002) 997 – 1010. doi:10.1016/S0890-6955(02)00040-8.

[35] D. Banjevic, A. Jardine, Condition Monitoring, 2014. doi:10.1002/9781118445112.stat03643.

[36] I. H. Witten, E. Frank, M. A. Hall, C. J. Pal, Data Mining: Practical machine learning tools and techniques, Morgan Kaufmann, 2016.

[37] D. H. Pandya, S. H. Upadhyay, S. P. Harsha, Fault diagnosis of rolling element bearing with intrinsic mode function of acoustic emission data using apf-knn, Expert Systems with Applications 40 (10) (2013) 4137 – 4145. doi:10.1016/j.eswa.2013.01.033.

[38] T. M. Mitchell, Machine Learning, McGraw-Hill Science/Engineering/Math, 1997.

[39] T. Cover, P. Hart, Nearest neighbor pattern classification, IEEE Transactions on Information Theory 13 (1) (1967) 21–27. doi:10.1109/TIT.1967.1053964.

[40] J. Keller, M. Gray, J. Givens, A fuzzy k-nearest neighbor algorithm, IEEE Transactions on Systems, Man, and Cybernetics - TSMC SMC-15.

[41] S. Wagh, G. Neelwarna, S. Kolhe, A comprehensive analysis and study in intrusion detection system using k-nn algorithm, in: C. Sombattheera, N. K. Loi, R. Wankar, T. Quan (Eds.), Multi-disciplinary Trends in Artificial Intelligence, Springer Berlin Heidelberg, Berlin, Heidelberg, 2012, pp. 143–154.

[42] Y. Lei, Z. He, Y. Zi, A combination of wknn to fault diagnosis of rolling element bearings, Journal of Vibration and Acoustics 131. doi:10.1115/1.4000478.

[43] Q. Wang, Y. B. Liu, X. He, S. Y. Liu, J. H. Liu, Fault diagnosis of bearing based on kpca and knn method, Advanced Materials Research 986-987 (1) (2014) 1491–1496. doi:10.4028/www.scientific.net/AMR.986-987.1491.

[44] P. Baraldi, F. Cannarile, F. D. Maio, E. Zio, Hierarchical k-nearest neighbours classification and binary differential evolution for fault diagnostics of automotive bearings operating under variable conditions, Engineering Applications of Artificial Intelligence 56 (2016) 1 – 13. doi:10.1016/j.engappai.2016.08.011.

[45] V. N. Vapnik, The Nature of Statistical Learning Theory, Springer-Verlag, Berlin, Heidelberg, 1995.

[46] L. Saidi, J. B. Ali, F. Fnaiech, Application of higher order spectral features and support vector machines for bearing faults classification, ISA Transactions 54 (2015) 193 – 206. doi:10.1016/j.isatra.2014.08.007.

[47] M. J. Zaki, W. Meira Jr, W. Meira, Data mining and analysis: fundamental concepts and algorithms, Cambridge University Press, 2014.

[48] T. G. Dietterich, G. Bakiri, Solving multiclass learning problems via error-correcting output codes, Journal of Artificial Intelligence Research 2 (1) (1995) 263–286.

[49] S. Escalera, O. Pujol, P. Radeva, On the decoding process in ternary error-correcting output codes, IEEE Transactions on Pattern Analysis and Machine Intelligence 32 (1) (2010) 120–134. doi:10.1109/TPAMI.2008.266.

[50] C. Bishop, Pattern Recognition and Machine Learning, Springer-Verlag New York, 2006.

[51] A. Widodo, B.-S. Yang, Support vector machine in machine condition monitoring and fault diagnosis, Mechanical Systems and Signal Processing 21 (6) (2007) 2560 – 2574. doi:10.1016/j.ymssp.2006.12.007.

[52] K. Gryllias, I. Antoniadis, A support vector machine approach based on physical model training for rolling element bearing fault detection in industrial environments, Engineering Applications of Artificial Intelligence 25 (2) (2012) 326 – 344, special Section: Local Search Algorithms for Real-World Scheduling and Planning. doi:10.1016/j.engappai.2011.09.010.

[53] Y. Zhang, H. Zuo, F. Bai, Classification of fault location and performance degradation of a roller bearing, Measurement 46 (3) (2013) 1178 – 1189. doi:10.1016/j.measurement.2012.11.025.

[54] W. Du, J. Tao, Y. Li, C. Liu, Wavelet leaders multifractal features based fault diagnosis of rotating mechanism, Mechanical Systems and Signal Processing 43 (1) (2014) 57 – 75. doi:10.1016/j.ymssp.2013.09.003.

[55] J. Wen, H. Gao, S. Li, L. Zhang, X. He, W. Liu, Fault diagnosis of ball bearings using synchrosqueezed wavelet transforms and svm, in: 2015 Prognostics and System Health Management Conference (PHM), 2015, pp. 1–6. doi:10.1109/PHM.2015.7380084.

[56] Y. Li, M. Xu, R. Wang, W. Huang, A fault diagnosis scheme for rolling bearing based on local mean decomposition and improved multiscale fuzzy entropy, Journal of Sound and Vibration 360 (2016) 277 – 299. doi:10.1016/j.jsv.2015.09.016.

[57] Y. Li, M. Xu, H. Zhao, W. Huang, Hierarchical fuzzy entropy and improved support vector machine based binary tree approach for rolling bearing fault diagnosis, Mechanism and Machine Theory 98 (2016) 114 – 132. doi:10.1016/j.mechmachtheory.2015.11.010.

[58] J. Saari, D. Strömbergsson, J. Lundberg, A. Thomson, Detection and identification of windmill bearing faults using a one-class support vector machine (svm), Measurement 137 (2019) 287 – 301. doi:10.1016/j.measurement.2019.01.020.

[59] B.-S. Yang, T. Han, W.-W. Hwang, Fault diagnosis of rotating machinery based on multi-class support vector machines, Journal of Mechanical Science and Technology 19 (2005) 846–859. doi:10.1007/BF02916133.

[60] M. F. Yaqub, I. Gondal, J. Kamruzzaman, Machine fault severity estimation based on adaptive wavelet nodes selection and svm, in: 2011 IEEE International Conference on Mechatronics and Automation, 2011, pp. 1951–1956. doi:10.1109/ICMA.2011.5986279.

[61] H.-E. Kim, A. C. Tan, J. Mathew, B.-K. Choi, Bearing fault prognosis based on health state probability estimation, Expert Systems with Applications 39 (5) (2012) 5200 – 5213. doi:10.1016/j.eswa.2011.11.019.

[62] Y. Wang, S. Kang, Y. Jiang, G. Yang, L. Song, V. Mikulovich, Classification of fault location and the degree of performance degradation of a rolling bearing based on an improved hyper-sphere-structured multi-class support vector machine, Mechanical Systems and Signal Processing 29 (2012) 404 – 414. doi:10.1016/j.ymssp.2011.11.015.

[63] S. Dong, T. Luo, Bearing degradation process prediction based on the pca and optimized ls-svm model, Measurement 46 (9) (2013) 3143 – 3152. doi:10.1016/j.measurement.2013.06.038.

[64] C. Lu, J. Chen, R. Hong, Y. Feng, Y. Li, Degradation trend estimation of slewing bearing based on lssvm model, Mechanical Systems and Signal Processing 76-77 (2016) 353 – 366. doi:10.1016/j.ymssp.2016.02.031.

[65] S. Kang, D. Ma, Y. Wang, C. Lan, Q. Chen, V. Mikulovich, Method of assessing the state of a rolling bearing based on the relative compensation distance of multiple-domain features and locally linear embedding, Mechanical Systems and Signal Processing 86 (2017) 40 – 57. doi:doi.org/10.1016/j.ymssp.2016.10.006.

[66] I. Guyon, A. Elisseeff, An introduction to variable and feature selection, Journal of Machine Learning Research 3 (2003) 1157–1182.

[67] G. H. John, R. Kohavi, K. Pfleger, Irrelevant features and the subset selection problem, in: W. W. Cohen, H. Hirsh (Eds.), Machine Learning Proceedings 1994, Morgan Kaufmann, San Francisco (CA), 1994, pp. 121 – 129. doi:10.1016/B978-1-55860-335-6.50023-4.

[68] R. Kohavi, G. H. John, Wrappers for feature subset selection, Artificial Intelligence 97 (1) (1997) 273 – 324, relevance. doi:10.1016/S0004-3702(97)00043-X.

[69] H. Liu, H. Motoda, Feature Selection for Knowledge Discovery and Data Mining, Kluwer, Norwell, MA, 1998.

[70] D. Huang, Z. Gan, T. W. Chow, Enhanced feature selection models using gradient-based and point injection techniques, Neurocomputing 71 (2008) 3114–3123.

[71] Z. Hu, Y. Bao, T. Xiong, R. Chiong, Hybrid filter–wrapper feature selection for short-term load forecasting, Engineering Applications of Artificial Intelligence 40 (2015) 17 – 27. doi:10.1016/j.engappai.2014.12.014.

[72] A. L. Blum, P. Langley, Selection of relevant features and examples in machine learning, Artificial Intelligence 97 (1) (1997) 245 – 271, relevance. doi:10.1016/S0004-3702(97)00063-5.

[73] J.-X. Peng, S. Ferguson, K. Rafferty, P. D. Kelly, An efficient feature selection method for mobile devices with application to activity recognition, Neurocomputing 74 (17) (2011) 3543 – 3552. doi:10.1016/j.neucom.2011.06.023.

[74] L. Breiman, Classification and regression trees, Routledge, 2017.

[75] M. Dash, H. Liu, Feature selection for classification, Intelligent Data Analysis 1 (1) (1997) 131 – 156. doi:10.1016/S1088-467X(97)00008-5.

[76] V. Gomez-Verdejo, M. Verleysen, J. Fleury, Information-theoretic feature selection for functional data classification, Neurocomputing 72 (16) (2009) 3580 – 3589, financial Engineering Computational and Ambient Intelligence (IWANN 2007). doi:10.1016/j.neucom.2008.12.035.

[77] Q. Hu, Z. He, Z. Zhang, Y. Zi, Fault diagnosis of rotating machinery based on improved wavelet package transform and svms ensemble, Mechanical Systems and Signal Processing 21 (2) (2007) 688 – 705. doi:10.1016/j.ymssp.2006.01.007.

[78] M. Zhao, X. Jin, Z. Zhang, B. Li, Fault diagnosis of rolling element bearings via discriminative subspace learning: Visualization and classification, Expert Systems with Applications 41 (7) (2014) 3391 – 3401. doi:10.1016/j.eswa.2013.11.026.

[79] I. El-Thalji, E. Jantunen, Fault analysis of the wear fault development in rolling bearings, Engineering Failure Analysis 57 (2015) 470 – 482. doi:10.1016/j.engfailanal.2015.08.013.

[80] F. Bolaers, O. Cousinard, P. Marconnet, L. Rasolofondraibe, Advanced detection of rolling bearing spalling from de-noising vibratory signals, Control Engineering Practice 12 (2) (2004) 181 – 190. doi:10.1016/S0967-0661(03)00048-0.

[81] Y. Gao, R. Randall, R. Ford, Estimation of envelope spectra using maximum entropy spectral analysis and spectrum interpolation, International Journal of COMADEM 1 (1998) 15–22.

[82] J. Antoni, Cyclic spectral analysis of rolling-element bearing signals: Facts and fictions, Journal of Sound and Vibration 304 (3) (2007) 497 – 529. doi:10.1016/j.jsv.2007.02.029.

[83] J. Antoni, P. Borghesani, A statistical methodology for the design of condition indicators, Mechanical Systems and Signal Processing 114 (2019) 290 – 327. doi:10.1016/j.ymssp.2018.05.012.

[84] P. Borghesani, P. Pennacchi, R. Randall, N. Sawalhi, R. Ricci, Application of cepstrum pre-whitening for the diagnosis of bearing faults under variable speed conditions, Mechanical Systems and Signal Processing 36 (2) (2013) 370 – 384. doi:10.1016/j.ymssp.2012.11.001.

[85] W. S. Siew, W. Smith, Z. Peng, R. B. Randall, Fault severity trending in rolling element bearings, in: Acoustics 2015, 2015.

[86] N. Sawalhi, Diagnostics, prognostics and fault simulation for rolling element bearings, Ph.D. thesis, The University of New South Wales (2007).

[87] Case Western Reserve University, Bearing Data Centre, data retrieved from, https://csegroups.case.edu/bearingdatacenter/pages/download-data-file.

[88] W. A. Smith, R. B. Randall, Rolling element bearing diagnostics using the case western reserve university data: A benchmark study, Mechanical Systems and Signal Processing 64-65 (2015) 100 – 131. doi:10.1016/j.ymssp.2015.04.021.

[89] P. Gehler, S. Nowozin, On feature combination for multiclass object classification, in: 2009 IEEE 12th International Conference on Computer Vision, 2009, pp. 221–228. doi:10.1109/ICCV.2009.5459169.

[90] P. Narendra, K. Fukunaga, A branch and bound algorithm for feature subset selection, IEEE Transactions on Computers 26 (09) (1977) 917–922. doi:10.1109/TC.1977.1674939.

V

SOFTWARE FRAMEWORK FOR TRIBOTRONIC SYSTEM

by

Jarno Kansanaho and Tommi Kärkkäinen 2019

A preprint available at arXiv:1910.13764

SOFTWARE FRAMEWORK FOR TRIBOTRONIC SYSTEMS

A PREPRINT

Jarno Kansanaho*
Faculty of Information Technology
University of Jyväskylä, FI-40014, Finland
jarno.m.kansanaho@jyu.fi

Tommi Kärkkäinen
Faculty of Information Technology
University of Jyväskylä, FI-40014, Finland
tommi.karkkainen@jyu.fi

October 30, 2019

ABSTRACT

Increasing the capabilities of sensors and computer algorithms produces a need for structural support that would solve recurring problems. Autonomous tribotronic systems self-regulate based on feedback acquired from interacting surfaces in relative motion. This paper describes a software framework for tribotronic systems. An example of such an application is a rolling element bearing (REB) installation with a vibration sensor. The presented plug-in framework offers functionalities for vibration data management, feature extraction, fault detection, and remaining useful life (RUL) estimation. The framework was tested using bearing vibration data acquired from NASA's prognostics data repository, and the evaluation included a run-through from feature extraction to fault detection to remaining useful life estimation. The plug-in implementations are easy to update and new implementations are easily deployable, even in run-time. The proposed software framework improves the performance, efficiency, and reliability of a tribotronic system. In addition, the framework facilitates the evaluation of the configuration complexity of the plug-in implementation.

***K*eywords** Software framework · Tribotronic system · Bearing diagnostics · Bearing prognostics · Vibration analysis

1 Introduction

The term 'tribology' was introduced and defined in The Jost Report [1] as "the science and technology of interacting surfaces in relative motion and of the practices related hereto." It was reported that enormous amounts of resources were wasted because mechanical surface phenomena was ignored [2]. However, The Jost Report did not pay much attention to wear, the most significant tribological phenomenon [2]. Tribology enables the effective design of both machines and lubrication to minimize the impact of friction and wear [3]. The successful implementation of tribological practices into design procedures for various machines and mechanisms has resulted in significant economic savings through improvements in machine performance and reliability [3]. Tribology combines physics, chemistry, materials engineering, machinery theory, and products of its own engineering science [4]. Holmberg [5] defined a taxonomy for different levels of occurrence of tribological phenomena: universe, global, national, plant, machinery, component, contact, asperity, and molecular. Each level of this classification comprises its own components and interactions between them.

A system is a set of related and interdependent elements that regularly interact to form an integrated whole [6]. At high levels of abstraction, a tribological system can be described with input and output variables and the interaction between these variables. The input variable is energy (e.g. force, moment and kinematics) and the output variables are matter and signals [4]. The interaction between elements causes friction and wear losses that are summarized as loss-outputs [7]. A tribosystem is a tribological system that includes at least two contacting tribological components [8]. A number of input and output variables in tribosystems can be infinite due to the number of physical and chemical properties of the surfaces in contact, the properties of the medium (i.e., the lubricant), and the environmental conditions [4]. For example, bearings, gears, and mechanical seals are tribological components. Glavatskih et al. [3] outlined a tribotronic

*Corresponding author

system that would unite the tribosystem, sensors, real-time control system, and actuators. The tribotronic system is distinct from a mechatronics system because tribosystems use loss outputs, such as wear, vibration, temperature, and friction. Controlling these outputs allows a tribosystem to try to improve the performance, efficiency, and reliability of the whole machine [3]. A desirable output for a tribotronic system should be expressed in terms of endurance life and probability of failure [5].

One of the main goals of software engineering is to reuse existing code [9]. A software's framework is a "skeleton" that can be used to supplement application-specific software, so recycling existing frameworks is a key technique when implementing software platforms. Software frameworks are customized to complete a software application by filling empty code blocks with product-specific code. An important property of software frameworks is inversion control, which enables the framework itself to call user-implemented methods, that is not possible in traditional procedural programming [10]. If frameworks were not reused during software development, a considerable amount of code would be written repeatedly. Our study focused on object-oriented frameworks. Abstract frameworks provide only software interfaces; they do not include any runnable code. White-box frameworks use subclasses as extensions, which allow the implementation of methods for base classes. Black-box frameworks use a composition approach and include ready-to-use classes. It should be noted that white-box frameworks evolve into black-box frameworks over time [10]. Gray-box frameworks merge black-box and white-box issues [11]. Layered frameworks can be applied to large-scale platforms when different frameworks need to be fused [12]. Plug-in frameworks are specialized because they implement application-specific interfaces, or plug-ins [13]. Caropreso et al. [14] presented a structured methodology to define the architecture for communication frameworks with multiframe capabilities. It is an example of maintainable object-oriented framework that is applicable for embedded systems.

Figure 1 depicts a schematic tribotronic system with a control unit and real-time software. In this paper, we introduce an object-oriented plug-in framework for such tribotronic systems. The main motivation for this work is to speed up and ease the deployment of diagnostic and prognostic algorithms into tribotronic systems. The purpose of the framework is to improve the performance, efficiency, and reliability of a tribotronic system. The framework covers asset and data management, fault detection, and RUL estimation. The plug-in implementation was targeted for REBs that were monitored using vibration sensors.

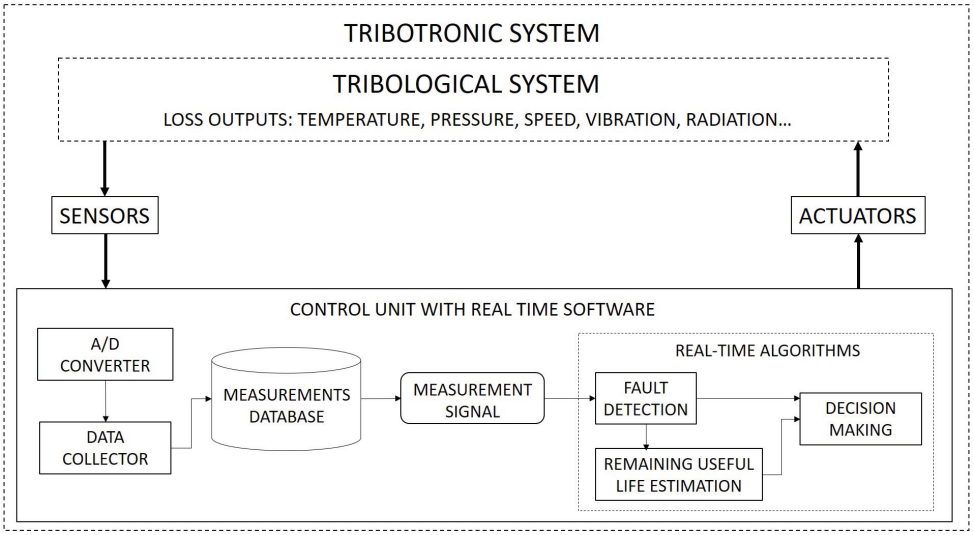

Figure 1: Tribotronic system [3]

The contents of this article are as follows. Bearings (tribosystem) and their wear evolution will be introduced in Section 2. Vibration analysis, fault detection, and RUL estimation will be explained in Section 3. Designed plug-in framework will be presented in Section 4. Evaluation of the framework will be presented in Section 5. Finally, conclusions and future work will be summarized in Section 6.

2 Tribosystem - Bearing

Bearings are widely used in rotating machinery to support shafts. Bearings are categorized as either REBs or journal bearings based on their structure [15]. REBs contain spherical, cylindrical, tapered, and needle-shaped rolling elements.

Journal bearings contain only sliding surfaces –no rolling elements. Monitoring the condition of these bearings is very important because a bearing failure is a very common reason for machine breakdowns. In general, the vibration and temperature of a tribological system (REB) are monitored to detect lost outputs.

2.1 Bearing failure

Bearing failures fall under six categories: fatigue, wear, corrosion, electrical erosion, plastic deformation, and fracture/cracking [16]. Wear is a cumulative quantity regularly measured by condition monitoring systems [17]. When a measured variable directly determines a bearing's failure, the condition monitoring method is direct; when a measured variable provides information associated with and affected by the bearing's condition, the condition monitoring method is indirect [17]. Common direct and indirect condition monitoring methods consist of the following [18, 19, 20, 21]: i) indirect methods include monitoring vibrations, acoustic emissions, basic physical quantities such as heat and pressure, basic electrical quantities such as voltage, current, power, and resistance, and ultrasound or infrared testing, and ii) direct methods include oil debris or corrosion analysis as well as visual inspection using a borescope. Furthermore, new methods are constantly being sought that would be more sensitive when measuring bearing defects [22].

Presenting wear evolution of REBs as a time series describes the wear interaction and evolution at different lifetime stages. A five-stage descriptive model of lifetime stages, as depicted in 2, was presented by El-Thalji et al. [23]: running-in, steady-state, defect initiation, defect propagation, and damage growth. First, during the running-in stage, the surface asperities and the lubrication film become uniform [23]. The length of the steady-state stage, the healthy stage of the lifetime, depends on maximum load-induced stress, material characteristics, and operating temperature [24]. The wear process starts and will affect surface roughness and waviness in the defect initiation stage [25]. According to [23], this stage can be further split into the sub-stages of defect localization, dentation, crack initiation, and crack opening. The linear elastic fracture mechanics commences in the defect propagation stage [26]. Incubation, stable, and crack-to-surface are then the main events that occur [27]. The defect starts to grow in three dimensions (length, width, and depth) and the effect of multiple asperities is prominent in the damage growth stage [23]. Direct condition monitoring makes it possible to detect lifetime stages of wear evolution directly from measurements; however, this is not possible using raw vibration measurements.

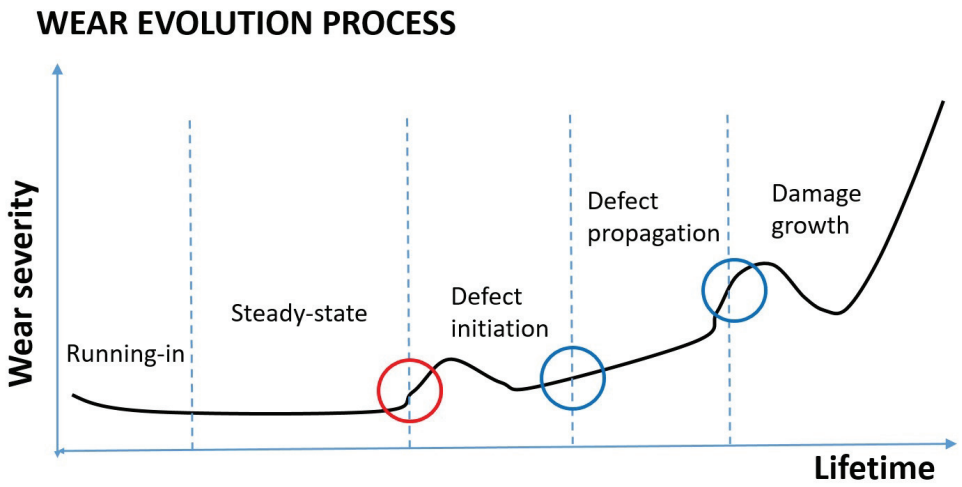

Figure 2: Wear evolution process [23]

3 Vibration analysis

Vibration sensors interpret vibration values indirectly using mechanical and optical quantities. Vibration sensors are categorized as contacting or non-contacting according to their measurement principles. Both contacting and non-contacting sensors are further divided according to path, speed, and acceleration measurement. Path measurement uses potentiometric transmitters and linear variable differential transformers; speed is measured using principles of electrodynamics and seismometers; acceleration is measured using piezoelectric, piezo-resistive, resistive, and inductive sensors [28].

A machine's vibrational signature is related to either a standard condition or a fault condition [29]. A tribotronic system measures vibrations and processes them to discover informative features using feature extraction. Frequently, features calculated from vibration signals are high-dimensional and non-Gaussian. Further, feature selection is applied to extracted features to leave over the most relevant features. Descriptive classification for features of vibration signals is the following: i) time-domain features; ii) frequency-domain features; iii) time-frequency-domain features; iv) phase-space dissimilarity measurements; v) complexity measurements; vi) other features [30]. A considerable amount of research has been directed towards the development of the digital signal processing of vibrational signals [22].

3.1 Fault detection

Randall stated [29] that "fault detection is the first step in the overall process of detection, diagnostics and prognostics. Since all signals have to be processed to determine whether a significant change has occurred, the techniques employed must be considerably more efficient than those which might be used for the latter processes." Early fault detection allows time to predict fault progression and estimate RUL before catastrophic failures occur [31]. Fault detection is one of the main functionalities in the designed framework. Depending on the response from the fault detection algorithm, the tribosystem (REB) would be controlled by actuators.

3.2 Remaining useful life estimation

RUL estimation is an important prognostic and health management task that enables optimized maintenance plans to enhance production, minimize costly downtime, and avoid catastrophic breakdowns [32, 33]. RUL estimation approaches are categorized into physical model approaches, data-driven approaches, and hybrid approaches [34, 32]. Further, the data-driven approaches can be categorized into knowledge-based, statistical, and supervised methods [35]. Recent machine learning approaches have frequently been applied to the diagnoses and prognoses of REBs [36]. However, the effectiveness of the machine learning methods rely on the quality of features of vibration signals.

An ideal signal processing method should be capable of detecting the bearing degradation phases on changing defect conditions [22]. Crucial for RUL estimation is to find the most suitable feature to describe the degradation process when vibration measurements are used. Measuring vibrations is an indirect methods to monitor the condition of REBs. RUL estimation is another main functionality of the framework.

4 Implementation of the framework

The plug-in framework designed for tribotronic systems supports asset and data management, feature extraction, fault detection, and RUL estimation. The framework design is shown in Figure 3. A measurement database can be deployed in a local or remote computer. The results of the fault detection and RUL estimation are inputs for a condition analyzer that passes the results to a module that decides how the tribosystem is controlled. The general architecture of the system has been presented Figure 1. A component linking the condition analyzer, the decision-maker, and the actual control of the system was not explicitly defined in the framework because it would depend on the machine, according to the sorts of actions needed to maintain running conditions or stop the machine's operation.

The framework includes interfaces for measurement data (`IMeasurementData`), asset data (`IAssetData`), feature extraction (`IFeatureExtractor`), fault detection (`IFaultDetector`), and RUL algorithms (`IRULalgorithm`). The measurement data is acquired from the sensor and the asset data is relates to the tribotronic component in question. Fault detection and RUL estimation are executed by the `CConditionAnalyzer` class. The `PluginLoader` class loads the desired plug-in that includes the appropriate implementations for the application in question. The `BearingApplication` plug-in implements the interfaces of the framework using inheritance (Figure 3). The presented plug-in was designed for REBs. The plug-in implementations are based on previous research on feature extraction from vibration signals, fault detection, and RUL estimation of REBs.

Technical bearing data is included in the `CBearingData` class. The bearing dimensions are the minimum data required to calculate characteristic fault frequencies, which are required for the fault detection algorithm. Measurement data is specialized as a `CVibrationData` class that handles vibration data. Vibration signals are loaded from the database as shown in Figure 1. Vibration data includes vibration signals and their measurement time and sampling frequency. Further, specialization of the measurement data could be easily done, for example, to address temperature and oil debris data that represent other commonly used condition monitoring measurements for REBs.

The `CConditionAnalyzer` class uses the `CBearingFeatureExtractor` that includes methods to extract specified features from vibrational signals. Methods used to calculate statistical features, such as RMS, skewness, and Kurtosis, include an optimal degradation parameter, a fast Fourier transform (FFT), and a squared envelope spectrum. The FFT is

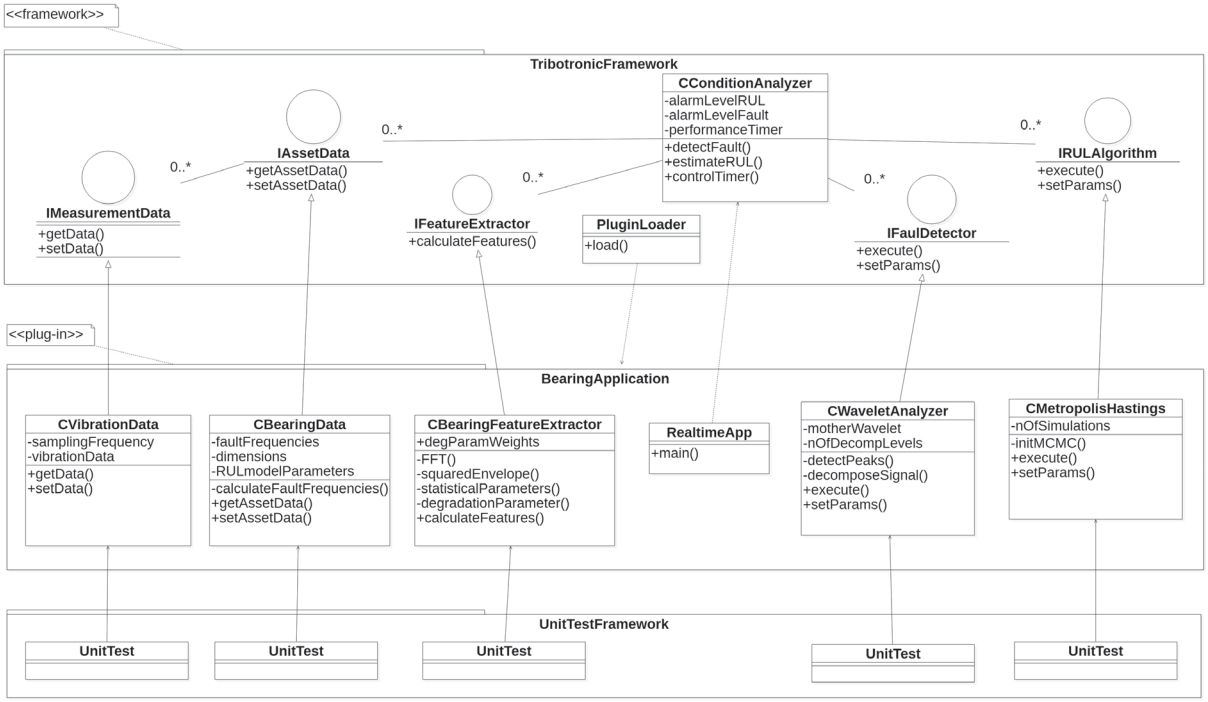

Figure 3: Tribotronic plug-in framework

a sub-routine for the squared envelope spectrum calculation. Previously, an introduced fault detection algorithm was implemented into `CWaveletAnalyzer`.

The fault detection algorithm is called by `CConditionAnalyzer` and implemented in the `CMetropolisHastings` class. The algorithm requires the characteristic fault frequencies of an REB and the sampling frequency of a vibrational signal as input parameters. The algorithm returns a boolean value indication of a fault or not-fault status.

Similar to fault detection, the RUL estimation algorithm is called by `CConditionAnalyzer`. The model parameters are stored in the `CBearingData` class when a model-based RUL estimation is applied. The accuracy calculations, as defined in equation 1refeq:1, which were used to determine degradation features were implemented in the `CBearingFeatureExtractor` class. The best degradation feature, the RUL model parameters, and the alarm level are input parameters for the RUL estimation algorithm that was implemented in the `CMetropolisHastings` class. The RUL algorithm returns the time of the last operation date.

The plug-in implementations are tested with unit tests. Unit tests are carefully designed to test the smallest components. Unclear definitions of unit testing leads to bad and inconsistent testing and makes the software error-prone [37]. This guarantees the reliability of the framework being run and can be updated in real-time.

A sequence diagram of fault detection and RUL estimation with the suggested realization of the framework are shown in Figure 4. The performance of the framework is measured by an internal timer initialized in the first call. Elapsed times for data loading, feature extraction, fault detection, and RUL estimation are recorded. However, RUL estimation is not executed if the result from fault detection is negative, indicating a non-faulty bearing.

A very important aspect of a system is its configuration complexity [38]. A complex algorithm does not need to be complex to configure; e.g. [39]. Complicated configurations can be error-prone and time-consuming, which increases the cost of the system. The meta-parameters of the algorithms play the key role in the evaluation of the configuration complexity. The configuration complexity can be evaluated based on the meta-parameters in the plug-in implementation: *alarmLevelFault*, *motherWavelet*, *nOfDecompLevels*, *degParamWeights*, *alarmLevelRUL*, *RULmodelParameters* and *nOfSimulations*.

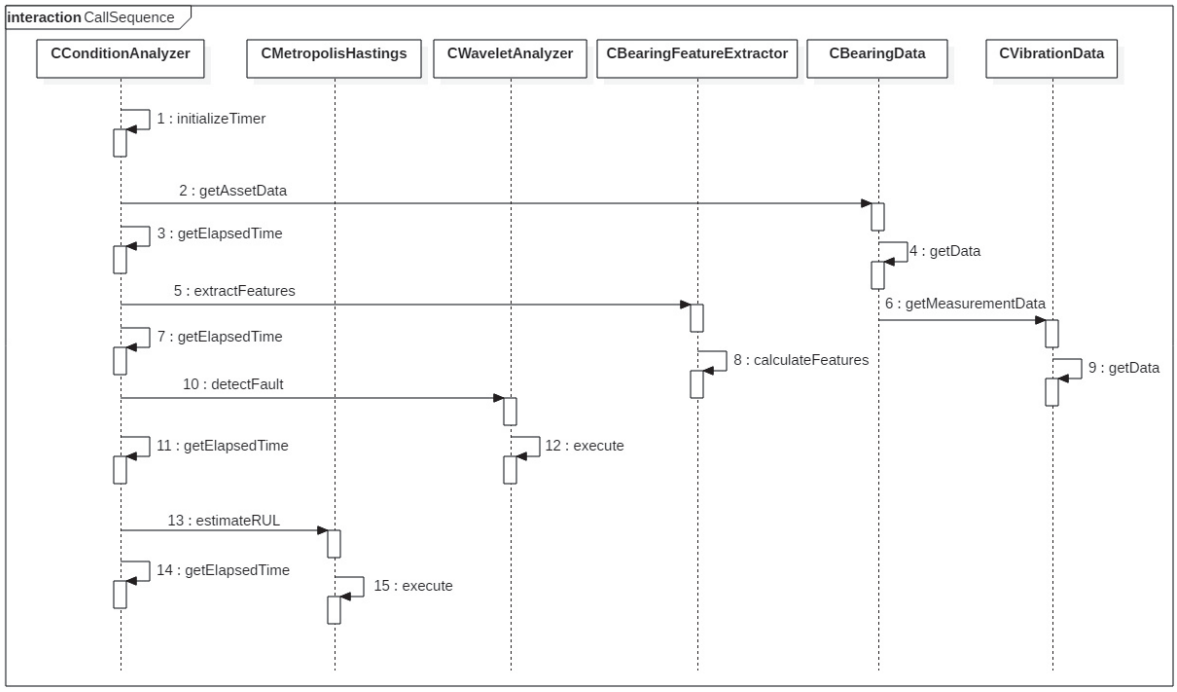

Figure 4: Sequence diagram of fault detection and RUL estimation

4.1 Specific algorithm descriptions

The plug-in's implementation of the fault detection algorithm uses time-frequency domain features. The algorithm exploits discrete spline wavelet decomposition with bior6.8 as the basis wavelet [40]. The squared envelope spectrum of the reconstructed signals is searched for characteristic fault frequencies for each wavelet decomposition level, and the peaks are detected based on local maxima. The peak detection algorithm uses a user-defined alarm level.

A method proposed by Zhang et.al. [41] for degradation feature selection was integrated into a plug-in; the method defines the feature goodness metrics of correlation, monotonicity, and robustness. The optimal degradation feature is selected using a weighted linear combination of the proposed metrics:

$$\max_{\mathbf{X}\in\mathbf{\Omega}} J = \omega_1 Corr(X) + \omega_2 Mon(X) + \omega_3 Rob(X), \tag{1}$$

where J is the score value, Ω is the set of candidate degradation features, and ω_i is the weight for individual metrics.

The implemented RUL estimation algorithm is based on the adaptive Metropolis-Hastings algorithm so it can calculate the parameters for the degradation model. The Metropolis-Hastings algorithm is a sampling algorithm based on Markov-Chain-Monte-Carlo (MCMC) algorithm [42]. MCMC methods aim to solve multi-dimensional integrals using numerical approximations. The Metropolis-Hastings algorithm generates a random walk using a proposal density and a method for rejecting some of the proposed moves. In our study, an Adaptive Metropolis (AM) algorithm is used where the Gaussian proposal distribution is updated along the process using the complete information cumulated so far [43]. A simple exponential degradation model is used in the evaluation [44, 45]:

$$\mathbf{Deg} = \mathbf{c}\exp(\mathbf{bt}), \tag{2}$$

where c and b are the model parameters, t is the time, and Deg is the degradation indicator. The exponential model is very often used in RUL estimation for REBs, although different modifications have been suggested [46].

5 Experimental results

A popular REB dataset from the Center for Intelligent Maintenance Systems (IMS) of the University of Cincinnati was used in the evaluation. Much research has analyzed the IMS dataset [48, 49, 50, 51, 47, 52, 53]. In these run-to-a-

Table 1: IMS BEARING DATA SPECIFICATIONS

BEARING INFORMATION	
Bearing model	Rexnord ZA-2115
Bearing type	Double row bearing
VIBRATION MEASUREMENTS	
Number of bearings	4
Sampling frequency	20480 Hz [47]
Sampling length	20480 data points
Shaft rotation speed	33.3 Hz
Inner race fault frequency (BPFI)	297 Hz
Outer race fault frequency (BPFO)	236 Hz
Rolling element fault frequency (BSF*2)	278 Hz
DATASET 1	
Number of measurements	2156
Recording duration	34 days 12 hours
Detected bearing faults	Bearing 3 / BPFI, Bearing 4 / BSF
DATASET 2	
Number of measurements	984
Recording duration	6 days 20 hours
Detected bearing faults	Bearing 1 / BPFO
DATASET 3	
Number of measurements	4448
Recording duration	31 days 10 hours
Detected bearing faults	Bearing 3 / BPFO

failure-tests, four Rexnord ZA-2115 double row bearings were installed on one shaft. The shaft rotation (2000 RPM) and the radial load (6000 LBS) were constant during the test-runs and all bearings were force-lubricated. During the test-runs, the designed lifetime of the bearing was exceeded for all failures. The IMS bearing data specifications are collected in Table 1.

Datasets for the evaluation were selected based on recent findings by [47]. Selected cases of faulty bearings include an inner fault in bearing 3 (Dataset 1) and an outer race fault in bearing 1 (Dataset 2). Vibration signals were processed through the realizations of the `IFilter` and `ITransform` interfaces, which provide feature extraction methods. The resulting features are shown in Table 2.

Table 2: VIBRATION SIGNAL FEATURES

STATISTICAL TIME DOMAIN FEATURES	
FEATURE	DESCRIPTION
1. Root Mean Square (RMS)	The power content
2. Crest Factor	The ratio of the peak amplitude to the RMS
3. Shape Factor	The RMS divided by the signal mean
4. Impulse Factor	The maximum of the peak amplitudes divided by the signal mean
5. Shannon Entropy	The degree of uncertainty
6. Log Energy Entropy	The degree of uncertainty
7. Skewness	Asymmetry measure of the PDF of the signal
8. Kurtosis	The impulsiveness of the signal
FREQUENCY DOMAIN FEATURES	
Squared Envelope Spectrum	
9. - Amplitude of characteristic defect frequency (1. harmonic)	
TIME-FREQUENCY DOMAIN FEATURES	
Re-constructed signal of Wavelet Decomposition Levels (bior6.8)	
Squared Envelope Spectrum	
10. - Amplitude of characteristic defect frequency (1. harmonic)	

The fault detection algorithm calculates the squared envelope spectrum of a vibration signal. The amplitudes of the characteristic fault frequencies are identified from the envelope spectrum using peak detection. The fault state indication

is determined using an alarm level three times the mean of the maximum amplitude of the envelope spectrum of the steady state (i.e., non-faulty) signal. The alarm level was justified earlier based on the noise level of non-faulty vibration signals.

The left side of Figure 5 illustrates the fault detection for both bearings, with bearing 3 on the top and bearing 1 on the bottom. The dotted red line represents the fault detection time. The blue line represents the amplitude of the ball pass frequency of the inner race (BPFI) in the envelope spectrum of the vibration signal. The orange plot is the highest amplitude of the BPFI in the envelope spectrum of the re-constructed signals. The BPFI was detected after testing bearing 3 for 31.5 days (Figure 5). The wavelet decomposition was determined for twelve levels, resulting in the highest frequency band from 5 kHz to 10 kHz. The wavelet filtering does not give any earlier indication of the fault compared to the envelope spectrum. The ball pass frequency of the outer race (BPFO) was detected at 3.8 days into the testing of bearing 1. The wavelet filtered signal provided fault detection 1.1 days earlier than the envelope spectrum.

RUL estimation was processed following fault detection using the adaptive Metropolis-Hastings MCMC algorithm. The best degradation feature was determined using the goodness metrics defined in equation 1. Table 3 includes the goodness metrics calculations for the selected features. All the features were normalized to the same sampling rate and the features were smoothened using a moving average with a window of 20 samples. In terms of time, the window is 3.3 hours to give adequate resolution for RUL estimation. The exponential model from equation (2) was fitted to the degradation curves of both cases using the least squares approximation. As a result, the prior estimates of the model parameters (c,b) and the error variance were obtained. The Metropolis-Hastings MCMC algorithm was executed with the prior parameters to estimate the RUL.

Table 3: DEGRADATION GOODNESS METRICS

1	2	3	4	5	6	7	8	9	10
0.438	0.342	0.418	0.348	0.424	0.453	0.359	0.328	0.270	0.235

Figure 5 represents RUL estimation with 5% - 95% confidence. RUL estimation was done after the last measurement date (the dashed black line). Time intervals between the fault detection time and the last measurement date were approximately two days in both cases. The solid blue line is the estimate of the degradation feature. The estimate was calculated using the exponential model with the model parameters obtained from the RUL algorithm at the last measurement date. The estimation confidence limits were calculated using the model parameters at 5% - 95% confidence. The alarm level for the degradation feature (the solid red line) was set to 3.5. The threshold was set higher than the last degradation feature values in both cases for evaluation purposes. The dashed red line represents the last operation date of the bearing. The last operation date was determined when the 5% confidence limit reached the alarm threshold.

Table 4: FRAMEWORK PERFORMANCE TESTS

Intel Core i5-6440HQ CPU 2.60GHz - 100 RUNS / FUNCTION

	FUNC.2	FUNC.5	FUNC.10	FUNC.13
Mean [s]	0.1616	0.0325	0.1303	24.6400
Std [s]	0.0313	0.0258	0.0365	0.5709

Intel Core i5-4300 CPU 1.90GHz - 100 RUNS / FUNCTION (Fig.4)

	FUNC.2	FUNC.5	FUNC.10	FUNC.13
Mean [s]	0.2385	0.0490	0.3256	56.1089
Std [s]	0.0137	0.0356	0.2200	2.7115

Performance tests for the developed framework were run on two CPUs. Table 4 includes averages of 100 runs for the main functions defined in the sequence diagram (Figure 4). It is notable that the function call `getAssetData()` (FUNC.2) also includes the function call `getMeasurementData()` that reads vibration signal data from external files, which is an operation dependent upon a hard drive. The function call `estimateRUL()` depends on how many measurements were collected since the bearings started to be used. Other than RUL estimation calculations, execution times of the main functions are not significantly large. However, the performance test should be run on embedded systems that include less computing power.

6 Conclusions

Tribotronic systems are installed in different environments with various configurations. These systems are vulnerable; consequently, complex algorithms are developed to interpret measurements from modern sensors and to make decisions

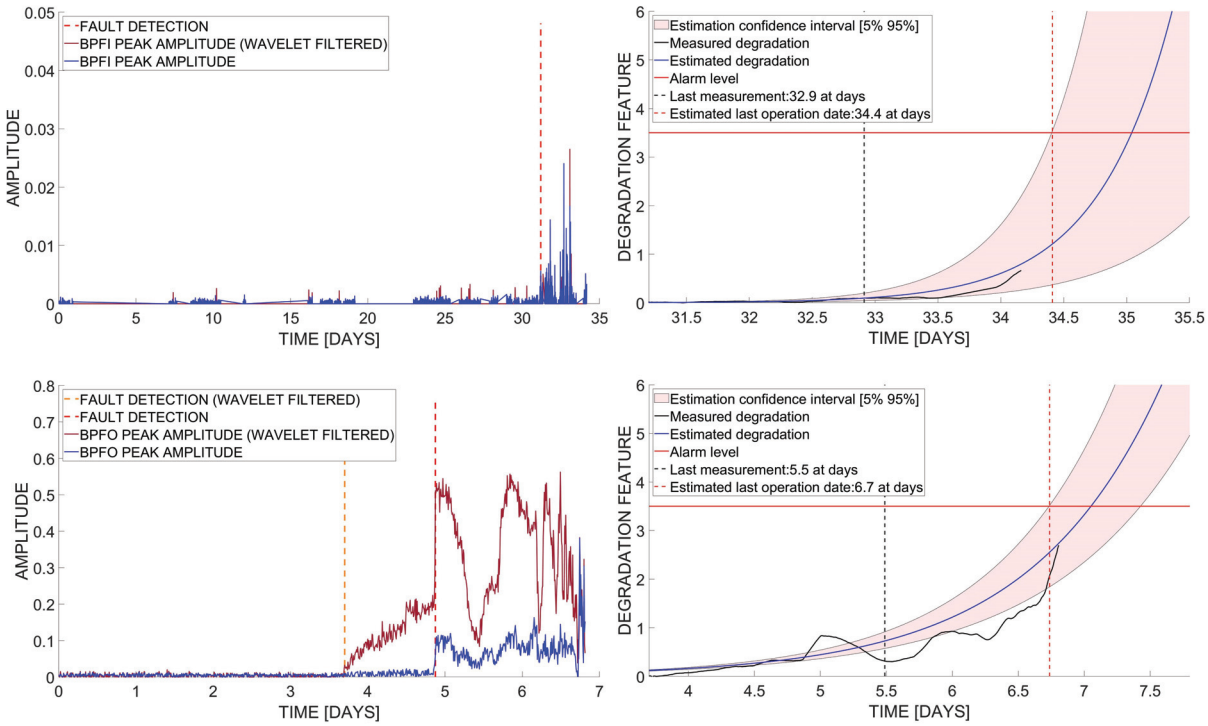

Figure 5: Fault detection (LEFT) and RUL estimation (RIGHT): Bearing 3(TOP), Bearing 1(BOTTOM)

to control the actuators that give feedback to a tribosystem. The fundamental phenomenon of interacting surfaces is the main motivator to build such self-adjusting tribotronic systems.

This paper introduced a unique Tribotronic plug-in software framework that offers assets and data management, feature extraction, fault detection, and RUL estimation for tribotronic systems. The plug-in implementation targets REBs. Further, the plug-in implementation is interchangeable; ergo, it perfectly fits with other tribosystems, such as gears. The framework is platform-independent and also applies to embedded systems. It is extensible and implements functionalities that require considerable amounts of computing power can be implemented in lower-level programming languages. Unit testing capabilities increase the reliability of the implemented plug-in.

The experimental evaluation of the tribotronic plug-in framework were done using bearing vibration data acquired from NASA's prognostics data repository. The evaluation included a run-through from feature extraction to fault detection to RUL estimation. The purpose of the evaluation was not to introduce fault detection or RUL estimation methods, but to show that the framework can handle complex algorithms and produce reliable results. The performance tests demonstrate that the running times are short on ordinary CPUs; however, the lengths of the vibration measurements can be considerably longer, which leads to longer running times. The configuration complexity of the implemented plug-in is low from the point of view of the total number of meta-parameters.

Future research should focus on performance testing of the framework on embedded systems and benchmarking the framework in other tribotronic systems.

References

[1] Great Britain. The jost report. Technical report, Department of Education and Science. Lubrication Engineering (Education and Research) Working Group., 1966.

[2] W Brostow, G Darmarla, and J Howe. Determination of wear of surfaces by scratch testing. *e-Polymers*, 4(1), 2013.

[3] Sergei Glavatskih and Erik Hoglund. Tribotronics towards active tribology. *Tribology International*, 41(9):934 – 939, 2008.

[4] S Kivioja, S Kivivuori, and P Salonen. *Tribologia - Kitka, kuluminen ja voitelu*. Otatieto, 2004. in Finnish.

[5] Kenneth Holmberg. Reliability aspects of tribology. *Tribology International*, 34(12):801 – 808, 2001.

[6] A Backlund. The definition of system. *Kybernetes*, 29(4):444 – 451, 2000.

[7] Horst Czichos. *Tribology: a systems approach to the science and technology of friction, lubrication, and wear*. Elsevier Science, 2000.

[8] P J Blau. *Tribosystem analysis: a practical approach to the diagnosis of wear problems*. CRC Press Taylor and Francis Group, 2016.

[9] Jan Bosch, Peter Molin, Michael Mattsson, and PerOlof Bengtsson. Object-oriented framework-based software development: Problems and experiences. *ACM Computing Surveys*, 32(1es), Mar 2000.

[10] R E Johnson and B Foote. Designing reuseable classes. *Journal of Object-Oriented Programming*, 1988.

[11] Michael Mattsson. *Object-Oriented Frameworks*. PhD thesis, Apr 1999.

[12] Stephen H. Kaisler. *Software Paradigms*. Wiley, 2005.

[13] Christoph Herrmann, Thomas Kurpick, and Bernhard Rumpe. Sselab: A plug-in-based framework for web-based project portals. *2012 2nd International Workshop on Developing Tools as Plug-Ins, TOPI 2012 - Proceedings*, Jun 2012.

[14] R. de T. Caropreso, R. A. S. Fernandes, D. P. M. Osorio, and I. N. Silva. An open-source framework for smart meters: Data communication and security traffic analysis. *IEEE Transactions on Industrial Electronics*, 66(2):1638 – 1647, Feb 2019.

[15] B J Hamrock and W J Anderson. Rolling element bearings. Technical report, NASA, Jun 1983.

[16] SKF Group. *Bearing investigation*. SKF Group, 2012.

[17] AH Christer and W Wang. A simple condition monitoring model for a direct monitoring process. *European Journal of Operational Research*, 82(2):258 – 269, 1995.

[18] D Banjevic and A K S Jardine. *Condition Monitoring*. John Wiley & Sons, 2008.

[19] E Jantunen. A summary of methods applied to tool condition monitoring in drilling. *International Journal of Machine Tools and Manufacture*, 42(9):997 – 1010, 2002.

[20] J-J Wang, Y-H Zheng, L-B Zhang, L-X Duan, and R Zhao. Virtual sensing for gearbox condition monitoring based on kernel factor analysis. *Petroleum Science*, 14(3):539 – 548, Aug 2017.

[21] P R Dongre, S S Chiddarwar, and V S Deshpande. Tool condition monitoring in various machining operations and use of acoustic signature analysis. *International Journal on Mechanical Engineering and Robotics (IJMER)*, 1(1):2321 – 5747, 2013.

[22] A Rai and S Upadhyay. A review on signal processing techniques utilized in the fault diagnosis of rolling element bearings. *Tribology International*, 96, Apr 2016.

[23] I El-Thalji and E Jantunen. A descriptive model of wear evolution in rolling bearings. *Engineering Failure Analysis*, 45:204 – 224, 2014.

[24] N K Arakere and G Subhash. Work hardening response of m50-nil case hardened bearing steel during shakedown in rolling contact fatigue. *Materials Science and Technology*, 28(1):34 – 38, 2012.

[25] J M Cookson and P J Mutton. The role of the environment in the rolling contact fatigue cracking of rails. *Wear*, 271(1):113 – 119, 2011.

[26] V V Panasyuk, O P Datsyshyn, and H P Marchenko. The crack propagation theory under rolling contact. *Engineering Fracture Mechanics*, 52(1):179 – 191, 1995.

[27] A V Olver. The mechanism of rolling contact fatigue: An update. *Proceedings of the Institution of Mechanical Engineers, Part J: Journal of Engineering Tribology*, 219(5):313 – 330, 2005.

[28] K H Ruhm. *Sensoren der Schwingungsmesstechnik*. 2010.

[29] R B Randall. *Vibration based Condition Monitoring: Industrial, Aerospace and Automotive Applications*. Dec 2010.

[30] W Caesarendra and T Tjahjowidodo. A review of feature extraction methods in vibration-based condition monitoring and its application for degradation trend estimation of low-speed slew bearing. *Machines*, 5:21, Sep 2017.

[31] B. Zhang, C. Sconyers, C. Byington, R. Patrick, M. E. Orchard, and G. Vachtsevanos. A probabilistic fault detection approach: Application to bearing fault detection. *IEEE Transactions on Industrial Electronics*, 58(5):2011 – 2018, May 2011.

[32] Q Wei and D. Xu. Remaining useful life estimation based on gamma process considered with measurement error. In *2014 10th International Conference on Reliability, Maintainability and Safety (ICRMS)*, pages 645 – 649, Aug 2014.

[33] Jinjiang Wang, Robert Gao, Zhuang Yuan, Zhaoyan Fan, and Laibin Zhang. A joint particle filter and expectation maximization approach to machine condition prognosis. *Journal of Intelligent Manufacturing*, Oct 2016.

[34] Kamal Medjaher, Diego Alejandro Tobon-Mejia, and Noureddine Zerhouni. Remaining useful life estimation of critical components with application to bearings. *IEEE Transactions on Reliability - TR*, 61:292 – 302, Jun 2012.

[35] J.Z. Sikorska, M. Hodkiewicz, and L. Ma. Prognostic modelling options for remaining useful life estimation by industry. *Mechanical Systems and Signal Processing*, 25(5):1803 – 1836, 2011.

[36] Q. T. Tran, S. D. Nguyen, and T. Seo. Algorithm for estimating online bearing fault upon the ability to extract meaningful information from big data of intelligent structures. *IEEE Transactions on Industrial Electronics*, 66(5):3804 – 3813, May 2019.

[37] Per Runeson. A survey of unit testing practices. *IEEE Software*, 23(4):22 – 29, Jul 2006.

[38] A Keller, B Brown, A Hellerstein, and J Hellerstein. A configuration complexity model and its application to a change management system. *IEEE Transactions on Network and Service Management*, 4:13 – 27, Jan 2007.

[39] K Saarinen and J Kansanaho. Decision of faulty bearing, WO2018069187.

[40] J Kansanaho, K Saarinen, and T Kärkkäinen. Spline wavelet based filtering for denoising vibration signals generated by rolling element bearings. *International Journal of COMADEM*, 21(4), 2018.

[41] Bin Zhang, Lijun Zhang, and Jinwu Xu. Degradation feature selection for remaining useful life prediction of rolling element bearings. *Quality and Reliability Engineering International*, 32(2):547 – 554, 2016.

[42] G O Roberts and J F Rosenthal. 2004 general state space markov chains and mcmc algorithms. *Probability Surveys 2004*, 1, Apr 2004.

[43] H Haario, E Saksman, and J Tamminen. An adaptive metropolis algorithm. *Bernoulli*, 7, Apr 2001.

[44] Kai Goebel, Bhaskar Saha, Abhinav Saxena, Jose Celaya, and Jon Christophersen. Prognostics in battery health management. *Instrumentation & Measurement Magazine, IEEE*, 11:33 – 40, Sep 2008.

[45] Dawn An, Joo-Ho Choi, and Nam Ho Kim. Prognostics 101 a tutorial for particle filter-based prognostics algorithm using matlab. *Reliability Engineering and System Safety*, 115:161 – 169, 2013.

[46] N. Li, Y. Lei, J. Lin, and S. X. Ding. An improved exponential model for predicting remaining useful life of rolling element bearings. *IEEE Transactions on Industrial Electronics*, 62(12):7762 – 7773, Dec 2015.

[47] W Gousseau, J Antoni, F Girardin, and J Griffaton. Analysis of the rolling element bearing data set of the center for intelligent maintenance systems of the university of cincinnati. In *CM2016*, Charenton, France, Oct 2016.

[48] Hai Qiu, Jay Lee, Jing Lin, and Gang Yu. Wavelet filter-based weak signature detection method and its application on rolling element bearing prognostics. *Journal of Sound and Vibration*, 289(4):1066 – 1090, 2006.

[49] A K Mahamad, S Saon, and T Hiyama. Predicting remaining useful life of rotating machinery based artificial neural network. *Computers and Mathematics with Applications*, 60(4):1078 – 1087, 2010.

[50] A. Soualhi, H. Razik, G. Clerc, and D. D. Doan. Prognosis of bearing failures using hidden markov models and the adaptive neuro-fuzzy inference system. *IEEE Transactions on Industrial Electronics*, 61(6):2864 – 2874, Jun 2014.

[51] G Gautier, R Serra, and J M Mencik. Subspace-based damage identification of roller bearing. *MATEC Web of Conferences*, 20, 2015.

[52] P. Arun, S. Abraham Lincon, and N. Prabhakaran. Reliability of using characteristic frequency components for the detection and characterization of bearing faults. *Procedia Computer Science*, 115:740 – 747, 2017.

[53] W. Ahmad, S. A. Khan, and J. Kim. A hybrid prognostics technique for rolling element bearings using adaptive predictive models. *IEEE Transactions on Industrial Electronics*, 65(2):1577 – 1584, Feb 2018.